EVIDENCE FOR THE INFLUENCE OF IRRIGATION ON PRECIPITATION

INTENSITY AND TOTALS IN THE MIDWESTERN UNITED STATES:

OBSERVATIONAL AND MODELING PERSPECTIVES

By

ROSS EVAN ALTER

A dissertation submitted to the

Graduate School-New Brunswick

Rutgers, The State University of New Jersey

In partial fulfillment of the requirements

For the degree of

Doctor of Philosophy

Graduate Program in Atmospheric Science

Written under the direction of

Ying Fan Reinfelder

And approved by

_____

_____

_____

_____

New Brunswick, New Jersey

October 2014

ABSTRACT OF THE DISSERTATION

Evidence for the influence of irrigation on precipitation intensity and totals in the Midwestern

United States: observational and modeling perspectives

By

ROSS EVAN ALTER

Dissertation Director:

Ying Fan Reinfelder

Significant increases in summer precipitation occurred in the Midwestern United States over the last century for reasons that remain unclear. It is postulated that the expansion of irrigation and cropland in the central US over the past sixty years has been a major contributor to these observed increases in precipitation. As a first step toward attribution of these regional precipitation changes, a detailed analysis of observed daily summer precipitation frequency and intensity is conducted for the contiguous United States over multiple spatial scales and time periods from 1895 to 2011. Robust increases in precipitation frequency, total precipitation, and moderate to heavy precipitation intensity are identified during July and August in the Midwestern US. Analysis of changes in mean monthly precipitation from the early- to late-20th century initially points to increasing frequency as the source of increasing monthly precipitation in the Midwestern US during the summer, especially during August; however, comparable increases in precipitation frequency occur during other times of the year. On the other hand, changes in precipitation intensity and total precipitation are both greatest during

July and August and coincide spatially in the Midwestern US. Additionally, the greatest intensity change occurs downwind of the most heavily irrigated regions, especially for the period between 1950 and 1980 when irrigation rapidly intensified. A 15-day simulation using the WRF regional climate model with a simplified irrigation scheme over Nebraska confirmed the postulated increase in moisture, decrease in temperature, and subsequent increases in both convective inhibition and convective available potential energy over Nebraska, which led to weakened convection over the irrigated areas. Wind anomalies produced by irrigation seem to be instrumental in enhancing precipitation intensity and totals downwind of Nebraska in general, and in the eastern Midwest region for one particular heavy precipitation event. The increases in Midwestern precipitation in both analyses – one based on observation and rooted in reality and one based on model experiments and controlled for irrigation – support the hypothesis that irrigation in Nebraska has led to an increase in the intensity and total of precipitation downwind of the irrigated regions.

office.   Stephen Nicholls also provided much assistance with Matlab and climate modeling when I was just beginning to learn about them, and our conversations and racquetball excursions were excellent opportunities for decompressing. All of my other friends in DES helped with academics whenever necessary, offered many useful discussions, and provided camaraderie during our forays into several intramural sports. In this regard, I especially thank the members of the ESGSA softball team – the Adiabats – who helped to provide me with five years of fun, hustle, and good times over the last five years. For all of the other friends I have made along the way, both inside and outside DES, I thank you so much for all of your assistance and for the joy that you gave to me over the last nine years.

Outside of DES were a number of others who greatly assisted me on my journey to earning a Ph.D. Haibin Li, a former postdoctoral fellow of Ying, first helped me to understand climate modeling three years ago and helped me with any questions I had about our research together in Ying's group. Yadu Pokhrel, another former post-doc of Ying, was indispensable in refreshing my modeling memory and helping me to develop my modeling skill to what it is today. Without his help, the modeling chapter of this dissertation would not have been possible. Paul Romero, a graduate student of Ying, offered plentiful conversation about academics and life in general and also helped immensely with his delivery of important paperwork to the Graduate Office for me while I was working in Boston. Other professors, graduate students, and post-docs outside of DES helped me to better understand other aspects of the world and enhanced my academic knowledge so as to round out my academic foundation for research.

Please note that Part I of this dissertation is currently undergoing revision as part of the peer review process for acceptance into the Journal of Hydrometeorology.

TABLE OF CONTENTS

LIST OF TABLES

LIST OF ILLUSTRATIONS

1. INTRODUCTION

1.1 Motivation and Summary

Over the last few centuries, humans have greatly modified the physical landscape of the Earth, resulting in widespread yet often unintentional consequences for the Earth's weather, climate, and biogeophysical processes. Understanding the causes and consequences of this land use and land cover change (LULCC) is critical to advancing our understanding of climate change and projecting its future impacts on society. The importance of LULCC to local and regional (and even global) climate has become apparent over the last decade with a bevy of modeling and observational studies taking place around the world (e.g., Boucher et al. 2004, Sacks et al. 2009, Puma and Cook 2010). However, the breadth, causes, mechanisms, and impacts of some aspects of LULCC are still not well understood. Because of this lack of definitive knowledge of the processes governing the intersection of LULCC and climate, attribution of past changes in climate also remains incomplete. To fill this attribution gap, LULCC processes have been gradually incorporated into global (e.g., IPCC 2013) and regional climate models (e.g., Ozdogan et al. 2010) as our understanding of these processes has solidified. Thereafter, climate simulations would be able to include these LULCC processes and perform sensitivity studies to determine the impact of LULCC on weather and climate. Over the past decade, many sensitivity studies to quantify the effects of LULCC on climate have been performed (e.g., Segal et al. 1998; Boucher et al. 2004; Diffenbaugh 2009; Harding and Snyder 2010a,b; Lo and Famiglietti 2013; Huber et al. 2014).

One particularly important aspect of LULCC that has had regional and global implications is the expansion of agriculture over the last few centuries. Over the last three centuries, cropland has expanded by 12 million km^2 around the world; in many areas of the world, cropland is nearly 100% of the current land cover (Ramankutty and Foley 1999).

Additionally, over the last sixty years, the world has experienced another agricultural renaissance: There has been a substantial, rapid, and global increase in irrigated cropland area and in the amount of water used for cropland irrigation. While there were approximately 108.4 million hectares of land equipped for irrigation in 1950, this area nearly tripled to 285.8 million hectares by 2007 (Freydank and Siebert 2008). This boom in large-scale cropland irrigation has had two main agricultural benefits: 1) it has enabled the production of more food in drier areas that would normally not produce significant crop yields and 2) it has allowed for the maintenance of consistent crop yields in more humid areas. The immediate economic and nutritional benefits of greater crop availability (e.g. in India and China) add to an argument that the worldwide expansion of irrigation in the second half of the 20th century has largely benefited society.

However, the process of irrigation expansion is a double-edged sword. In order to accommodate the expansion in cropland and crop yields, this development has required the eradication of native vegetation and/or traditional agricultural practices (Ramankutty and Foley 1999) and has added copious amounts of water to the surface in several regions that did not previously irrigate cropland. One unintended consequence of this irrigation-induced land use/land cover change is the altering of two aspects of the climate system: 1) the surface energy balance, through changes to albedo and sensible and latent heat

ratios, and 2) the amount of water that is available for evapotranspiration (ET) – the transfer of water to the atmosphere via evaporation and transpiration from plants. Additionally, in areas where groundwater aquifers (reservoirs of water below ground level) are the dominant irrigation source, groundwater levels and streamflow patterns may also be shifted. These changes in hydroclimate – the interdependency of climatic and hydrologic processes – are large enough to throw off the energy and moisture balance in the more intensely irrigated regions. However, because the irrigation expansion took place over the course of several decades and is regionalized in scope, the issue of weather and climate modification due to irrigation has only garnered significant scientific attention since the peak of irrigation in the 1970s and 1980s.

Nevertheless, the last 30-40 years has produced an array of studies that illustrate potential climate effects resulting from large-scale irrigation. Mean temperatures (e.g. Barnston and Schickedanz 1984; Adegoke et al. 2003), extreme temperatures (Lobell et al. 2008), dewpoint temperatures and low-level moisture (e.g. Mahmood et al. 2008), mean precipitation (e.g. Barnston and Schickedanz 1984; Sacks et al. 2009), streamflow (Kustu et al. 2010, 2011), sensible and latent heat fluxes (e.g. Adegoke et al. 2003; Douglas et al. 2009), and other hydroclimate variables have likely changed in and around irrigated areas due to the increase in irrigation regionally and globally. Unfortunately, these studies are made more difficult by a lack of continuous historical data (e.g., radiative fluxes), too much background noise to sort out a signal (e.g., precipitation variability), and a multitude of other environmental factors that could influence observations (e.g., El Niño Southern Oscillation, synoptic weather patterns, climate change, etc.). In short, despite evidence that suggests hydroclimate can be significantly

altered by large-scale irrigation, it remains a challenge to attribute the noted "irrigation" effects" to irrigation alone.

In particular, precipitation changes are difficult to attribute to large-scale irrigation development. Studies involving irrigation-induced precipitation often involve multiple statistical tests (e.g. Barnston and Schickedanz 1984), radar estimates of precipitation (Moore and Rojstaczer 2002), and/or climate model simulations (e.g. Adegoke et al. 2003; Sacks et al. 2009) because analyzing station observations alone presents a great deal of weather "noise", and the result may be influenced by several other local and regional factors. Furthermore, one recent study (e.g. DeAngelis et al. 2010) suggests that precipitation impacts from irrigation may be felt as far as several hundred kilometers downwind of the irrigated areas. It is for this reason that this dissertation research focuses on both observational analysis of irrigation impacts on precipitation and on modeling the "irrigation effect" on precipitation both around and downwind of intensely irrigated areas. Because North America holds a bevy of historical climate and irrigation data, and since the climate model being utilized has been extensively tested over North America, the analyses are conducted with regard to large-scale irrigation in the Great Plains of the United States.

The following sections entail two separate aspects of this dissertation research. In Section 2, precipitation observations are analyzed across the United States in an attempt to attribute irrigation and agricultural expansion as a primary cause of increasing precipitation intensity and totals in the Midwestern US. In Section 3, a regional climate model is used to conduct a sensitivity study for the impact of irrigation in Nebraska on

precipitation in the central US during June of 2002. Section 4 delineates the conclusions that can be drawn from these analyses.

2. OBSERVATIONAL ANALYSIS

2.1 Introduction

Over the course of the 20th century, statistically significant increases in precipitation have occurred in the Midwestern United States (Karl et al. 1996; Angel and Huff 1997; Pryor et al. 2009; Groisman et al. 2012; Villarini et al. 2013, Melillo et al. 2014), especially during the summer (June-July-August) (Changnon and Kunkel 1995; Karl and Knight 1998; Groisman et al. 2004; DeAngelis et al. 2010; Higgins and Kousky 2013). Several potential drivers of such increases have been proposed, including large-scale atmospheric circulations and teleconnections, e.g., the El Niño Southern Oscillation (Groisman et al. 2012), shifts in the nocturnal Great Plains low-level jet (Weaver and Nigam 2008), and increases in temperature as a result of greenhouse gas emissions (Groisman et al. 2004; Villarini et al. 2013). Land use and land cover changes (LULCC) over the last century, such as dam and reservoir construction (Hossain et al. 2009), conversion of forest and grassland to cropland (Baidya Roy et al. 2003), increasing crop acreage and yield (Groisman et al. 2012), and the development of large-scale cropland irrigation (Barnston and Schickedanz 1984; DeAngelis et al. 2010), have also been hypothesized as potential drivers of precipitation change. However, uncertainty remains in the relative importance of each driver in explaining the observed changes in total precipitation.

In the present study, we analyze observed changes in regional precipitation characteristics in the Midwestern US and consider how these may relate to the historical intensification of irrigation and expansion of cropland in the central US, especially Nebraska. Irrigation in the US Great Plains began rapidly developing in Texas in the 1930s and across the rest of the Great Plains in the 1940s and 1950s. In Nebraska – the most densely irrigated of the Great Plains states – the abundance of water from the Ogallala Aquifer combined with lower energy costs and improved technology (Guru and Horne 2000) facilitated expansion of irrigated acreage from approximately 876,000 acres in 1949 to 5,700,000 acres in 1978, and further to 8,559,000 acres in 2007 – almost twice the area of the state of New Jersey (NASS 2013). Groundwater withdrawal for irrigation experienced similar rapid development from about 600,000 acre-feet in 1950 to about 6,500,000 acre-feet in 1980 (USGS 2013). In 2013, total irrigation-related groundwater withdrawal for Nebraska counties over the Ogallala Aquifer was estimated at 7,960,000 acre-feet, or 13 times larger than estimated amount in 1950 (NRCS 2013).

As a result of the expansion of irrigation, irrigated cropland became the dominant type of warm-season agriculture in Nebraska (see Figure 1): In 1950, approximately 7% of corn and soybean acreage in Nebraska was irrigated; by 2011, approximately 54% of the same crop acreage was irrigated (NASS 2013). A similar change occurred for production of these crops: In 1950, approximately 12% of corn and soybean production was irrigated, while in 2011, approximately 64% of that production was irrigated (NASS 2013). Generally, the expansion of crops in Nebraska over the last sixty years, in acreage by a factor of two and in production by a factor of seven, may be largely attributed to enhanced cropland irrigation during this time period.

In the 1970s and 1980s, several studies analyzed station observations of precipitation to demonstrate a supposed "irrigation effect" on local precipitation, i.e., precipitation enhancement in the vicinity of heavily irrigated regions (Stidd et al. 1975; Barnston and Schickedanz 1984). These early studies indicated elevated precipitation about 50-100 km downwind of heavily irrigated areas in Washington State during July and August, and in the Texas Panhandle during June, respectively. Later studies focused on larger regions of the US (Segal et al. 1998) and analyzed precipitation patterns using weather radar (Moore and Rojstaczer 2002) and water vapor tracking (DeAngelis et al. 2010; Harding and Snyder 2012a) to demonstrate the plausibility of irrigation effects on precipitation. Recent numerical modeling experiments for the US (Ozdogan et al. 2010; Lo and Famiglietti 2013; Qian et al. 2013) and other areas globally (e.g., De Ridder and Gallée 1998; Douglas et al. 2009; Sacks et al. 2009; Jódar et al. 2010; Puma and Cook 2010; Lee et al. 2011; Wei et al. 2013) provide additional support for irrigation-related influences on precipitation patterns, both locally and remotely.

In the current study, we perform a comprehensive analysis of station observations of summer precipitation and attempt to identify signals in precipitation frequency, intensity, and totals that are indicative of an irrigation-induced enhancement of precipitation. While the analyses cover the entire contiguous US (CONUS), we emphasize two target regions – the Upper Midwest (Minnesota, Wisconsin, Michigan, and Iowa) and the Midwest (Missouri, Illinois, Indiana, Ohio, Kentucky) – which, together, form the Midwestern US. The Midwestern US is downwind of Nebraska, which contains more irrigated acres than any state in the US; thus, this is the area where the largest irrigation-induced enhancement in precipitation is expected to occur. In

Section 2, we describe potential mechanisms for how irrigation affects precipitation as well as related hypotheses, while in Sections 3 and 4, we describe our methodology and results. As a first step toward attribution, we discuss in Section 5 how the results compare with expectations based on the mechanisms outlined in Section 2.

2.2 Potential mechanisms for LULCC enhancement of precipitation

2.2.1 Irrigation

Figure 2 illustrates several potential influences of irrigation on atmospheric thermodynamics and associated precipitation processes. The basic premise of an irrigation effect on precipitation is that irrigation increases soil moisture, thereby lowering surface albedo (Eltahir 1998; Pielke 2001) and repartitioning the surface energy budget toward larger latent heat flux, smaller sensible heat flux, and consequently, a lower Bowen ratio (Eltahir 1998; Adegoke et al. 2003; Betts 2004; Mahmood et al. 2004). Both the lower albedo and repartitioned energy budget may increase net radiation at the surface: Reduced albedo increases the absorption of incident solar radiation, while the repartitioning of sensible and latent heat fluxes results in decreased outgoing surface longwave emission, both through lower surface temperatures as well as an amplified water vapor greenhouse effect (Eltahir 1998). Since increasing net radiation at the surface necessitates an increase in total outgoing surface heat fluxes (Betts et al. 1996; Eltahir 1998), the flux of moist static energy (MSE) into the atmospheric boundary layer (ABL) should increase (Eltahir 1998; Pal and Eltahir 2001). However, the dense crop cover during the summer may prevent a noticeable change in soil albedo even under irrigated conditions. In fact, other studies suggest that net radiation is rather insensitive

to soil moisture (Betts 2004; Jones and Brunsell 2009), so the hypothesized enhanced flux of MSE into the ABL may be overemphasized. The historical increase of (irrigated) crop acreage, density, and greenness as a result of irrigation further strengthen the magnitude of these moisture and energy fluxes into the ABL (Wang et al. 2003).

In contrast, the effects of the repartitioned radiative budget have rather direct implications for ABL structure and thermodynamics. The smaller sensible heat flux and the associated decrease in temperature (Adegoke et al. 2003, 2007; Mahmood et al. 2004, 2006; Lobell et al. 2008) lower ABL height, which simultaneously reduces entrainment of low-MSE air at the top of the ABL (Betts et al. 1996) and increases the MSE per unit mass of ABL air (Eltahir 1998), both of which are expected to encourage atmospheric convection. Additionally, the greater latent heat flux is indicative of increased evapotranspiration (ET) from the surface (Pielke 2001; Ozdogan et al. 2010), which moistens the ABL. This moistening of the ABL over irrigated areas, which has been documented in studies of changes in dewpoint temperature (Mahmood et al. 2006, 2008) and specific and relative humidity (Brown and DeGaetano 2013; Qian et al. 2013), lowers the lifting condensation level (LCL - cloud base) (Betts 2004; Sun et al. 2007), allowing rising air parcels to more readily form clouds and potentially reach their level of free convection (LFC). Increased moisture in the ABL also enhances convective available potential energy (CAPE) (Pielke and Zeng 1989; Pielke 2001; Qian et al. 2013; Huber et al. 2014), which represents the conduciveness of the upper-air environment for convective development.

However, it is also possible that irrigation-induced radiative changes may reduce the potential for convection over the irrigated areas. In particular, the expected decreases

in the LCL over the irrigated areas are likely to be greater than those of the LFC because the LCL is closer to the surface and therefore would likely respond more readily to increased irrigation. The greater decrease of the LCL is evident in the irrigation-induced changes to the atmospheric vertical profile depicted in Huber et al. (2014). If the LCL of a parcel is lowered more than its LFC, then the vertical distance over which a saturated air parcel must rise to reach its LFC, attain positive buoyancy, and utilize CAPE would increase. The increasing distance between the LCL and LFC would likely increase convective inhibition (CIN), i.e., the energy needed for a saturated parcel to overcome negative buoyancy and reach its LFC, thus reducing the likelihood of deep, moist convective development and precipitation (Huber et al. 2014; Im et al. 2014). Additionally, since the height of the LCL may be lowered more than the height of the ABL, it is possible that shallow convective clouds would preferentially develop (Qian et al. 2013). Since enhanced CIN hinders the development of convective precipitation, these shallow, non-precipitating clouds may block incoming solar radiation, thereby reducing net surface radiation and creating a negative feedback on the initial flux perturbations caused by irrigation (Qian et al. 2013). Such mechanisms may account for the results of some studies showing reduced frequency of summer precipitation events over irrigated areas (Harding and Snyder 2012b; Huber et al. 2014; Im et al. 2014).

The aforementioned mechanisms are effectively local responses to irrigation. However, the advection of air with additional moisture and moist static energy from irrigated areas to more convectively favorable areas downwind, e.g., where CIN is not enhanced, could increase the frequency and/or intensity of storms in downwind regions (DeAngelis et al. 2010). This is especially true during the summer, when the

characteristics of the ABL can be important in determining the probability of rainfall occurrence (Findell and Eltahir 2003a,b). The downwind enhancement of irrigation on precipitation has already been demonstrated on local scales (see above) and remotely (e.g., DeAngelis et al. 2010; Harding and Snyder 2012a; Lo and Famiglietti 2013; Wei et al. 2013; Huber et al. 2014), but uncertainty remains in the degree and location of irrigation impacts on more regional scales. Average winds during July and August at the 850 hPa pressure level, which is often used to diagnose moisture transport (Harding and Snyder 2012b; Huber et al. 2014), are generally southwesterly over eastern Nebraska, where extensive cropland irrigation occurs. Thus, if irrigation in Nebraska were to cause downwind enhancement of precipitation via an increase in moisture (convergence), it would likely be in the Upper Midwest states of Iowa, Minnesota, Wisconsin, and Michigan, assuming enough vertical transport of the air parcels to reach the 850 hPa pressure level; otherwise, winds at the surface are generally more southerly and would likely lead to precipitation enhancement in the Dakotas and Minnesota. Note that the scale of irrigation in the states downwind of Nebraska is much less than that of Nebraska itself due to the more humid climate; thus, irrigation in these downwind regions are not expected to significantly add to the rainfall effects expected from irrigation in Nebraska.

The contrasts in phenology between irrigated crops, rain-fed crops, and potential vegetation are important for determining the most appropriate timing for an irrigation effect. Most irrigation occurs during July and August in Nebraska, when ET is highest and crop water demand is maximized (Suyker and Verma 2008; Ozdogan et al. 2010; see Fig. 1c in DeAngelis et al. 2010 for a depiction of monthly crop water use in the Great Plains). For both semi-arid and sub-humid climates within Nebraska, irrigated corn has

been demonstrated to have a longer growing season than rain-fed corn and grass, which results in higher values of ET lasting into August (Mahmood and Hubbard 2002). While peak ET from irrigated corn is in July, the largest difference between ET from irrigated corn fields and that of rain-fed corn and grass is in August; this is also reflected in a modeling study done by Ozdogan et al. (2010). Hence, if more irrigation-induced moisture is available in August, then the largest, most expansive irrigation effect on precipitation would be expected in August, a more moderate irrigation effect in July, and not much effect at all in June.

2.2.2 Other potential mechanisms

A similar mechanism may apply to the expansion of non-irrigated cropland in the Corn Belt of the US, which extends eastward from Nebraska to Ohio and northward to Minnesota and the eastern Dakotas. Instead of a soil moisture-precipitation feedback, plant transpiration would increase as a result of increasing crop acreage, density, and greenness. From 1940 to 2011, the acreage of corn and soybeans roughly doubled in Iowa and Illinois, and production of corn and soybeans increased in the two states by a factor of five (NASS 2013). However, the degree to which this increase in non-irrigated crop acreage and production affects precipitation is unclear. Latent heat flux, and thus ET, has been shown to increase when converting from grassland to rain-fed cropland (Wang et al. 2003), and specific humidity (Bonan 1997) and precipitation (Bonan 1997; Raddatz 2007) have also exhibited increases as a result of land cover conversion to cropland. However, Adegoke et al. (2003) demonstrate that increases in latent heat flux in Nebraska are stronger for conversion from rain-fed to irrigated agriculture than for conversion from natural vegetation to rain-fed agriculture. Additionally, Baidya Roy et

al. (2003) show no significant change in July precipitation in the Midwestern US between 1910 and 1990 when accounting solely for changes in historical land cover fractions (without irrigation). Therefore, while the potential contribution of non-irrigated cropland expansion and greater crop production to changes in precipitation patterns cannot be ruled out, it may be secondary to the forcing caused by irrigation development.

Other studies have demonstrated potential impacts of irrigation on the dynamical forcings of summer precipitation, e.g., the Great Plains low-level jet (Weaver and Nigam 2008; Huber et al. 2014) and monsoonal circulations (Douglas et al. 2009; Lee et al. 2011, Im et al. 2014). Moisture convergence may be enhanced in certain areas if monsoonal winds are changed or if additional moisture around irrigated croplands enhances moisture gradients. However, further attribution of long-term precipitation changes to these phenomena would require the long-term (>60 years) determination of observational or modeled changes to the Great Plains low-level jet and/or to wind speed and direction over time, both of which are not readily available. Though the limited observational nature of the present study precludes diagnosis of potential circulation changes, they are likely important links between irrigation and its effects on precipitation patterns.

Finally, climate change (CC) from greenhouse gas emissions may be a potential mechanism. For CC, enhancements in ET and saturation vapor pressure from rising temperatures (Clausius-Clapeyron relation) may cause distinct changes in precipitation patterns that, along with those caused by irrigation, may be ascertained from analysis of the observational record. Therefore, our hypotheses, outlined in the next subsection, describe the expected precipitation effects from both CC and irrigation (or more

generally, LULCC) to determine which one has been more important in influencing observed changes in summer precipitation patterns.

2.2.3 Hypotheses

While the aforementioned mechanisms are each plausible, it is difficult to establish direct causal linkages, especially with observations. Some of this difficulty may be the result of not separating changes in precipitation frequency from those of precipitation intensity; the relative contributions of frequency and intensity change may provide insight into mechanisms. Moreover, it is possible that distinct mechanisms account for changes in different portions of the precipitation distribution, e.g., the controls on light precipitation events may differ from those on heavy events. Therefore, our hypotheses incorporate both of these dichotomies – frequency and intensity, and lighter and heavier precipitation – to better attribute the observed changes in precipitation.

We hypothesize that CC and LULCC (specifically, irrigation and non-irrigated crop expansion) have distinct signatures in changes of the precipitation distribution. If CC is the main driver, warmer temperatures would increase ET, saturation vapor pressure, and atmospheric water vapor, thus stimulating more intense and more frequent heavy precipitation events (Trenberth et al. 2003). However, the overall frequency of precipitation events – especially those of light and moderate intensity – would likely stay roughly the same or decrease (Hennessy et al. 1997; Sun et al. 2007). This expected decrease in overall precipitation frequency would largely cancel out the effects on total precipitation of general increases in precipitation intensity (due to the extra water vapor). Indeed, an ensemble of global climate model simulations using the RCP8.5 scenario

(business as usual greenhouse gas emissions) indicates that total summer precipitation is projected to either remain roughly constant or increase slightly (less than 10%) in the Midwestern US by the years 2081-2100, even though annual average surface temperature in the same region is projected to be 5-7 K greater than present (IPCC, 2013). Thus, it is expected that increases in surface temperature due to CC would likely result in only a small (if any) net change in total precipitation.

On the other hand, if LULCC is the main driver, the combination of enhanced MSE from greater net radiation and enhanced atmospheric water vapor from greater ET could destabilize the ABL and create more frequent convective precipitation events over the entire precipitation distribution (Findell and Eltahir 2003a). However, LULCC likely does not have as much of an effect on precipitation frequency compared with precipitation intensity since 1) the increase in net radiation, and therefore, in MSE, is less prominent than the repartitioning of heat fluxes and consequent increase in water vapor, and 2) non-local (synoptic and mesoscale) forcings likely determine the periods during which convective precipitation is most favorable (Allard and Carleton 2010; Huber et al. 2014). On the other hand, the added moisture in the ABL and increased moisture convergence downwind would very likely enhance precipitation intensity. Therefore, we expect that LULCC would have a stronger effect on precipitation intensity than on precipitation frequency in the Midwestern US. The increase in precipitation intensity (combined with potentially greater precipitation frequency) would likely enhance total precipitation if LULCC is the main driver. It is expected that the largest increases in total precipitation would occur downwind of the irrigated regions due to the offsetting effects of greater CIN and greater shallow cloud cover directly over the irrigated areas.

In summary, if CC is the main driver, the precipitation distribution would shift toward more frequent and intense heavy events, less frequent lighter events, and small changes in total amounts. If LULCC is the main driver, the precipitation signal would be weak over the irrigated areas but more pronounced downwind, especially in the Upper Midwest spatially and in August temporally. In this region, we would expect to see enhancements in intensity and perhaps frequency, giving higher total precipitation amounts. These are the signals that we attempt to detect in the following data analyses.

2.3 Data and Methods

Daily precipitation data were obtained from the Global Historical Climatology Network - Daily (GHCND) archive of the National Climatic Data Center (NCDC). The GHCND dataset and its predecessor, the Global Daily Climatology Network, have been utilized by several previous works to analyze extreme precipitation patterns, determine historical precipitation frequencies, and calculate long-term trends in precipitation (e.g., Groisman et al. 2005; Alexander et al. 2006; Sun et al. 2006; Degu et al. 2011; Utsumi et al. 2011; Peterson et al. 2013). Another advantage of GHCND is that in 2011, it became the official archive of all US daily climate data, including the U.S. National Weather Service Cooperative Observer Network, which has been previously used in long-term precipitation studies (e.g., Karl and Knight 1998, Kunkel et al. 2003, Groisman et al. 2004, Groisman et al. 2012). With these updates, GHCND now features unparalleled spatial coverage and hundreds of long-term precipitation stations throughout the contiguous US. Additionally, the GHCND dataset is regularly subjected to a suite of 19 quality control tests, as well as format testing and record integrity checks (Menne et al.

2012). The main caveat with GHCND is that it is not adjusted for systematic biases resulting from instrument and/or reporting changes that may have occurred over the period of record for a particular station. A more systematic and extensive quality control effort, e.g., removal of statistical biases resulting from the above issues, is beyond the scope of this paper; thus, it is worth noting that the results may be affected by inconsistencies in data homogeneity. However, given the pros and cons of the dataset, we believe that inclusion of multiple overlapping temporal and spatial scales (described below), precedent in other peer-reviewed literature, and unparalleled spatiotemporal coverage of daily data permit the use of GHCND in determining long-term, observed changes in precipitation.

To further enhance the robustness of the following analyses of long-term precipitation changes, only those stations containing at least 90 years of data over 1895-2011 were considered for this study. Data flagged for potential quality concerns were not included in the analysis, and missing values were removed. A total of 1736 stations were retained for analysis, with the highest station densities in the central US, Texas, and California [Fig. 3a].

Our choice of spatial aggregates (climate divisions and regions) is motivated by NCDC practice. While the former match the standards used by the NCDC, the latter are defined by the authors and differ slightly from the NCDC definitions (not shown) (Karl and Koss 1984). Among the principal differences are: 1) redistribution of climate regions in the southeastern United States to isolate potential impacts of shifts in tropical storm activity; 2) partitioning of the "Northern Rockies and Plains" region into "Northern Rockies" and "Northern Plains", to isolate the Plains from the more topographically

diverse Northern Rockies; and 3) redistribution of states within the Midwest and Northeast regions to even out the areal coverage of the climate regions.

To reduce the sensitivity to temporal period, precipitation was compared across different temporal segments [Fig. 3b, vertical axis]. The precipitation data were first sorted into ten bins of different intensity, ranging from 0.25-2.5 mm (0.01-0.1 in) to 152+ mm (6+ in) [Fig. 3b, horizontal axis]. A time-series of 117 data points – one for each year from 1895 to 2011 – was compiled for each intensity bin for frequency, intensity, and total precipitation, with each datum representing a per-station average for each climate region or division. Segments of different temporal length (e.g., 36 values each for 1895-1930 and 1976-2011) were then compared using a two-sample t-test to determine the significance of any changes between the means of the distributions. The results were concatenated into "time period-intensity" plots [Fig. 3b].

Similar to the methodology of Groisman et al. (2012), use of irregularly-spaced widths of precipitation intensity bins reflects the nature of the original precipitation measurements (reported in inches, rather than mm). The first two bins are termed "light precipitation" (0.25-6.4 mm [0.01-0.25 in] per day); the third and fourth bins, "moderate precipitation" (6.4-25 mm [0.25-1 in] per day); the fifth and sixth bins, "heavy precipitation" (25-76 mm [1-3 in] per day); and the remaining four bins, "very heavy precipitation" (>76 mm [3 in] per day).

2.4 Results

2.4.1 Statistically significant changes in precipitation

2.4.1.1 PRECIPITATION FREQUENCY

The middle row of Figure 4 summarizes changes in the frequency of precipitation events in June, July, and August. The Midwest and the Upper Midwest clearly stand out, with significant increases ($p \leq 0.05$) over the second half of the 20th century during July and August [Figs. 4e-f]. In the Upper Midwest, almost all precipitation bins exhibit significant increases in precipitation frequency during these two months, especially during August, when nearly every temporal period experiences significant increases. In the Midwest during July, significant increases in precipitation frequency are evident for the heavier precipitation bins when evaluated over longer temporal periods, but almost no significant increases occurred in August. Overall, the magnitude and robustness of these increases far exceed those elsewhere in the CONUS domain: aside from a few significant increases in moderate precipitation frequency in the Northwest and West, no other region exhibits consistent, significant frequency increases outside of the lightest two bins [Figs. 4d-f].

Figure 5 summarizes changes in June, July, and August precipitation frequency across the 344 climate divisions, giving a finer spatial view of the changes in precipitation frequency. In the top row, total counts of significant increases ($p \leq 0.05$) over all precipitation intensity bins and comparison periods are indicated for each climate division, e.g., a total of seven significant increases, colored darker green, and are counted in Fig. 3b. Again, the Midwest and Upper Midwest regions stand out. Most of Iowa, southern Minnesota, Wisconsin, and Michigan experienced widespread significant

increases in precipitation frequency over the observational record in both July and August and to a lesser degree in June, while eastern Illinois and Indiana experienced many significant increases in precipitation frequency in July only. These results correlate reasonably well with the expected areas of a LULCC impact on precipitation frequency, as discussed in Section 2.

The lower two rows of Figure 5 depict the results of similar climate division analyses but for the lightest four bins (≤25 mm or 1 in) [middle row] and for the heaviest six bins (>25 mm) [bottom row]. Partitioning the analysis into these bins is useful for distinguishing between the CC (i.e., heavy precipitation) and LULCC (i.e., light and heavy precipitation) hypotheses. In general, the results from the lighter bins are nearly identical to that of all precipitation bins (top row). However, the heavier bins only show isolated significant increases in Iowa, Illinois, and Indiana in July and in Iowa and some climate divisions in the Upper Midwest in August. We note that differences in station density are likely not an issue: e.g., central Indiana and eastern Indiana have 11 and 2 stations, respectively, yet both show widespread significant increases in July.

2.4.1.2 PRECIPITATION EVENT INTENSITY

The bottom row of Figure 4 summarizes the changes in precipitation event intensity by climate region. The Midwest and Upper Midwest show significant increases in event intensity for the moderate and heavy precipitation bins during each summer month. However, several other regions also show significant increases. Changes in event intensity by climate division [Fig. 6] are more scattered and generally less robust, though climate divisions in the north-central United States – especially near Nebraska and Iowa – reflect more significant changes than elsewhere. Overall, since the pattern of

significant increases in precipitation intensity is not unique to the Midwestern US, an LULCC signal on precipitation intensity is not readily apparent in these figures.

2.4.1.3 TOTAL MONTHLY PRECIPITATION

Spatially, changes in total monthly precipitation [top row in Fig. 4] correlate well with changes in precipitation frequency [middle row in Fig. 4]. For a more quantitative comparison, Figure 7 depicts the mean monthly changes in frequency, intensity, and total precipitation for each climate region. From 1895-1933 to 1973-2011 (row 6 on the time period-intensity plots), the average June, July, and August precipitation in the Upper Midwest increased by 12.5, 13.4 and 20.7 mm, respectively, while July precipitation in the Midwest increased by 11.3 mm [Figure 7a]. These increases exceed those of the other regions in all three months (except the Southern Plains in June), usually by a factor of two or greater, mirroring the large increases in precipitation frequency [Fig. 7b].

At first glance, the results in Figure 7 point to daily frequency change as the principal determinant of total precipitation change. However, while changes in frequency dominate the magnitude of total monthly precipitation changes in the Midwestern United States, changes in intensity exert a notable secondary influence. For frequency change, the differences between June, July, and August are relatively small in both the Midwest and Upper Midwest [Fig. 7b]. However, intensity changes are much less negative in the Midwest during July and in the Upper Midwest during August [Fig. 7c], and total precipitation changes are likewise amplified in the Midwest and Upper Midwest during July and August, respectively, when compared to the other summer months [Fig. 7a]. Further evidence of this influence is seen in the Southern Plains, which experiences intensity increases in June but intensity decreases in July and August. Thus, anomalous

intensity changes do exert some influence on month-to-month patterns of total precipitation change.

2.4.2 Absolute and percent changes

Figure 8 depicts the absolute changes in mean monthly total precipitation, frequency, and intensity from pre- to full-irrigation. We analyze absolute changes because more distinct patterns may emerge using mean changes rather than only analyzing statistically significant changes, especially for precipitation intensity, which displays weak spatial patterns in Figure 6. Additionally, whereas the previous figures sum the significant changes over all ten temporal pairings, Figure 8 specifically illustrates changes that occurred from pre- to post-irrigation. In particular, we focus on precipitation changes between 1895-1933 and 1973-2011, i.e., row 6 on the temporal axis of the time period-intensity plots [Fig. 3b], for a few reasons: 1) It is one of the rows that compares a pre-irrigation to full-irrigation period; 2) it avoids the Dust Bowl drought of the mid-1930s, unlike rows 1-4; and 3) it utilizes more years than rows 8 and 9, thereby improving the robustness of any potential conclusions.

In summary, Figure 8 displays mixed correlations between absolute changes in precipitation frequency and total precipitation in the Midwestern US. In August, absolute frequency changes [Fig. 8f] match up well with the pattern of changes in total precipitation [Fig. 8c], though they are displaced a bit farther north than the total precipitation swath. Intensity increases [Fig. 8i] only slightly overlap with the southern edge of the total precipitation swath [Fig. 8c]. In this way, it seems that frequency changes dominate the changes in August total precipitation, while intensity changes exert a small secondary influence. However, in July, the larger frequency changes lie much

farther north than those of total precipitation; intensity changes, on the other hand, spatially coincide with the total precipitation changes. Maps of percent changes (not shown) are almost exactly the same east of the Rocky Mountains; the main difference is larger increases in frequency and total precipitation in the West Coast states, where summer season rainfall is sparse. Hence, frequency changes do not always dictate the patterns of total precipitation change during the summer months in the Midwestern US, and intensity changes may actually exert a notable influence.

2.4.3 Monthly ranks of absolute and percent changes

Since the patterns of absolute frequency change are inconsistent with those of total precipitation change, the rank of each variable is computed relative to the other months of the year in Figure 9 to provide an additional means of determining the seasonal intercorrelation and uniqueness of these frequency, intensity, and total precipitation changes. Climate divisions with a monthly value that ranks as one of the three highest of the year (out of 12) are illustrated in darker green; the three lowest values of the year are shaded in darker brown.

Ranking the absolute changes highlights a distinct relationship between the three variables: Intensity patterns, rather than those of frequency, coincide better with total precipitation patterns (in terms of both magnitude and location) in all three summer months [Fig. 9 – top and bottom rows]. On the other hand, it seems as though the large absolute changes in frequency [Figs. 8d-f] are not as unique in the Midwestern US during the summer months. The spatial distribution of top-three August frequency changes in the Upper Midwest is disjointed and, unlike those of intensity and total precipitation, does not extend into northern New England. In July, top-three frequency rankings only

overlap with those of total precipitation for six climate divisions in Iowa and Indiana; in contrast, top-three intensity rankings overlap those of total precipitation in at least 18 climate divisions throughout the Midwestern US. Additionally, the total precipitation rankings for percent change show an even stronger correlation with those of intensity and even weaker correlation with those of frequency (not shown). In summary, the rankings suggest that changes in both intensity and total precipitation in the Midwestern US are greatest during the summer, especially during July and August.

2.5 Discussion

We now interpret the above results in the context of the CC and LULCC hypotheses. The argument that CC is the main driver of the observed precipitation changes is supported by the significant increase in the frequency of heavy and very heavy precipitation events in the Midwestern US, with no other region showing changes of similar magnitude. The increases in precipitation intensity for moderate and heavy precipitation bins are also consistent with a CC signal. Combined with observed increases in growing season temperature over the Midwestern US over the last century (Villarini et al. 2013) and large increases in specific humidity since 1947 (Brown and DeGaetano 2013), one might conclude that CC has been a major factor in influencing precipitation changes over this region.

However, total monthly precipitation increased significantly throughout the Midwestern US during July and August, sometimes by more than 25 mm (1 in) [Figs. 8b,c], which is counter to changes expected from CC. The frequency of light and moderate precipitation events also significantly increased [Figs. 4 and 5 – middle rows],

which is not accounted for by changes outlined in the CC hypothesis. Temporally, the most robust increases in precipitation frequency and total precipitation are evident when comparing pre-1950 time periods with post-1975 time periods [Fig. 4 – top and middle rows]: The timing here is consistent with the rapid development of cropland and irrigation between 1950 and 1980 in the central US. Spatially, the location of the strongest increases in precipitation, i.e., downwind of a major irrigated region in the Great Plains, is consistent with the argument of a LULCC influence on precipitation patterns. Together, these results suggest that LULCC, or a driver with similar spatial and temporal characteristics, may have exerted a significant impact on precipitation changes over the Midwestern US. While CC may still have influenced precipitation changes in the Midwestern US, especially those of precipitation frequency, the patterns of spatiotemporal changes in total precipitation and precipitation intensity seem to favor a stronger influence from LULCC.

Furthermore, our analyses of absolute and percent changes in mean frequency, intensity, and total precipitation from pre- to full-irrigation shed light on how changes in frequency and intensity may have affected the observed changes in total precipitation. While the analysis of absolute (and percent) changes seems to indicate that frequency is the main determinant of total precipitation patterns [Fig. 8], a comparison of the monthly rankings for each variable [Fig. 9] reveals that changes in intensity and total precipitation are both greatest during July and August in the Midwestern US and are spatially coincident. Meanwhile, the large increases in frequency evident during July and August are not unique to the summer, as large increases in frequency also occur in other months of the year. In other words, because these large increases in frequency are not isolated to

the summer, they are not necessarily responsible for large increases in Midwestern precipitation during the summer; the anomalously high changes in precipitation intensity, on the other hand, may be more closely linked to changes in total precipitation than originally implied by Figure 8.

The unique correlation of summer intensity rankings with summer monthly precipitation rankings is consistent with the hypothesis that increased moisture from irrigation and/or cropland expansion, and thus increased moisture convergence, is responsible for a non-negligible portion of total precipitation change during July and August in the Midwestern US. This is even more apparent when comparing the intensity changes of the Midwest and Upper Midwest to those of other regions. Since summer frequency increases have generally exceeded those of total precipitation across the US [Fig. 7], decreases in intensity would appear to be favored; indeed, most climate regions across the US have exhibited decreases in intensity during the summer. One potential explanation for this intensity decrease is that with CC, increasing temperatures around the US would cause more atmospheric instability near the surface, increasing the frequency of precipitation events; however, intensity would decrease if water vapor does not increase sufficiently to compensate for the greater incidence of precipitation events. The changes of intensity in the Midwest during July and in the Upper Midwest during August are much less negative than the strongly negative mean established by the other climate regions in the summer and are thus anomalously high. Therefore, even though most of the intensity changes in the US have been negative and seemingly antithetical to increasing total precipitation, the anomalously high intensity changes in the Midwestern US are likely indicative of an increase in moisture and/or moisture convergence in this

region. This is consistent with observational evidence of increased moisture across the

Corn Belt during the second half of the 20th century (Mahmood et al. 2004; Brown and

DeGaetano 2013) and with the numerical model simulation of Huber et al. (2014) that

shows large increases in precipitation intensity (though not in precipitation frequency)

because of irrigation development.

Two other mechanisms that may factor into the observed increases in

precipitation intensity and frequency are non-classical mesoscale circulations (NCMCs)

and precipitation recycling. Similar in concept to the dynamics of classical mesoscale

circulations like land-sea breezes, NCMCs may form at the boundary between two land

types with different radiative and/or roughness characteristics, such as cropland and

forest (Segal et al. 1988; Carleton et al. 2001; Weaver 2004; Allard and Carleton 2010).

The horizontal gradients of temperature and moisture between irrigated and non-irrigated

regions may induce ascent and moisture convergence on the non-irrigated, warmer side

[see Fig. 2], which can potentially enhance convective rainfall under relatively weak

synoptic conditions (Carleton et al. 2008). Because enhanced precipitation from NCMCs

tends to occur within 100 km of the boundary (see Carleton et al. 2008), one might

anticipate enhanced uplift and rainfall over western Iowa, the non-irrigated region

immediately adjacent to the heavily irrigated areas in eastern Nebraska. Incidentally, a

regional simulation of irrigation-induced radiative changes during the summer by Qian et

al. (2013) depicts an area in western Iowa with higher LCL and ABL heights

immediately adjacent to a wide swath of (irrigation-induced) lower LCL and ABL

heights, which is indicative of greater sensible heat flux on the Iowa side and potentially

an irrigation-induced NCMC. Our analyses show that frequency, intensity, and total

precipitation have increased in western (and often, most of) Iowa in the figures with climate division analyses, especially during July for frequency and total precipitation [e.g., Fig. 8]. Though the mechanism posited here would need to be validated using a climate model, the coincident location of the observed precipitation increases adds evidence to the notion that an NCMC has influenced local precipitation patterns.

Another potential mechanism for expanding the swath of enhanced precipitation is precipitation recycling. Precipitation recycling occurs when soil moisture from rainfall in a particular area is evaporated into the ABL and cycled back into precipitation downwind of its source (Eltahir and Bras 1996; Zangvil et al. 2004; Dominguez et al. 2006). This mechanism may be a secondary transport of moisture downwind of Iowa, where total precipitation in July increased by at least 20% (~12.7 mm) from pre- to full-irrigation. Wind vectors at the 850 hPa level illustrate that the areas in August with the largest increases in total precipitation (Great Lakes and northern New England) are downwind of Iowa, so this mechanism has some physical plausibility. However, numerical modeling experiments are necessary to diagnose the degree to which precipitation recycling may have contributed to the observed increases in precipitation downwind of Iowa.

Other potential forcings, such as changes to the Great Plains low-level jet (GPLLJ), urban heat island effects, and large-scale atmospheric circulations may also be important in causing the observed changes in precipitation. For example, Weaver and Nigam (2008) indicate that the GPLLJ index and Great Plains precipitation index (which includes eastern Nebraska and Iowa) have a correlation of 0.71 during July, and the first principal component of GPLLJ variability explains up to 1.6 mm/day (~50 mm/month) of

July precipitation in Iowa. Additionally, while the indices of various circulation patterns (e.g., ENSO, NAO, AMO) are not strongly correlated with monthly precipitation during July and August in the Midwestern US (with the exception of August PDO) [Fig. 10], there is slightly better correlation between the Niño 3.4 index and July and August precipitation when the Niño 3.4 index leads by 1-3 months (e.g. June Niño 3.4 vs. July precipitation) (not shown). It is also possible that the large increases in Texas precipitation during June could be linked via precipitation recycling or the GPLLJ to the increases in the Midwestern US during July and August. The accumulation of aerosols in the US over the last century also has the potential to alter precipitation patterns, especially those of heavy precipitation (Tao et al. 2012). Connecting the observed increases in rainfall with all of these potential factors requires a more comprehensive investigation that is beyond the scope of this paper.

We point out a few caveats on these interpretations. First, observations of dynamic variables such as vertical wind are not readily available, precluding further attribution of these changes. Second, the location and strength of irrigation-induced impacts may vary depending on mesoscale or synoptic conditions, so the overall signature in precipitation may be weakened with averaging over long temporal or coarse spatial scales. Third, while LULCC is hypothesized as an important contributor to the observed changes in precipitation, quantification of its contribution to precipitation (and those of other factors) requires further research. We anticipate that future sensitivity studies using regional model simulations may reduce these uncertainties.

In conclusion, this study sheds new light on the possible causes of the observed increase in summer precipitation in the Midwestern US. The balance of evidence

suggests that while changes in frequency appear to exert a strong control on the magnitude of changes in total precipitation, the moderate to strong correlations of intensity changes with total precipitation changes (especially when ranked against other non-summer months) implies an increase in atmospheric moisture and/or moisture convergence. We speculate that the rapid development of irrigation and expansion of cropland in the central US may have contributed to this increase in atmospheric moisture and moisture convergence. In combination with previous studies, these analyses strengthen the argument that historical, large-scale LULCC was a key factor in enhancing summer precipitation in the Midwestern US over the late 20th century. Understanding the drivers of such precipitation changes is essential for sound management and adaptation strategies in a changing climate.

3.   MODELING ANALYSIS

3.1 Previous studies

In recent years, many modeling studies have been conducted regarding the effects of irrigation on hydroclimate. To start, initial models were one-dimensional, column models that only simulated the effects of irrigation over one particular grid cell. As an example, DeRidder and Gallée (1998) used one of these models to simulate the effect of irrigation on precipitation over southern Israel, and they determined that convective activity was enhanced by irrigation.

Many other modeling studies since then have been two-dimensional, i.e., simulations were performed over horizontal areas. Over the United States, Segal et al. (1998) conducted a nationwide modeling simulation that concluded irrigation only influences the intensity of rainfall and not the location of the precipitation. Adegoke et al. (2003) simulated weather over Nebraska for 15 days and determined that there was a 36% increase in the surface latent heat flux and a 2.6 K increase in dewpoint temperature as a result of irrigation. Diffenbaugh (2009) also conducted a nationwide simulation of the United States and found increases in precipitation from both irrigation and other land use change in the Northern Plains of the US. DeAngelis et al. (2010) showed observationally that the precipitation increases in the Midwestern US in July correlated with the development of irrigation; a water vapor tracking model based on NARR reanalysis products showed strong sensitivity of downwind precipitation to upwind ET from the High Plains. Ozdogan et al. (2010) demonstrated strong increases in ET in Nebraska and in other irrigated areas when irrigation was included in their land surface

model. Harding and Snyder (2010a,b) ran nine years of growing-season simulations with the WRF model and determined that irrigation results in enhanced rainfall over and immediately downwind of Nebraska. Guimbertau et al. (2011) showed precipitation increases over and to the northwest of Nebraska but precipitation decreases southeast of Nebraska due to irrigation. Lo and Famiglietti (2010) discovered a remote enhancement of precipitation in the US Southwest due to irrigation in California. Qian et al. (2013) simulated the effects of irrigation in the Great Plains and determined that shallow cumulus convection is more likely in the irrigated areas since the LCL drops more than the height of the planetary boundary layer. Huber et al. (2014) showed in a WRF simulation that precipitation intensity increases in select areas downwind of the irrigated areas of the Great Plains when irrigation saturates soil moisture. The main conclusion to be derived from the above modeling studies is that precipitation, and relevant surface and atmospheric variables, are indeed affected by irrigation in the United States, and further investigation into irrigation effects is warranted.

Elsewhere around the world, other modeling studies have come to similar conclusions. Douglas et al. (2009) found that irrigation in India caused latent heat flux to increase and sensible heat flux to decrease, and precipitation exhibited both increases and decreases as a result.

Most of the above modeling studies have been on monthly, seasonal, or annual time scales. Since irrigation impacts on precipitation may vary widely on shorter timescales with changing synoptic and mesoscale conditions, a modeling analysis of the daily and sub-daily impacts of irrigation is warranted. As in the observational study, the

modeling analyses attempt to determine these daily and sub-daily changes in precipitation from irrigation in the Great Plains.

3.2 Experimental setup

The model being utilized in this study is the Weather Research and Forecasting (WRF) – Advanced Research WRF regional climate model, version 3.3.1. The WRF model is fully compressible, Eulerian, and nonhydrostatic with a run-time hydrostatic option (NCAR 2011). The model uses a terrain-following, hydrostatic-pressure vertical coordinate with the top of the model being a constant pressure surface. WRF is a versatile model: It has been used to simulate weather and climate on time scales of hours to decades, spatial scales of meters to hundreds of kilometers, and has a multitude of available physics options.

The impacts of irrigation on precipitation are analyzed during June of 2002. The original intent was to simulate June, July, and August for the proposed model experiments, but due to time limitations, the simulation was stopped after a 15-day simulation beginning on June 1. The year 2002 was chosen for a few reasons. First, the Great Plains region was under drought conditions during the summer of that year, with above-average temperatures and low precipitation (low Palmer Drought Severity Index). This would increase the crop water demand during these months and lead to more irrigation water being used. Second, much more precipitation fell in the Upper Midwest than in Nebraska during the summer of 2002; the difference in precipitation between the two regions was actually the largest such difference in the 21st century (NCDC 2013). Third, the above precipitation difference matches what one might expect from an

irrigation effect on precipitation, i.e., that is enhanced rainfall downwind of the irrigated areas, and reduced rainfall over the irrigated areas. During the summer of 2002, an El Niño was present, so this bears consideration when interpreting the final results. It is also important to note that because of the short simulation, spin-up time was not accounted for or removed from the analysis. This may cause some artifacts in the model results for the first several days as the model reaches more of a realistic equilibrium.

The model is run at 10 km spatial resolution, which is fine enough to capture the effects of larger convective systems yet coarse enough that it did not use too much of the limited computational resources. The experiment uses 28 vertical levels and a model top of 100 hPa, both standard configurations for WRF. The model time step is set at 60 seconds, following the WRF guideline of six times the spatial resolution. The Kain-Fritsch cumulus parameterization is utilized in the model run, and the microphysics option used is the Morrison 2-moment scheme. The radiative longwave scheme used is the RRTM (Rapid Radiative Transfer Model), and the radiative shortwave scheme used is the Dudhia scheme. All of the above are standard recommendations for climate simulations using the WRF model. The domain covers the northern Great Plains from Kansas north to the Dakotas, and from central Colorado to Indiana [Figure 11]. This domain is large enough to encompass most of the irrigation impacts, even those that are non-local, and is small enough to have run in a reasonable amount of time given the limited computational resources.

The land surface model being used in conjunction with WRF is the Noah land surface model (LSM). Noah is the standard LSM used with the WRF model. There are four soil layers in the Noah LSM, which are 10, 30, 60, and 100 cm thick, respectively.

Thus, all soil layers in Noah combined reach a depth of two meters below the ground; any additional water that filters through the bottom of the deepest soil layer is returned to the surface as runoff.

The irrigation scheme implemented in WRF focuses exclusively on a subdomain of the model that is placed roughly over Nebraska. If any of the four soil layers at a particular grid cell within the Nebraska subdomain are at less than half of field capacity (i.e., the level of soil moisture after excess water has drained away), then all four soil layers are filled up to field capacity. Raising the soil moisture within a grid cell once it reaches a certain soil moisture threshold has some precedent in previous works (Ozdogan et al. 2010; Qian et al. 2013), though this scheme is much simpler. Actual irrigation practice would involve watering the surface, either through sprinkler or flood irrigation. It would also be more prudent to use root zone soil moisture as the variable to test for a soil moisture threshold. However, time limitations prevented the usage of more complicated irrigation schemes. The simple one used here is deemed appropriate for an exploratory study on the effects of irrigation in Nebraska on precipitation.

Land use categories were those used by the United States Geological Survey. There are 24 categories in this dataset, which is the default configuration for the Noah LSM. Much of the Great Plains and the Midwestern US are cropland or in a cropland mosaic. While the irrigated land in Nebraska would normally be grassland or cropland, this model run was set to irrigate any type of land as long as it was in the Nebraska subdomain. This is due to the simplicity of the irrigation scheme.

The WRF model was initialized with the North American Regional Reanalysis product, which has 32-km horizontal and 3-hour temporal resolution. Simulations were

initialized on June 1 at 00Z and ended on June 15 at 21Z, updating with new lateral NARR boundary conditions every 3 hours. A buffer of five grid cells transitioned from the NARR background to the experimental domain. No spectral or analysis nudging was performed, and nested domains were not used so that computation resources could be conserved. Additionally, leaf area index was initialized at summer values (only summer and winter values are available for standard Noah configurations), and soil moisture was initialized at values specified by NARR on June 1 at 00Z. Note that the irrigation scheme takes effect by the second time step. Because of the short duration of the model runs, any grid cells that were irrigated in the model run usually retained anomalously high soil moisture values during the entire run and did not necessitate further irrigation during the 15-day period.

Validation of the precipitation model run was performed by comparing the precipitation output from the WRF model to that of cli-MATE, an online precipitation repository from the Midwestern Regional Climate Center [Figure 12]. Values of total precipitation were obtained from the cli-MATE gridded precipitation observations. In comparing the WRF model precipitation to the cli-MATE precipitation, it is apparent that while there are regional variations in the spatial distribution of precipitation, it seems that the overall pattern of precipitation is preserved. The major precipitation maxima near the intersection of Iowa-Wisconsin-Illinois and in northern Minnesota are reproduced fairly well by the WRF model, and the local maximum near the Kansas-Oklahoma border in cli-MATE is reproduced in WRF but shifted to the northeast. Meanwhile, the dry patch in Nebraska and South Dakota is also captured in the WRF model. Some of the more noticeable errors in the WRF representation of precipitation are anomalous dry patches in

southern Minnesota and northern North Dakota and anomalous wet patches in Indiana and around the southern and eastern edges of the model domain. The actual values of WRF precipitation also seem to be roughly in line (plus or minus one inch) with what is shown in the cli-MATE precipitation. In general, WRF precipitation seems to be close enough to cli-MATE precipitation that sensitivity studies to an irrigation forcing in the model can be conducted with reasonable correspondence to reality.

The WRF model was run two separate times: once with the irrigation scheme being implemented and once without the irrigation scheme. All absolute and percent changes in the upcoming sections are the irrigation run minus the non-irrigation run, unless otherwise noted. To better isolate changes in precipitation between different regions of the central US, the domain is split into nine regions [Figure 11]: Nebraska (NE), Kansas (KS), Colorado Rockies (CR), east and west Northern Plains (NPE and NPW), east and west Upper Midwest (UME and UMW), and east and west Midwest (MWE and MWW). The NE region is the only one that was subject to irrigation; all other regions are considered to be downwind and are non-irrigated. In particular, we focus on the subregions of the Midwest and Upper Midwest, since these are the regions in which the observational analysis suggests that there may be precipitation increases due to irrigation in the Great Plains.

3.3 Results

The spatial distribution of total precipitation for the simulated 15-day period is very similar between the irrigated and non-irrigated model runs [Figure 13]. As is suggested in other studies of irrigation impacts on precipitation (e.g., Segal et al. 1998;

Huber et al. 2014), irrigation does not seem to create any new areas of precipitation. Rather, if there is an irrigation effect on precipitation, it seems to be in intensifying the precipitation already falling at a particular location. Some areas where precipitation seems to intensify are at the border between Illinois and Wisconsin, the border between Illinois and Indiana, and the border between Kansas and Missouri. However, simple comparison of these two plots does not seem to indicate any widespread changes in precipitation. Initially, this seems to contradict the main findings of the observational study, where widespread increases in total precipitation are evident across the northeastern quadrant of the US during the summer. Furthermore, there is also a comparable number of areas where precipitation seems to decrease across the domain. Thus, initially the effect of irrigation on precipitation in the Midwestern US seems to be muted.

However, the absolute difference map between the two model runs depicts a slightly different picture, with seemingly more areas with precipitation increases (warmer colors) than with precipitation decreases (cooler colors) [Figure 14]. In particular, it seems that the eastern part of the model domain, i.e. the Midwest and Upper Midwest subregions, exhibit more precipitation increases than decreases, which corresponds with the increases in total precipitation found in the observational study. Masking all differences less than 12.5 mm depicts a much more scattered precipitation change distribution, yet still there seem to be more increases than decreases east of Nebraska [Figure 14]. Masking all differences less than 25 mm (1 inch) shows that even though some isolated pockets of both increases and decreases remain, there are still larger areas of precipitation increases in Illinois and Indiana, along with one area of major

precipitation decrease [not shown]. Thus, while precipitation increases are not a strong majority in the modeled domain, there are still more (and stronger) increases in precipitation in general than there are precipitation decreases.

The percent difference between irrigated and non-irrigated model runs is shown in Figure 15. The pattern depicted here is very similar to that of Figure 14, but the main variation is in the intensity of the changes. It seems that in general, the percent increases in precipitation are of a higher magnitude than those of the precipitation decreases. In particular, southern Minnesota, northern Michigan, eastern Illinois, the northern part of South Dakota, western Nebraska, and eastern Colorado all have much larger magnitudes of percent increases in precipitation than is indicated by the absolute increases. Meanwhile, central Lake Michigan, southern South Dakota, and much of Nebraska all exhibit stronger magnitudes of percent decrease in precipitation than is indicated by the absolute changes. The large number of "intensified" magnitudes of percent changes versus absolute changes is due mainly to the lower overall precipitation recorded in the aforementioned areas. In general, most of the areas with the elevated magnitudes recorded less than 25 mm (1 inch) of precipitation during the 15 day period, and many areas recorded less than 12.5 mm (0.5 inch) of precipitation. For reference, more than half of the eastern part of the domain (east of Nebraska) received at least 50 mm of precipitation during the 15-day period.

Masking percent changes that have a magnitude of less than 25% defines the precipitation patterns very clearly [Figure 15]. While large percent increases in precipitation seem to be occurring downwind of Nebraska, the major areas of percent decreases in precipitation occur over or slightly to the north of Nebraska. Masking the

percent changes with a magnitude of less than 75% depicts an even starker pattern: While there are a few larger areas and many isolated areas of greater than 75% increase in precipitation, there are virtually no areas with greater than 75% decrease in precipitation [not shown]. In other words, the largest percentage changes in total precipitation are increases rather than decreases.

Changes in precipitation intensity are now examined across the whole domain and within each subregion. Total precipitation over the 15 simulated days for the irrigation and non-irrigation runs and the absolute and percent differences between them are listed in Table 1. Averaged across the whole domain for the whole 15-day period, total precipitation increases by 0.13 mm, or 0.26%. Thus, irrigation leads to a net increase in precipitation over the whole domain during the 15-day period, though the increase is very small. Regionally, there exists a west-east precipitation gradient, where more rain falls in the humid east and less rain falls in the semi-arid west; this is expected climatologically. As for the absolute changes, the MWE and UMW subregions have the top two absolute increases in precipitation due to irrigation, and the NE subregion exhibits the greatest absolute decrease. This is consistent with what would be expected from the observational analyses, though the UME subregion (which exhibited long-term significant increases in precipitation in the observational analysis) exhibits a decrease in precipitation in this modeling experiment. The magnitude of the NE decrease in precipitation is almost equal to the combined magnitude of the MWE and UMW increases; in other words, its absolute changes are highly anomalous compared to the other subregions. Comparing percent changes in precipitation due to irrigation depicts an even starker contrast between NE and the other subregions: While MWE and UMW exhibits increases in precipitation of

2.46% and 4.07%, respectively, the NE region exhibits a decrease of 19.42%. Overall, only the two Midwest subregions and the UMW subregion experience increases in precipitation over the 15 days; the other six subregions experience precipitation decreases due to irrigation.

The timelines for daily precipitation intensity for the irrigated and non-irrigated model runs are shown for all subregions (except for CR) in Figure 16. When comparing these timelines of daily precipitation intensity, it is apparent that while a few larger changes exist on a daily basis, the majority of irrigation-induced changes in daily precipitation seem to be relatively minor [Figure 16]. Only for a select few events is there a sizeable gap between the two model runs. Some larger increases occurred in the MWE subregion on June 12, UME on June 14, UMW on June 3 and 13, and NPE on June 8. Some larger decreases occurred in the NPE subregion on June 2, NPW on June 9, KS on June 4, and NE on June 2-3 and 10-12. The absolute decreases in NE on June 10-12 seem to be the largest of any daily change in the combined subregions. Following the pattern described above, it seems that large increases are more likely to occur in the eastern part of the domain, while large decreases are more likely in the western part of the domain, especially over Nebraska. Additionally, examination of these timelines imply that precipitation frequency is unaffected by irrigation; only the intensity of individual precipitation events changes on any given day.

These relatively minor changes in precipitation intensity are further elucidated when comparing absolute differences between the irrigated and non-irrigated runs in each subregion [Figure 17]. Typical daily changes in precipitation between the two model runs are less than 0.25 mm (0.01 inch) per day. Absolute changes in precipitation are

seldom greater than 0.5 mm (0.02 inch) per day in the western part of the domain, and precipitation changes greater than 1 mm (0.04 inch) occur only five times among all of the subregions combined. The MWE region contains the most drastic changes in precipitation: three increases of at least 0.5 mm per day (two of which are greater than 1 mm per day) and one decrease of at least 0.5 mm per day. The CR region contains the least drastic changes in daily precipitation: Its largest change is 0.38 mm per day [not shown]. This generally follows the climatological west-east precipitation gradient where less precipitation falls in the semi-arid west and more in the humid east.

However, Figure 18 illustrates that percent decreases in daily precipitation paint a very different picture than that indicated by the absolute differences. While the majority of precipitation changes have a magnitude of less than 10%, there are several daily events that exceed a 25% change in almost every subregion. There are even nine instances of greater than 50% precipitation change within the subregions. One caveat with the larger percent changes is that oftentimes the large percent change is caused by a small absolute increase from very small initial precipitation values, e.g., a change from 0.01 to 0.02 mm would yield a 100% change. While this situation occurs for roughly half of the anomalously high percent changes, there also exist many instances of greater percent changes that correspond to anomalously high absolute changes. This situation is less likely to occur in the eastern part of the domain, where precipitation is generally higher.

Robust changes in hourly precipitation intensity are much more difficult to parse out. The main subregions where there seem to be consistent precipitation changes in one direction more than another are the MWE region (increases on June 10-14) and the NE region (decreases on June 11-13) [not shown]. Otherwise, precipitation changes flip-flop

between positive and negative too frequently to determine any real robust trends. Thus, the main focus of the upcoming analyses will be on 6-hourly and daily precipitation values.

To delve more deeply into the mechanisms that may be causing an irrigation effect on precipitation, the focus is narrowed to individual precipitation events. Because of the brevity of the time period that is simulated, there are not many events that can be discussed in detail where irrigation seems to have had a significant effect. One precipitation event stands out – the precipitation on June 12 in the MWE subregion – where irrigation may have had a robust effect on the precipitation intensity and totals. Thus, we focus on this event in the upcoming analysis. In the upcoming analysis, the times of analysis are from June 11 at 0Z until June 14 at 0Z unless otherwise noted.

3.3.1 Precipitation comparison

First, it is instructive to compare precipitation characteristics and changes over the domain for the event to be studied. For the period June 11 at 0Z to June 14 at 0Z, the average precipitation change over the whole domain is -0.08 mm, or -0.44%. However, on June 12 specifically, precipitation over the whole domain increased by 0.09 mm, which is close to the averaged increase over the domain for the entire 15-day period. The percent increase of 1.48% for June 12 dwarfs that of the 15-day period (0.26%). Thus, even for the whole domain, June 12 represents a day with anomalously strong, irrigation-induced rain. In the subregion of note – MWE – average precipitation increased by nearly 2 mm (0.08 in) [Figure 17], or ~11% [Figure 18] on June 12. This absolute increase is the largest among all precipitation days in all subregions, thus it represents one of the largest irrigation-induced precipitation increases in the 15-day record.

Precipitation is compared for both irrigated and non-irrigated model runs for 6-hour periods on June 12 in Figure 19. Each of the panels represents the precipitation that began falling at the specified time for six hours; e.g., the precipitation panels for June 12 at 0Z represent precipitation that fell from 0Z to 6Z on June 12. The changes that stick out most are increases in precipitation intensity in one of the stronger storms in the MWE region. Specifically, the storm that moves across Illinois and Indiana shows stronger precipitation intensities in the irrigated run than in the non-irrigated run, especially in the heavier intensity categories. The largest increases are evident in the 0Z and 6Z panels. Conversely, the storm that traverses Kansas and Missouri shows stronger intensities in the *non*-irrigated run, especially at 6Z. Overall at first glance, there seems to be indication of heavy precipitation enhancement in the MWE region on June 12.

Absolute and percent changes in the same 6-hourly precipitation are shown in Figure 20. For absolute changes, it is evident that precipitation at 0Z and 6Z exhibits the larger and more distinct increases of all four panels. At 0Z, there is a widespread swath of greater than 5 mm (0.2 in) increase in precipitation, with many areas exhibiting increases of greater than 12.5 mm (0.5 in). At 6Z, the overall increases seem to be smaller than for 0Z, but there are isolated, very large increases in precipitation of 12.5 mm or more. At 12Z and 18Z, there are also areas of strong precipitation increase, but they are more balanced by decreases in precipitation than the first two panels.

For percent changes, the majority of the aforementioned strong absolute increases at 0Z generally correspond to increases of 10-50%, though some isolated areas exhibit increases of >100% [Figure 20]. At 6Z, more of the larger absolute increases represent larger percent increases of greater than 100%. At 12Z and 18Z, similar patterns are also

present.   Overall, on June 12, there are large absolute and percent increases in precipitation in the MWE region, especially earlier in the model day, which warrant further investigation.   The mechanisms that may have led to these increases are now investigated by examining different surface and atmospheric variables in the following section.

3.3.2 Surface Variables

First, soil moisture is compared between the irrigated and non-irrigated runs, since this is the initial effect of irrigation on the land surface [Figure 21]. As expected, the irrigation scheme over Nebraska results in much higher soil moisture values for the irrigated model run, especially in the western part of Nebraska. Physically, the higher soil moisture differences in the western part of Nebraska are feasible; since western Nebraska is semi-arid (as compared to the humid eastern part), it has a greater atmospheric demand for water vapor, which would normally lower the ambient soil moisture.   Irrigation to field capacity across Nebraska would thus result in a larger difference in western Nebraska. Indeed, at most grid cells in western Nebraska, the soil moisture in the irrigated run is twice the value of the non-irrigated run (not shown). Elsewhere across the model domain, soil moisture does not experience increases at the same scale as in Nebraska. Isolated increases occur in several places due to prolonged rainfall that may be influenced by irrigation.

The large increase in soil moisture results in a similarly large increase in latent heat flux, and thus, ET [Figure 22]. Since ET (represented by upward moisture flux) is the hydrological component of the surface change and latent heat flux is the radiative component, it is intuitive that the spatial patterns for both of these variables are nearly

identical. It is evident, especially during the afternoon and early evening hours, that both latent heat flux and upward moisture flux are much higher during the irrigation run over Nebraska. Interestingly, though, comparable increases in both variables occur downwind of the irrigated regions in the Upper Midwest and Midwest subregions at 18Z on the given days [Figure 22]. It is possible that these increases downwind of Nebraska are due to irrigation-induced rainfall in these areas, though the extra rain that usually falls is relatively light (< 5 mm in 6 hours). Regardless, the large increase in both latent heat flux and upward moisture flux means that there is an influx of moisture to the atmosphere, both over Nebraska and downwind where rain has recently fallen.

This extra atmospheric moisture can be measured in either absolute or relative terms. When measuring by absolute terms, e.g., by changes in dewpoint temperature, Nebraska again is at the epicenter of the increase in surface moisture, with increases in dewpoint temperature of greater than 5 K in the western part [Figure 22]. Dewpoint temperature also increases downwind at similar scales, again usually following rain, but is often accompanied by complementary decreases. This implies that the difference in dewpoint temperature is not necessarily due to irrigation-induced moisture transport but perhaps due instead to a slight change in storm track. The two lobes of complementary increases and decreases would cancel if averaged over a large enough subdomain. Regardless, it seems that dewpoint temperature does not exhibit a large increase in the MWE region until June 13, which would make sense if it had rained the previous day and the ground contained a greater amount of soil moisture. However, surface dewpoint temperature differences do not seem to impact precipitation in the MWE subregion on the day of the precipitation (June 12).

Relative humidity also exhibits increases of greater than 15 percentage points over western Nebraska and eastern Colorado [Figure 22], mimicking the locations of the major increases in dewpoint temperature. Increases of this magnitude downwind are infrequent during the 3-day period. One reason for this behavior could be that a given absolute increase in dewpoint temperature in the semi-arid west would likely raise relative humidity by more percentage points than if it were in the humid east, since the east is likely already closer to saturation and thus has fewer percentage points to give. On the other hand, decreases of a similar magnitude do occur downwind, especially in southern Nebraska and southern South Dakota. Over the MWE region, no major increases in relative humidity occur until June 14 [not shown]. Thus, it seems that changes in surface relative humidity in the MWE region have little bearing on the increase in rainfall in the region on June 12.

It is also instrumental to compare changes in temperature, for which we use the potential temperature (which is conserved for dry adiabatic processes) [Figure 23, top row]. Strong decreases in potential temperature at the surface (often exceeding 2 K) are evident over Nebraska for the whole 3-day period, while equally strong increases in temperature occur downwind in the Midwest and Upper Midwest regions. By June 12 at 18Z, strong temperature increases are evident across the MWE subregion, potentially destabilizing the lower atmosphere and thus contributing to an increase in convection over the area [Figure 23].

With the aforementioned changes in temperature, surface pressure is likely to change as well. Consistent with expected physical processes, there is an area of higher pressure in the vicinity of the temperature decreases over Nebraska [Figure 23, bottom

row]. Colder air is more stable and denser than warmer air, so it would be anticipated that this would result in sinking air and thus higher pressure. Conversely, over the MWE region by 12Z on June 12, the increases in temperature form an area of lower pressure, which lasts until 0Z on the next day. The warmer surface temperatures may have caused atmospheric instability and thus rising air, which lowers the surface pressure and may have enhanced precipitation on June 12. Of note is that the other major area of lower pressure in southwestern Minnesota is also associated with increased precipitation at 18Z on June 12.

3.3.3 Environment Aloft and Downwind

The atmospheric environment above the surface is also affected by the introduction of irrigation into the WRF model. The changes in surface variables due to irrigation cause reactions in the troposphere that could have important impacts on precipitation.

As mentioned in the observational analysis, some atmospheric indices that could be affected by irrigation are lifting condensation level (LCL), level of free convection (LFC), convective available potential energy (CAPE) and convective inhibition (CIN). A rising air parcel encounters the LCL when it reaches saturation, and it rises further to the LFC if it can overcome CIN. CAPE is then available to the rising parcel if it passes the LFC. Greater values of CIN could prevent convection from occurring or greatly reduce its severity, whereas greater values of CAPE could intensify convection and increase rainfall totals. If the LCL drops more than the LFC, then CIN would likely increase and hinder convection, and convection would be more likely if the LFC drops more than the LCL. It is expected that CIN and CAPE would be enhanced over the irrigated areas,

while only CAPE would be enhanced over the downwind areas; the lack of temperature decrease downwind would allow CIN to remain the same.

The LCL generally experiences large decreases in western Nebraska and isolated large changes elsewhere [Figure 24]. In the northern part of the MWE region, major LCL increases tend to occur, though they are still rather isolated. By June 13, major LCL increases are present in eastern Nebraska and western Iowa, which are likely indicative of warming at the surface [Figure 23]. Meanwhile, neither LFC nor the difference between LFC and LCL (LFC-LCL) exhibits a definitive direction of change anywhere in the domain for the three chosen days [Figure 24]. Because of the heterogeneity in these individual values, it is hard to determine if LFC and LFC-LCL have any impact on the processes governing irrigation-precipitation interactions.

Changes in CIN and CAPE are depicted in Figure 25. Areas of major CIN change are scattered, though it seems that decreases in CIN are more likely downwind of Nebraska than are increases. Adding to the increased potential for convection in the MWE region is a broad area of large increases in CAPE on June 12 [Figure 25]. Large changes in CAPE seem to be confined mainly to the eastern part of the domain.

Not surprisingly, changes in surface moisture likely fuel the increases in CAPE and decreases in CIN. As evidenced by the water vapor mixing ratio, the atmosphere near the surface of Nebraska is moister because of irrigation, while the rises in temperature immediately east of Nebraska correspond to decreases in water vapor mixing ratio [Figure 26]. The water vapor at 850 mb, however, exhibits both increases and decreases over Nebraska during the three given days [Figure 26]. Downwind the patterns

are also heterogeneous. Thus, while surface moisture seems to uniformly increase over Nebraska, higher levels of the atmosphere exhibit patterns that vary daily.

Figure 27 displays the inter-level variability of water vapor mixing ratio differences in a time series of cross-sections at latitude 40.5 degrees North and from longitude 107 degrees West to 85 degrees West (line drawn in Figure 26, bottom left panel). While increases in the boundary layer moisture are apparent in Nebraska in most of the panels, changes at level 9 (~800 mb) and higher are either constant or decreasing over Nebraska. This time series of cross-sectional plots also shows the apparent advection of positive, lower-level anomalies in water vapor toward the east. These positive anomalies end up over the MWE subregion by June 12 at 12Z, at the end of the peak increase in precipitation. By 12 hours later, the anomalies over MWE are negative, perhaps due to most of the moisture being rained out in the irrigation run. Thus, it is possible that the positive moisture anomaly that ended up over the MWE region and contributed to excess precipitation on June 12 may have originated from Nebraska a day or two earlier.

Finally, the wind patterns likely play an important role in both the transport of water vapor from Nebraska to regions with irrigation-induced precipitation and also in convergence in the same areas. We diagnose in Figure 28 the winds at 850 mb, since this is a standard height at which moisture transport is determined. The winds at 850 mb are generally southwesterly over the MWE subregion; thus, moisture transport would seem to come from south of the Nebraska region. Indeed, this pattern is typical of that seen from the Great Plains low-level jet (GPLLJ), which derives its moisture from the Gulf of Mexico. As the hours progress from June 11 into June 12, the winds over the MWE

subregion shift eastward, especially after 18Z on June 11, and the moisture source seems to emanate from farther and farther south of Nebraska. Thus, moisture transport from Nebraska may not be a direct cause of the increases in precipitation in the MWE subregion.

To better determine the mechanisms behind the increase in precipitation in the MWE subregion, the differences in water vapor mixing ratio and wind vectors at 850 mb, along with the absolute and percent differences in precipitation, are plotted together in Figure 29. A striking pattern emerges: The areas of strongest wind differences at 850 mb largely coincide with the precipitation differences, especially the percent differences. The areas just downwind of the strongest wind vector differences are in areas of increased wind convergence at 850 mb, which can lead to more frequent storms and stronger convection. Even though moisture transport does not generally seem to originate from Nebraska during this period, the wind convergence seems to be effective in building water vapor anomalies in the area and causing storms to be more intense. Although there is no water vapor anomaly in the MWE region on June 11, there is a larger positive anomaly in the region on June 12, when much of the increased precipitation occurs. Since this new area of enhanced water vapor is ahead of the more prominent arc of water vapor increases progressing southeast from the Upper Midwest, it can be estimated that this anomaly originates more from the wind convergence in the MWE subregion than from distant moisture transport.

Finally, to get a better idea of the progression of the wind anomalies over time, a vertical cross-section of the differences in horizontal wind vectors is illustrated in Figure 30. In this figure, the large vertical extent of these wind anomalies (at almost every level

of the troposphere) is evident on June 11. Here, the eastward movement of the wind anomalies is also apparent in the panels for June 11. On June 12, the anomalies in the lower levels of the troposphere remain on the eastern fringe of the MWE subregion, likely contributing to the increased precipitation in the area on that day. So even though moisture transport from Nebraska may not have played a major role in the enhancement of precipitation in the MWE subregion, the wind anomalies may have originated from the irrigated region of Nebraska.

3.4 Discussion

In summary, this modeling experiment performed over 15 days in June of 2002 simulated increases in precipitation in both Midwest subregions and the UMW subregion due to irrigation in Nebraska. In the NE subregion, on the other hand, strong precipitation decreases (~20% decrease, on average) occurred over the 15 day period. Some absolute increases eclipsed 12.5 mm (0.5 in) in the MWE region, and many percent increases eclipsed 50%.

When the focus is shifted to one particular event – June 12 in the MWE region – it becomes evident that strong increases in surface moisture and decrease in temperature occur over western Nebraska. This forms an area of high pressure over Nebraska and a subsequent moisture gradient between Nebraska and other states. While moisture is seemingly transported in different directions, wind anomalies in all levels of the atmosphere are advected downwind, i.e., toward the east, where they may create wind and moisture convergence in the lower atmosphere and enhance already existing rainfall. Areas of higher temperature elsewhere (e.g., southern Minnesota at 18Z on June 12) lead

to higher values of upward moisture flux and lower pressure, which also subsequently lead to enhanced precipitation (albeit, lighter than that of the MWE subregion). While these mechanisms seem to be physically sound, more work is needed to verify them with longer simulations and more realistic irrigation schemes.

3.5 Future Work

To create a comprehensive picture of the effects that irrigation exerts on precipitation, more detailed simulations need to be performed. The following subsections detail additional model experiments to run, variables to analyze, and adjustments to be made in future work.

3.5.1 Additional model experiments

The first and most important limitation on the above model experiments was a shortage of time to complete more and longer simulations. Given more time, several aspects of the simulations would have been changed. To start, at least three ensemble runs of the irrigation sensitivity studies would have been performed, where the start date and initial conditions of the model vary by a day or two. Performing ensemble runs can better isolate any potential signal of irrigation on precipitation from the noise of the precipitation patterns themselves. The danger in relying on only one model run is that it is difficult to determine if the patterns seen are manifestations of, e.g., the irrigation effect on precipitation, or from a particular setup of initial conditions that led to coincident effects. In the future, running at least three simulations will allow for more robust characterization of the causes of precipitation change seen in the above analyses.

Secondly, future work will also need to focus on running the simulations for longer periods of time. The above analyses were limited to 15 days because of constraints on timing, but simulations of at least one growing season (roughly May-September) would be necessary to determine the monthly variability of the irrigation effect on precipitation, especially during the most heavily irrigated months of July and August. Ensemble runs of one growing season would provide a secondary measure of significance to the monthly variability that would be present in the model runs. If time allows, simulations of multiple growing seasons would yield even more robust changes in precipitation that would be due to irrigation in the Great Plains since they would not be limited to the meteorological conditions of one particular year.

Conducting a parameter sensitivity analysis would also be helpful for determining the robustness of the changes outlined in the above experiments. For example, while the above experiments were run at 10-km horizontal resolution with a Kain-Fritsch cumulus parameterization, it would be instructive to choose a finer spatial resolution that would not require a convective parameterization or to remove the cumulus parameterization from the 10-km resolution domain and compare the irrigation effects on precipitation. Removing the cumulus parameterization could result in significantly different precipitation patterns, with or without irrigation, since convection may be more realistically simulated, so this would be a critical future experiment. Along a similar line, while this study used a single unnested domain, using one or two nested domains in these modeling experiments would facilitate determination of local vs. short-distance vs. remote effects of irrigation on precipitation. Conducting these experiments with different radiation and microphysics options, different vertical resolutions (e.g., fewer or more

model levels, or more model levels concentrated in the PBL) or model tops (e.g., 200 vs 50 hPa), and different boundary conditions with and without spectral nudging could be helpful in determining the sensitivity of the irrigation effect on precipitation to these parameters and whether the changes induced by these different parameters would outweigh the changes in precipitation induced by irrigation itself. Finally, enlarging or shrinking the domain and moving it to a different location (even in different irrigated areas) could indicate if the above changes were unique to the chosen domain or if they could be duplicated elsewhere. For example, enlarging the domain to include the Northeast US could yield interesting results because there may even be influences of irrigation on precipitation in that region (e.g., August changes in total precipitation in the observational study). Finally, irrigating a smaller or larger area could drastically affect the precipitation distribution and degree of changes locally and downwind and will be investigated in future work.

It would also be instructive to conduct a climate change experiment to complement the irrigation study performed above and more completely verify the hypothesis set forth in the observational study regarding the effects of irrigation and climate change on summer precipitation. One option is to artificially raise the temperature of the boundary conditions so as to induce warming in the actual domain during the model run. Another option is to increase incoming solar radiation by a certain percentage for the duration of the model such that temperature would increase in the experimental domain (while also accounting for spin-up time so surface temperature can reach equilibrium); however, this would require a very lengthy model run, so it is not as feasible as simply altering the boundary conditions. Other options will be explored in the

future with regard to creating a warmer environment in the experimental domain for testing the climate change hypothesis.

3.5.2 Additional analyses within model experiments

An important aspect of the climate system that was not analyzed in the above model experiments was vertical velocity. Vertical velocity is critical to determining the mechanisms by which irrigation would change precipitation patterns because of its importance in connecting surface changes with the lower atmosphere and in determining the favorability of the lower atmosphere for convection. In future studies, vertical velocity at different levels of the atmosphere, especially at 700 mb (a common level for diagnosing vertical motion for convective purposes), will be analyzed for the whole time period and for individual storms to see how irrigation affects upward motion. Connecting the vertical motion fields with other atmospheric variables such as convergence, CAPE, CIN, LCL, and others will be important for connecting the processes together in a cohesive, mechanistic argument. This will also be helpful for determining any anomalous NCMCs in the vicinity in the irrigated regions, as this would be evident in the vertical velocity fields.

To better ascertain the transport of water vapor in the vicinity of the irrigated region, it is also imperative to conduct a back-trajectory water vapor analysis. Similar analyses have already been conducted in DeAngelis et al. (2010), Wei et al. (2013), and other studies regarding the effects of irrigation on precipitation. The objective would be to determine two things: 1) how much irrigation-induced water vapor from the Great Plains contributes to increased rainfall over and downwind of the irrigated areas, and 2) how much of the rain that falls in the areas downwind originates as water vapor from the

irrigated regions.   These water vapor tracking analyses can be done using wind, temperature, and moisture information already produced by the WRF model simulations.

It may also be necessary to directly quantify atmospheric quantities like LCL, LFC, CAPE, etc. to verify the authenticity of the results calculated by WRF.   For example, LFC may not even exist on a given day if the vertical profile of atmospheric temperature and moisture is not conducive for convection, and it is possible that WRF's pre-processed values for LFC do not correctly account for the missing data on those days when LFC is not present.   Therefore, independent confirmation of these values is necessary to determine the precise mechanisms by which irrigation may influence rainfall via these variables.

4. CONCLUSIONS

This study investigates the causes of the observed increases in summer precipitation in the Midwestern US and attempts to attribute, through observational analysis and model simulations, these changes to irrigation development in the Great Plains of the United States. Attribution of these observed increases in summer precipitation is important to better understand the causes of climate change; if irrigation development is part of the mechanistic linkages leading to these changes, then this adds a new issue to address in terms of our physical understanding of anthropogenic influence on the climate system. The main hypothesis postulated in the observational study is that climate change (CC) and land use and land cover change (LULCC) would cause different shifts to the precipitation distribution in the Midwestern US and that the changes in precipitation evident in the Midwestern US observational record would more closely match those predicted by LULCC – or more specifically, irrigation development. The irrigation portion of this hypothesis is further explored by conducting a brief sensitivity study of the effects of irrigation on precipitation in the central US.

The effects of irrigation on precipitation were first investigated through analysis of long-term, daily precipitation observations. Time segments of precipitation were compared for statistically significant changes using the Student t-test over multiple precipitation intensities and over two spatial scales – climate regions and climate divisions. It was found that large increases in precipitation frequency, total precipitation, and moderate to heavy precipitation intensity have occurred over the last half-decade. While increases in precipitation frequency are the most significant during JJA, the

increases in intensity are most unique to the summer and seem to exert the most influence on the month-to-month variations in total precipitation differences. Also, the largest increases in frequency, intensity, and total precipitation are between pre- and full-irrigation periods in the Great Plains (i.e., pre-1950 versus post-1975). Furthermore, the spatial distribution of precipitation increases is consistent with a downwind effect of irrigation on precipitation. It is postulated that increases in CIN over Nebraska due to irrigation prevent convection from occurring as frequently and dampen precipitation amounts, while the increase in CAPE and moisture downwind allow for increases in convection to occur. These mechanisms postulated in the observational analyses seem to be physically feasible given the results of that analysis. Finally, the increases in total precipitation and anomalous increases in precipitation intensity when ranked against other months counter the notion that CC is a major factor in influencing these precipitation increases. Thus, the main conclusion from the observational study is that the hypothesized changes in precipitation due to irrigation development display a greater agreement with the observed increases in summer precipitation than those of CC and may be indicative of a causal link.

A modeling experiment was then performed with the WRF regional climate model to verify the feasibility of the mechanisms postulated in the observational section and to attempt to duplicate the results derived from the observational analysis. The model was run at 10-km spatial resolution with a convective parameterization for 15 days in June of 2002. Additionally, the model run was initialized with the 32-km, 3-hourly NARR reanalysis product and coupled to the Noah LSM. A subdomain over Nebraska

was subjected to a simplified irrigation scheme where soil moisture was filled to field capacity if any of the four soil moisture layers fell below half of field capacity.

Overall, convective precipitation seemed to increase north and east of Nebraska (and decrease over Nebraska) due to irrigation. The increases in moisture, decrease in temperature, and subsequent increases in both CIN and CAPE over Nebraska predicted in the observational section were also verified. It was initially hypothesized that moisture transport to the Midwestern US from Nebraska would be the major cause of enhancements in rainfall. However, analyzing one particular event shows that intensification of rainfall in the Midwest coincides with anomalous wind convergence created by the inclusion of irrigation into WRF. Thus wind and circulation anomalies seem to be more important than previously realized in enhancing the precipitation over the downwind areas, especially in the MWE subregion on June 12.

The modeling analysis also determined that while precipitation intensity exhibited increases in some downwind regions, the frequency of precipitation was largely unaffected by irrigation. This supports the observational evidence of anomalously high changes in intensity during the summer, despite a lack of actual increases, and also seems to discourage the notion that irrigation is primarily responsible for the significant increases in precipitation frequency that are evident in the observation study. Thus, it is possible that some other forcing – perhaps climate change – is responsible for the frequency changes while irrigation is more responsible for the changes in intensity. Naturally, further modeling studies will have to be completed to verify this postulation. However, the spatial pattern of increases in total precipitation and intensity downwind of Nebraska in the model simulation seems to support the hypothesis that the intensity

increases (and maybe even part of the total precipitation increases) implied by the observational analysis are more a result of irrigation development than from climate change.

Admittedly, due to time and computing constraints, this initial modeling experiment only scratches the surface of what would need to be done to more comprehensively verify the existence of an irrigation enhancement of precipitation. Future work in this regard would involve several ensemble runs of at least one growing season and sensitivity analyses to parameters such as convective parameterizations, microphysics options, and size and location of the model domain. Adding nested grids could help to isolate local, short-range, and remote effects of irrigation on precipitation. Additionally, the vertical wind field needs to be analyzed, as this is extremely important in piecing together the mechanisms that would result in irrigation enhancement of precipitation. Water vapor tracking analyses would also be critical for identifying the directionality and contribution of moisture transport to downwind regions so that the impact of irrigation on precipitation can be quantitatively assessed. Many atmospheric variables associated with the vertical profile, such as LFC, LCL, CAPE, and CIN, should also be explicitly calculated to verify the accuracy of the pre-processed values given by WRF. Additional experiments will also further analyze specific storm events and determine changes to the overall precipitation distribution given more model runs and longer simulations. Finally winds, convergence, and additional diagnostic atmospheric variables will be analyzed in more detail in these future experiments to better determine the pathway from irrigation to the enhancement of precipitation in these downwind areas.

A few caveats remain in these analyses. Though both observations and modeling simulations support the hypothesis that precipitation intensity and totals downwind of Nebraska have likely been enhanced by irrigation in Nebraska, the simulations found a decrease in precipitation due to irrigation over western Nebraska that is not unambiguously supported by observations; future work should be done to verify this simulated result in the observational record. Also, the amount of precipitation enhancement is highly dependent on location and timing. In other words, the scale of enhancement is localized, and the effects may be in different places depending on where the ambient precipitation is located. Future research in this subject will be conducted to better determine and predict the location and degree effects of irrigation on precipitation. Also, a complete dynamical assessment of other potentially confounding factors is beyond the scope of this paper but should be conducted in the future to rule out other large-scale climate factors such as ENSO and the Great Plains low-level jet.

Overall, this work attempts to fill a gap in our current mechanistic understanding of the causes behind the observed increase in summer rainfall in the Midwestern US. Implicating irrigation as a potential cause of these changes in precipitation opens up a relatively new nexus between anthropogenic activities and climate change that could have societal and economic consequences. If these linkages are verified in the near future, the irrigation effect on precipitation intensity and totals may warrant consideration for climate change planning and adaptation measures on local and regional scales in the Midwestern United States.

TABLES

	Precipitation - irrigated run (mm)	Precipitation - non-irrigated run (mm)	Absolute difference (mm)	Percent difference (%)
MWE	104.85	102.33	2.52	2.46
MWW	85.76	85.14	0.62	0.73
UME	45.13	45.51	-0.38	-0.84
UMW	50.77	48.79	1.98	4.07
NPE	28.94	29.59	-0.64	-2.17
NPW	22.39	22.66	-0.26	-1.16
NE	18.15	22.52	-4.37	-19.42
KS	41.97	42.17	-0.19	-0.46
CR	19.19	19.23	-0.05	-0.26
Whole Domain	49.68	49.55	0.13	0.26

Table 1 – Average values of total precipitation and their differences between the irrigated and non-irrigated WRF model runs for the whole 15-day simulation period, June 1-15. Note that because the regions are different sizes and don't encompass the whole domain, the 9 values listed above do not add up to the values for the whole domain.

ILLUSTRATIONS

Nebraska Crops - Harvested Acreage

Nebraska Crops - Production
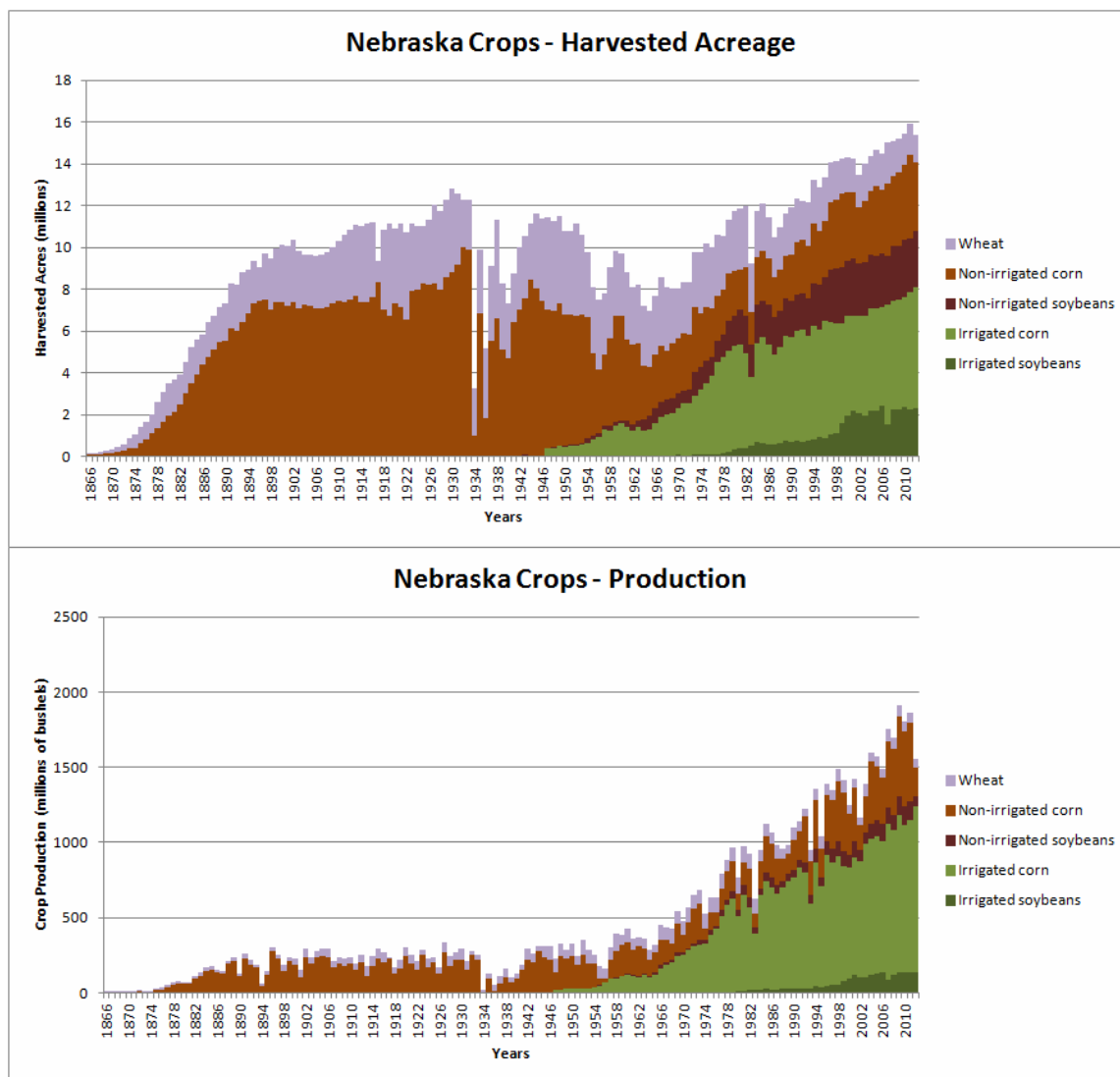
Figure 1: Timelines of harvested acreage [top] and production [bottom] of major crops in Nebraska since 1866. Note that the data for irrigated crops only begins in 1947.
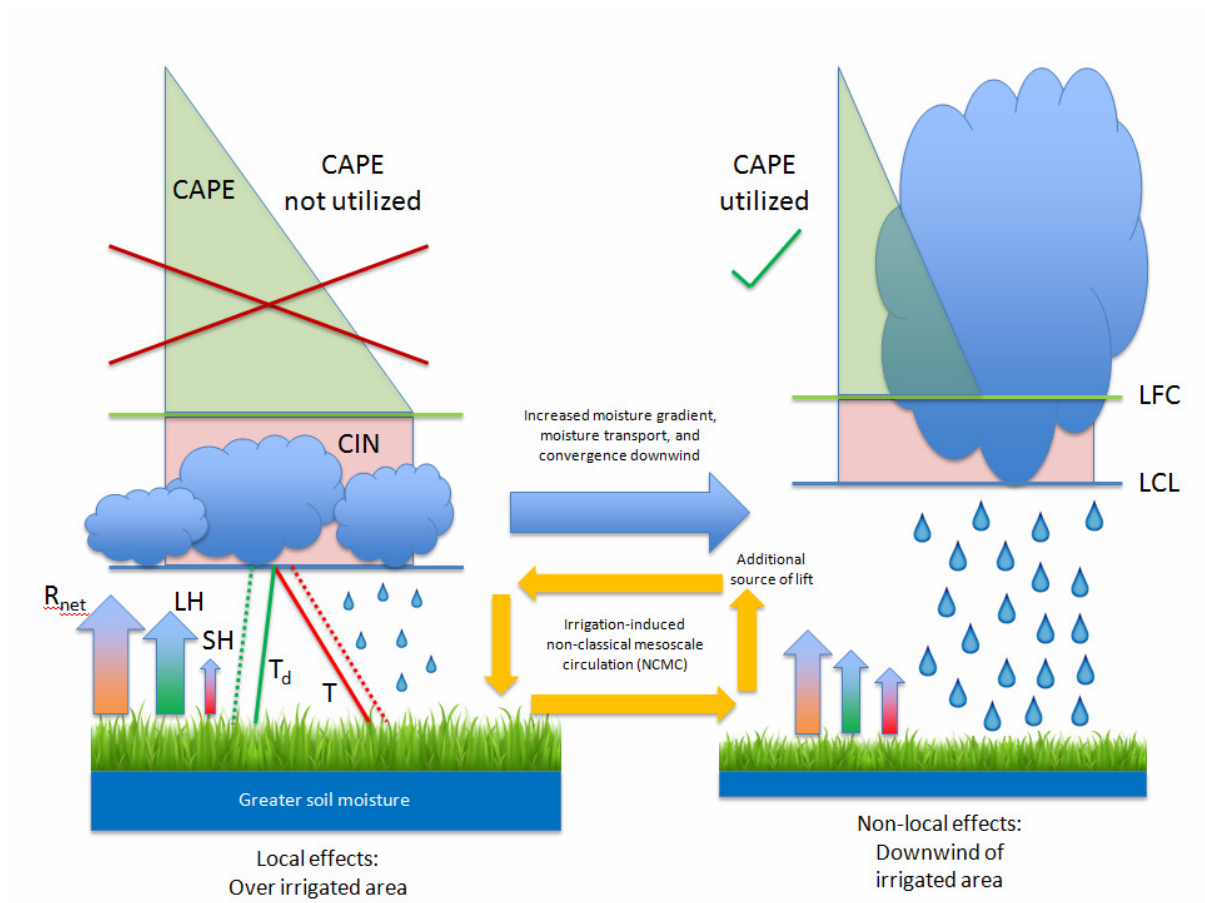
Figure 2: An idealized schematic depicting the local and non-local effects of irrigation on atmospheric thermodynamics and precipitation processes. R_{net} = net surface radiation, LH = latent heat flux, SH = sensible heat flux, T_d = dewpoint temperature, T = temperature, CIN = convective inhibition, CAPE = convective available potential energy, LCL = lifting condensation level (cloud base), and LFC = level of free convection. The linear depictions of T_d and T show the changes in mixing ratio and dry adiabatic lapse rate, respectively, given near-surface T_d and T from pre-irrigation (dotted lines) to full-irrigation (solid lines). The intersection of these lines gives the approximate height of the LCL. Note that the downwind area on the right can be considered to be in a "pre-irrigation" condition, with either non-irrigated crops or grass.

(a)

(b)
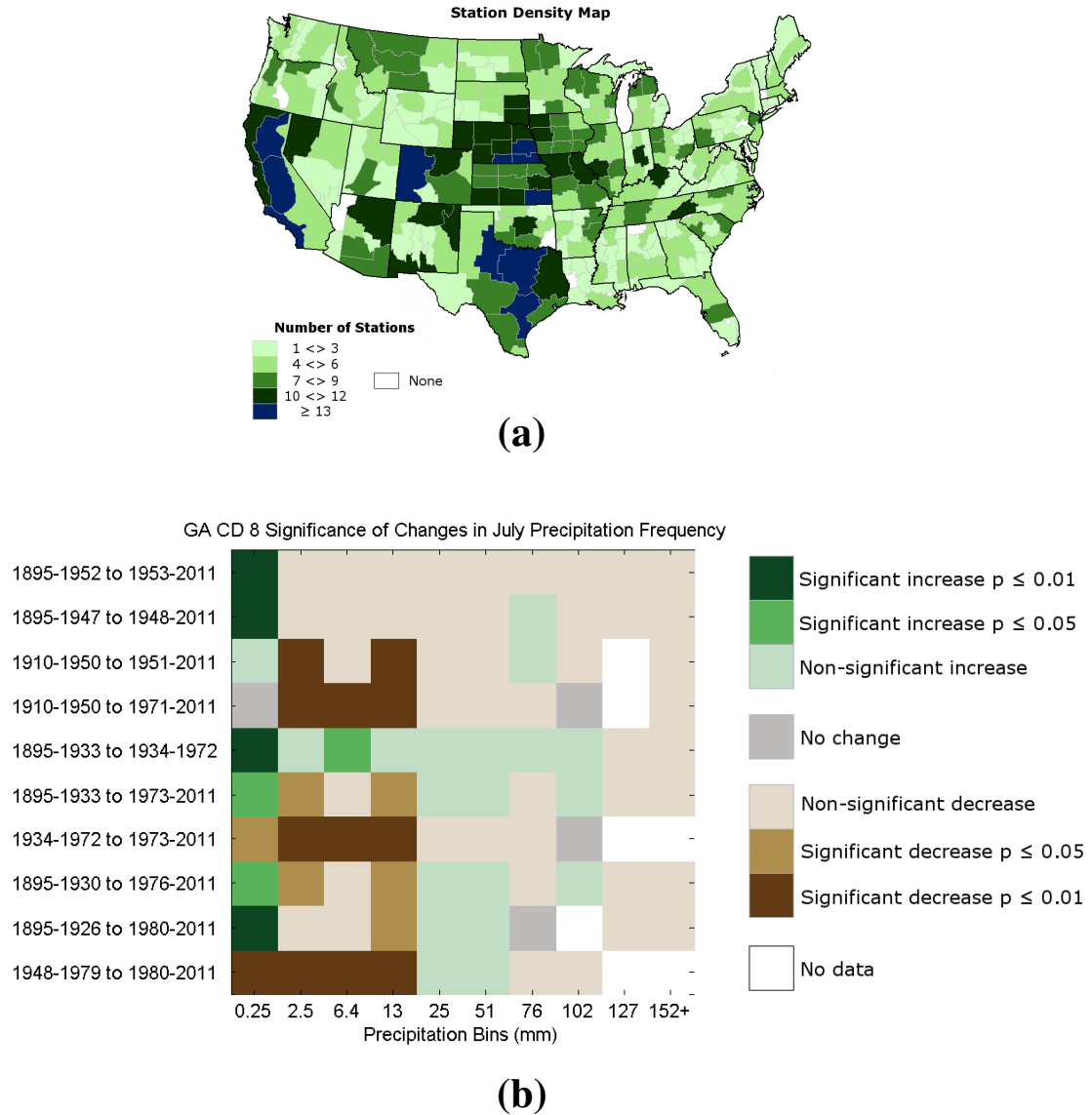
Figure 3: (a) Map of station density by climate division. (b) Example of a "time period-intensity" plot from south-central Georgia (climate division 8). The precipitation bins are specified by their lower bounds, e.g., the lightest bin is 0.25-2.5 mm (0.01-0.1 inches), followed by 2.5-6.4 mm (0.1-0.25 inches), etc. Information from this plot is used in Figure 5 (and similarly in Figure 6, for intensity): e.g., south-central Georgia has a total of seven significant increases across the entire intensity distribution in July (see Figure 5b).

67

June   **July**   **August**

Total Precipitation

A = Gulf Coast
B = Southeast Interior
C = Northeast
D = Midwest
E = Upper Midwest   H = Southwest
F = Southern Plains   I = Northern Rockies
G = Northern Plains   J = Northwest
K = West

(a)   (b)   (c)

Frequency

(d)   (e)   (f)

Intensity

(g)   (h)   (i)
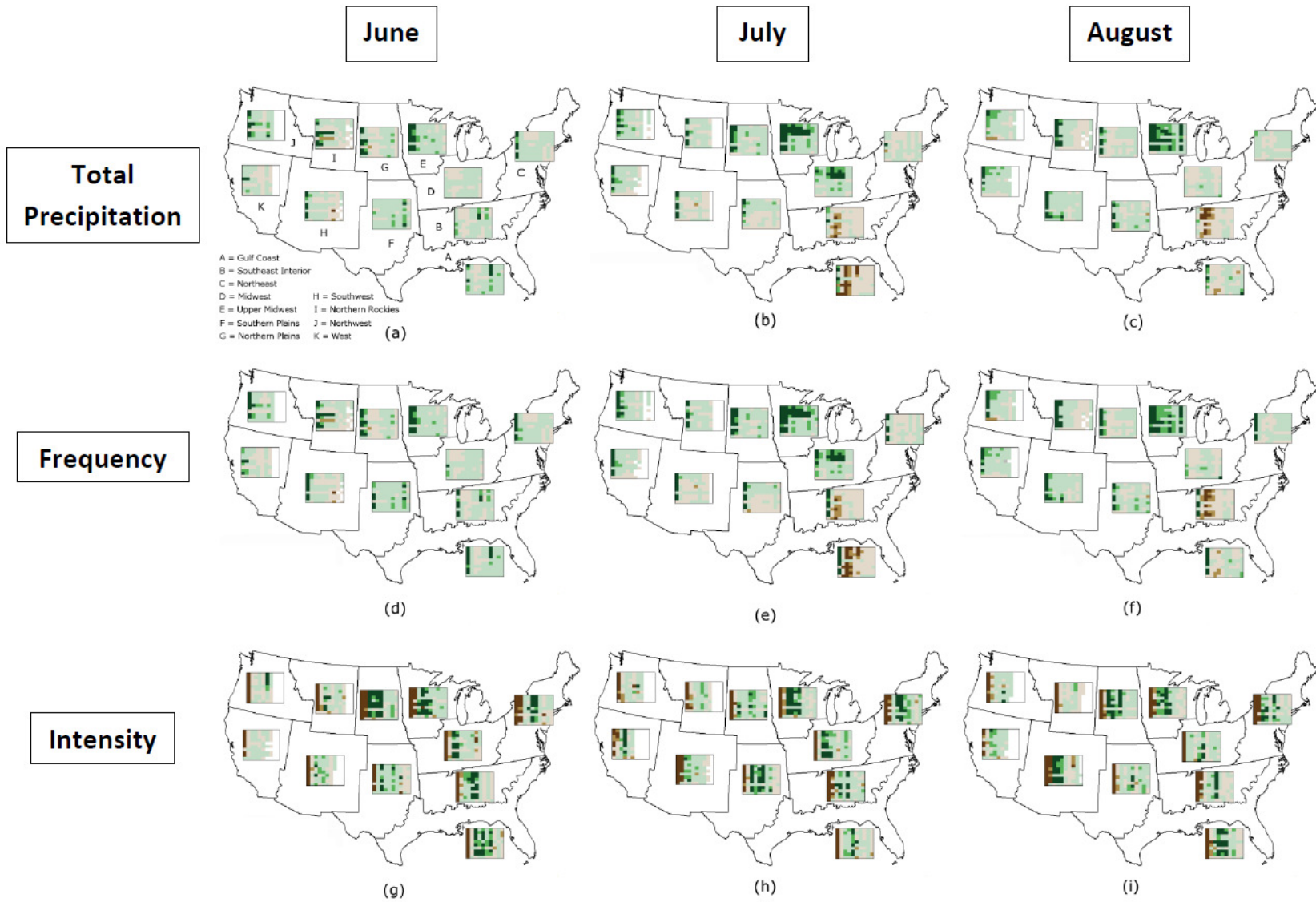
Figure 4: Regional maps of changes in total precipitation [top row], precipitation frequency [middle row], and precipitation event intensity [bottom row] during June [left column], July [middle column], and August [right column]. The time period-intensity plots within each region have the same axis labels as in Figure 3b.

FREQUENCY | June | July | August
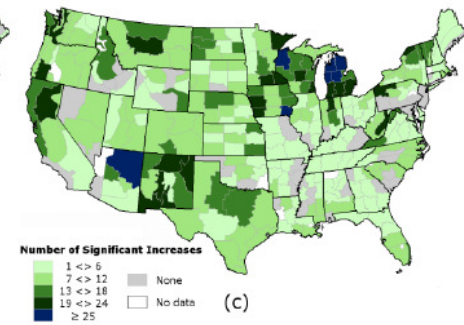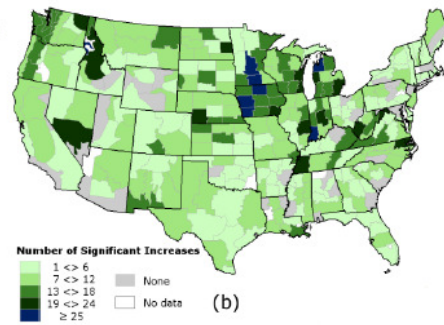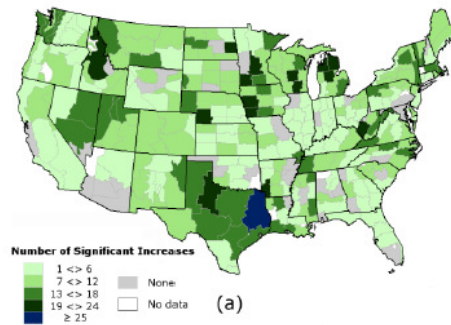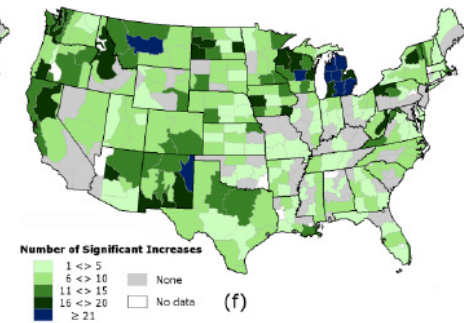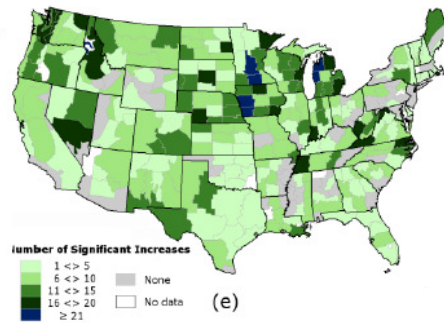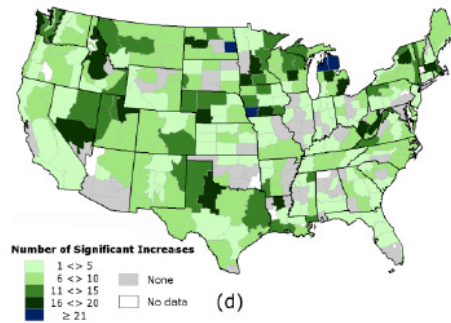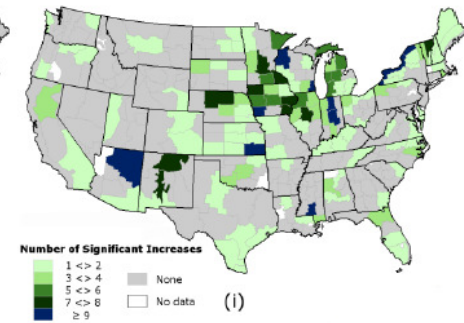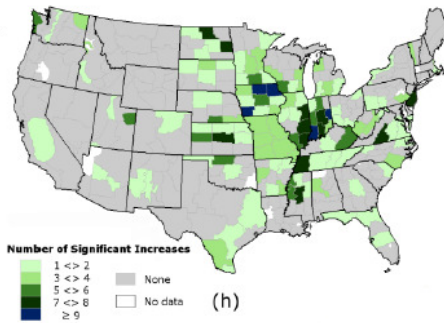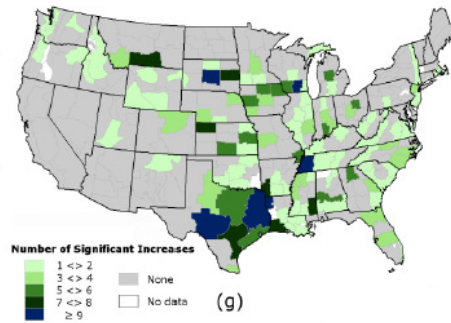
Figure 5: The sum of significant increases (p ≤ 0.05) in precipitation frequency over all precipitation intensity bins [top row], over the lightest four bins (0.25-25 mm) [middle row], and over the heaviest six bins (>25 mm) [bottom row] for each climate division during June [left column], July [middle column], and August [right column].
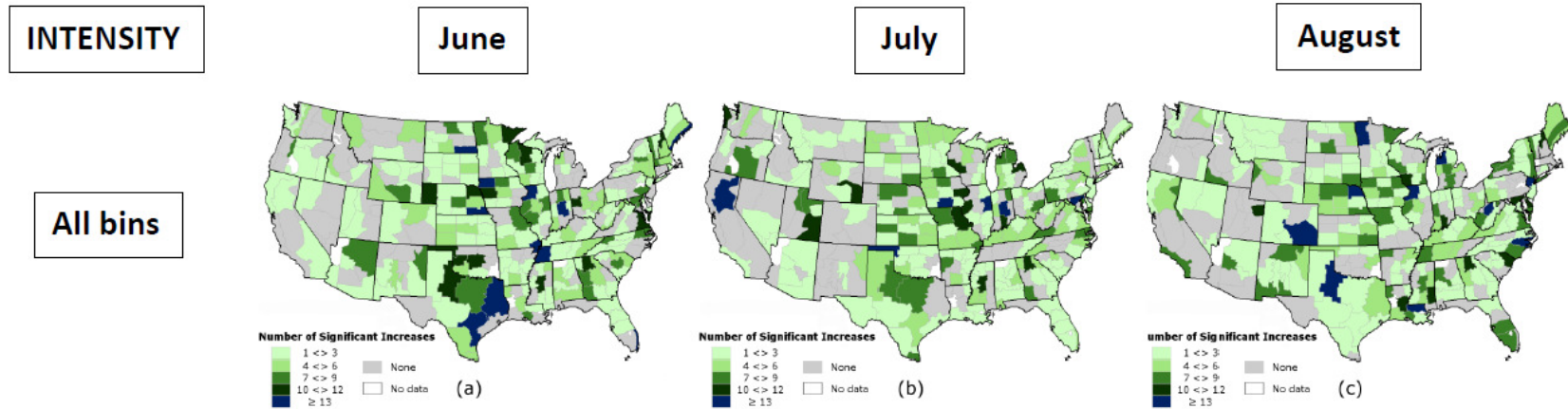
Figure 6: The sum of significant increases (p ≤ 0.05) in precipitation event intensity over all precipitation bins for each climate division during (a) June, (b) July, and (c) August.
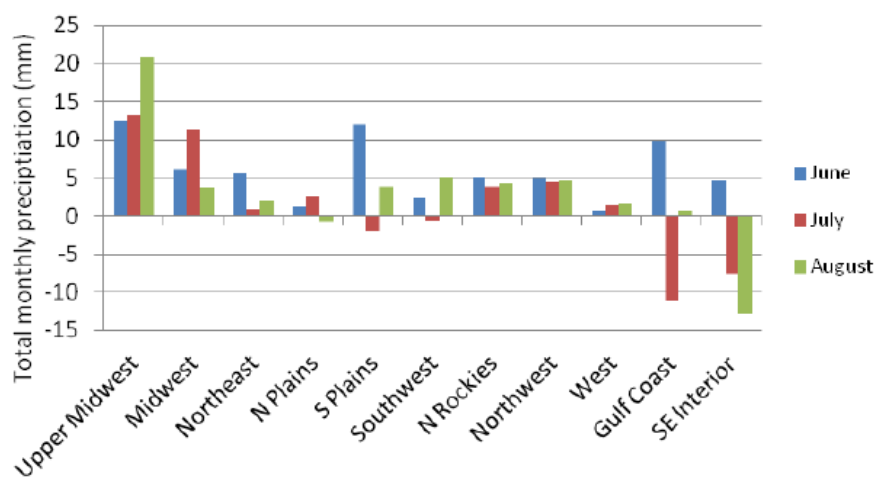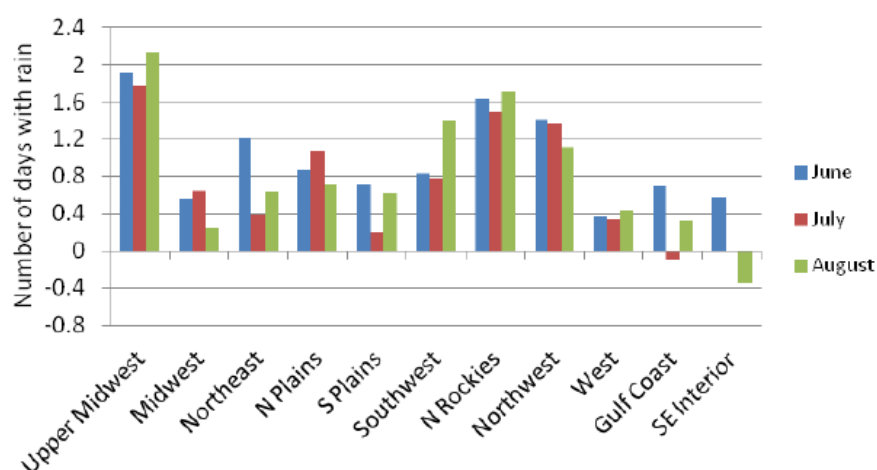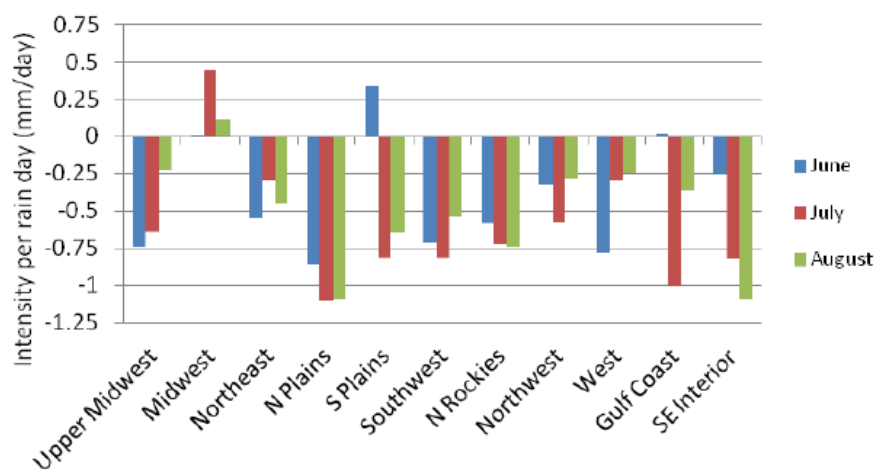
Figure 7: Regional changes in mean monthly total precipitation [top], precipitation frequency [middle], and precipitation intensity [bottom] during June [blue], July [red], and August [green] between 1895-1933 and 1973-2011, corresponding to row 6 of the time period-intensity plots.
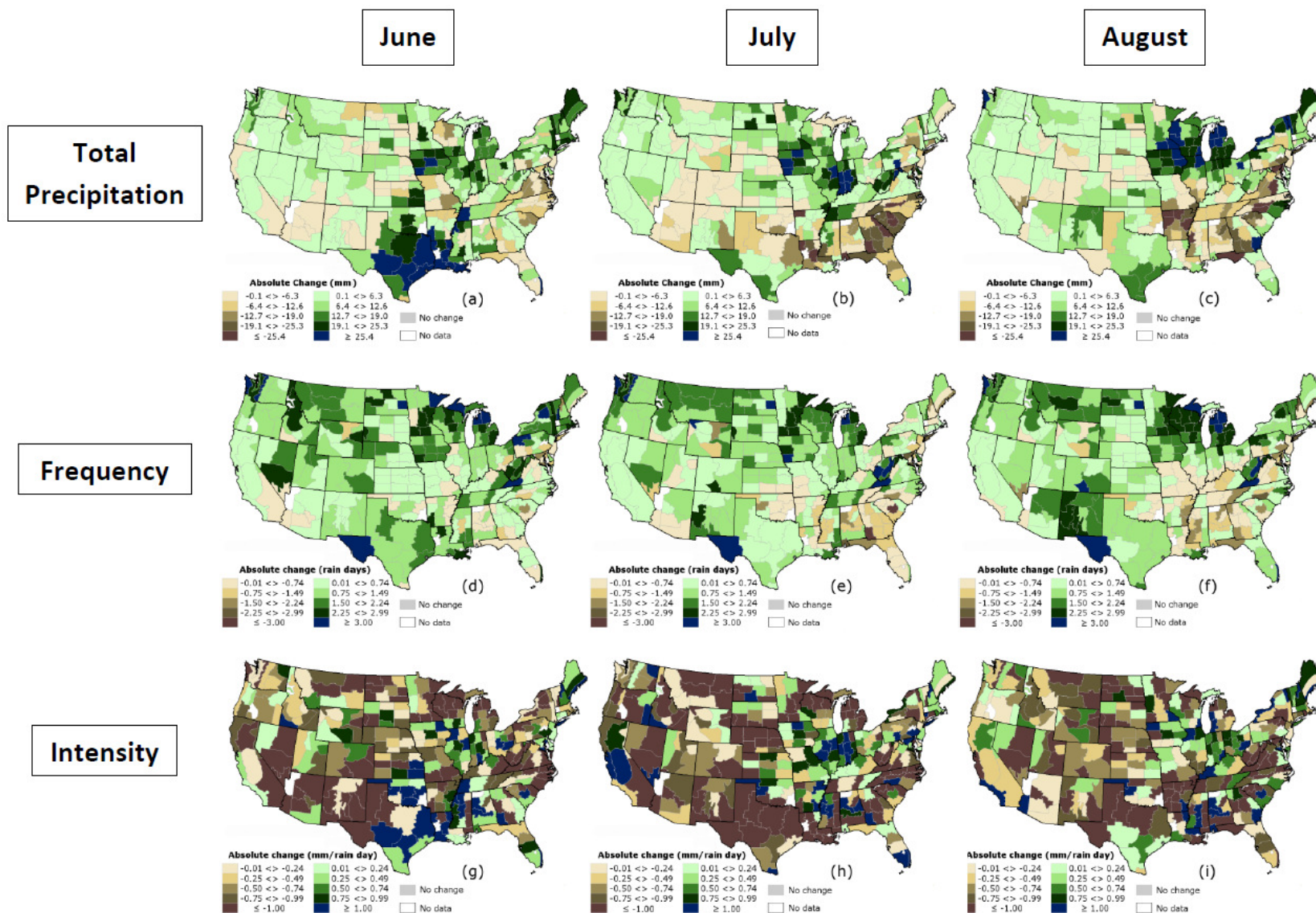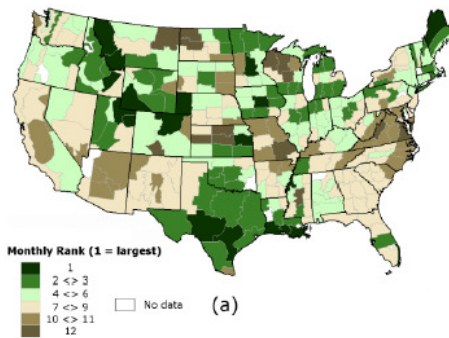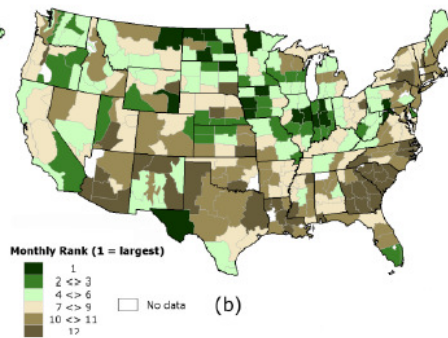
Figure 8: Absolute changes in total precipitation [top row], precipitation frequency [middle row], and precipitation intensity [bottom row] during June [left column], July [middle column], and August [right column] between 1895-1933 and 1973-2011, corresponding to row 6 of the time period-intensity plots.

	June	July	August
Total Precipitation	(a)	(b)	(c)
Frequency	(d)	(e)	(f)
Intensity	(g)	(h)	(i)

Monthly Rank (1 = largest)

1
2 <> 3
4 <> 6   No data
7 <> 9
10 <> 11
12
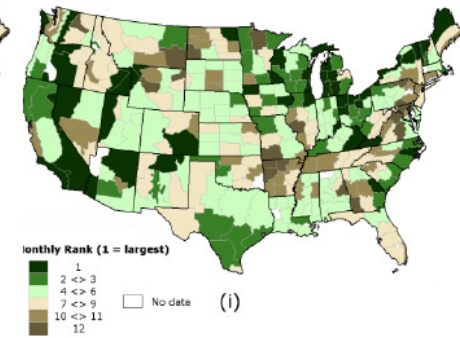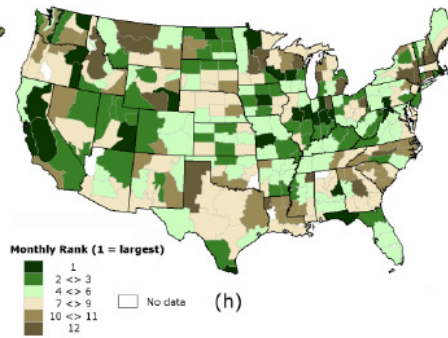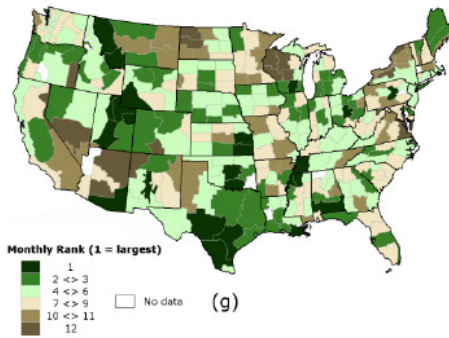
Figure 9: Monthly ranks (out of 12 months) of absolute changes in total precipitation [top row], precipitation frequency [middle row], and precipitation intensity [bottom row] for June [left column], July [middle column], and August [right column] between 1895-1933 and 1973-2011, corresponding to row 6 of the time period-intensity plots.

July   August

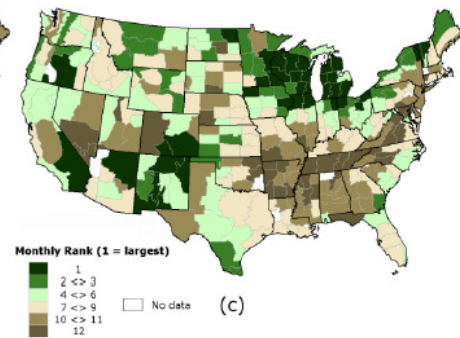Niño 3.4
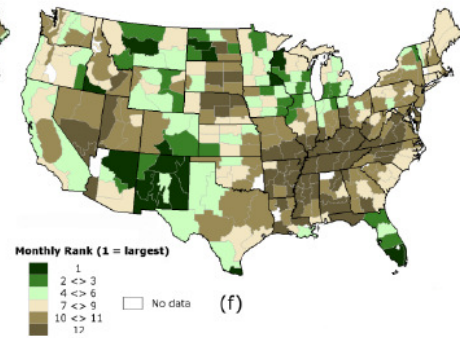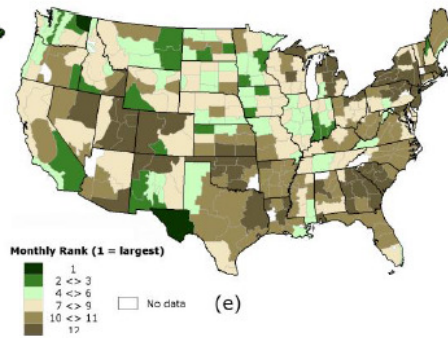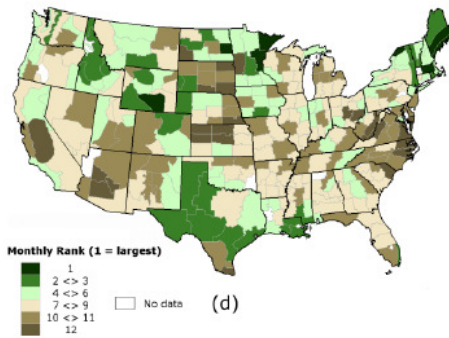
NAO

AMO

PNA

PDO

NOAA/ESRL PSD and CIRES–CU

Absolute change in mean monthly precipitation
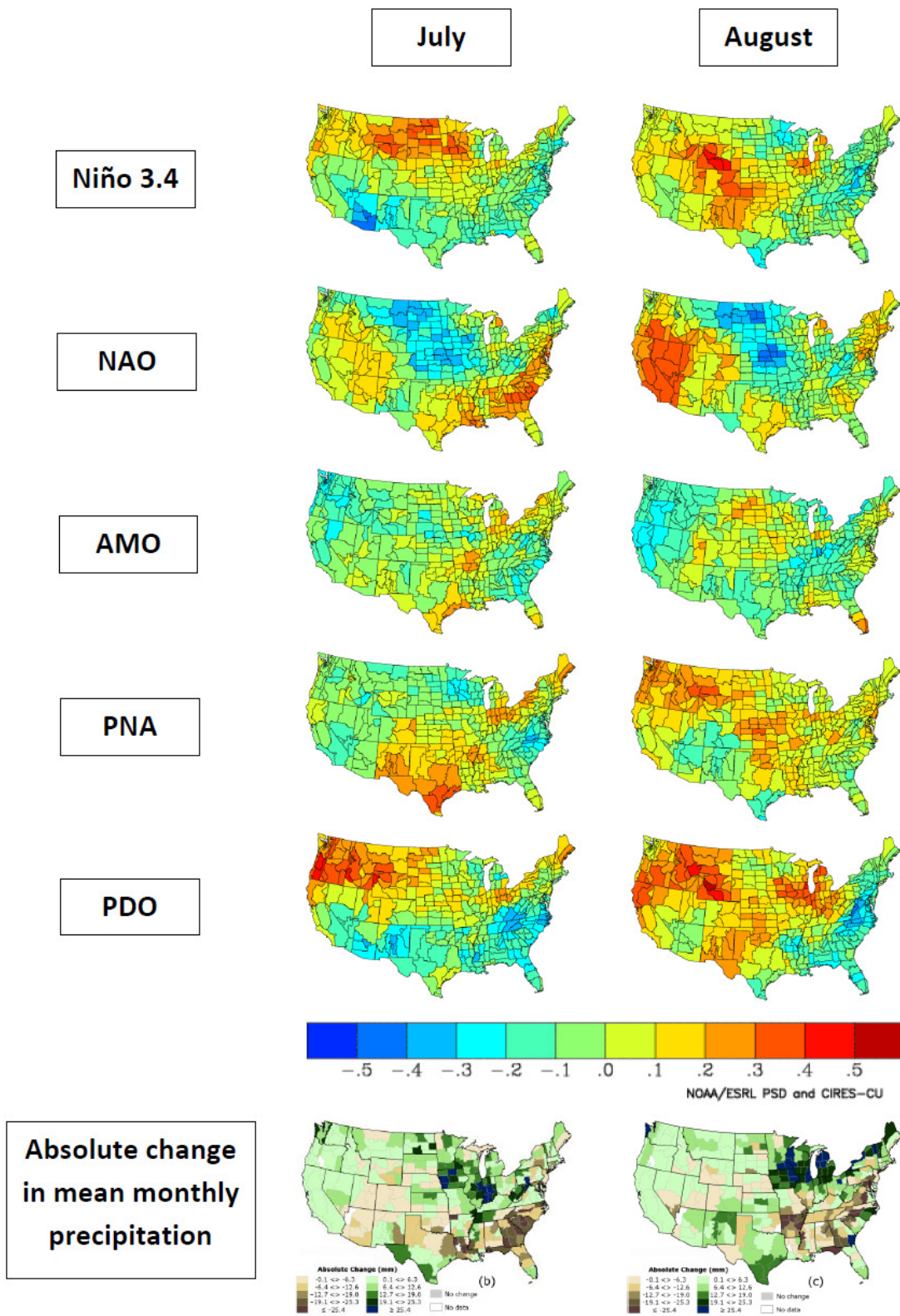
Figure 10: Correlations of monthly mean precipitation during July [left column] and August [right column] with monthly indices of various large-scale atmospheric circulations (averaged over 1948-2012). Niño 3.4 measures sea surface temperature anomalies in the tropical Pacific Ocean and corresponds to the state of the El Niño Southern Oscillation, NAO = North Atlantic Oscillation, AMO = Atlantic Multidecadal Oscillation, PNA = Pacific/North American teleconnection, and PDO = Pacific Decadal Oscillation. Absolute increases in July and August total precipitation from Figure 8 are included on the bottom for reference. Correlations are calculated from the US Climate Division Dataset Seasonal Correlation Page (http://www.esrl.noaa.gov/psd/data/usclimdivs/correlation/).
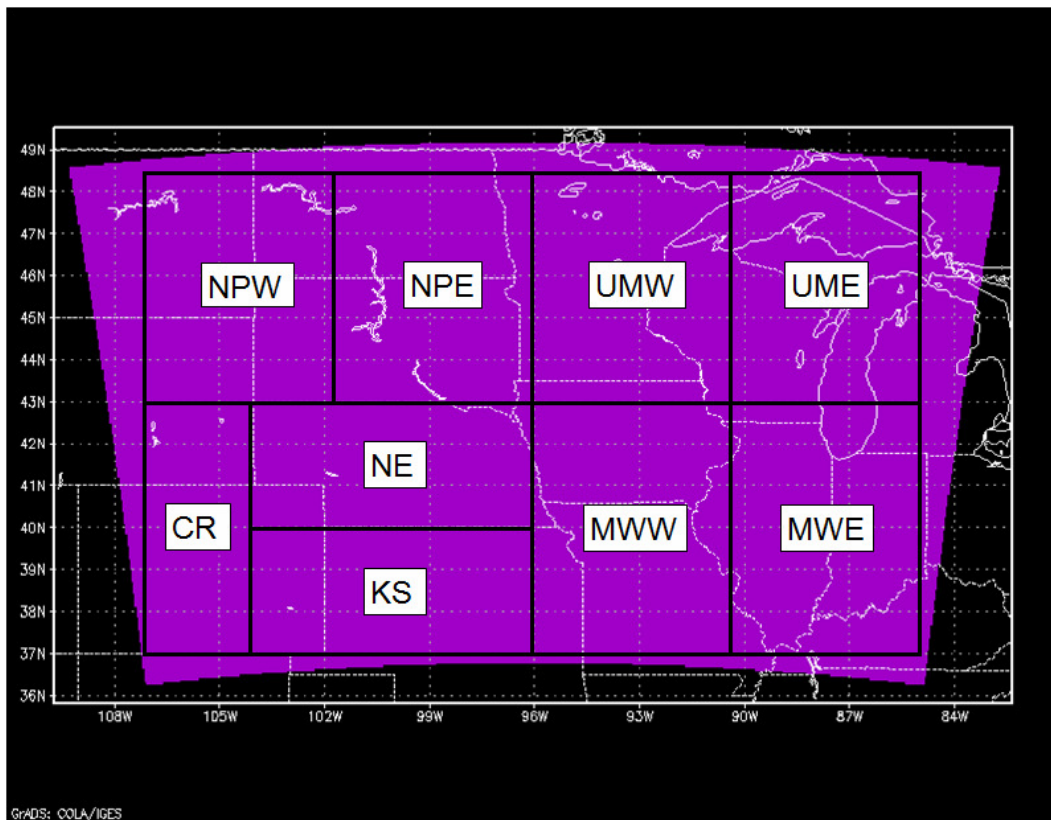
Figure 11 – A map of the WRF model domain (in purple) and of the nine subregions used to more closely determine regional changes in precipitation. MWE and MWW are eastern and western Midwest, respectively; UME and UMW are eastern and western Upper Midwest, respectively; NPE and NPW are eastern and western Northern Plains, respectively; NE is Nebraska; KS is Kansas; CR is Colorado Rockies.
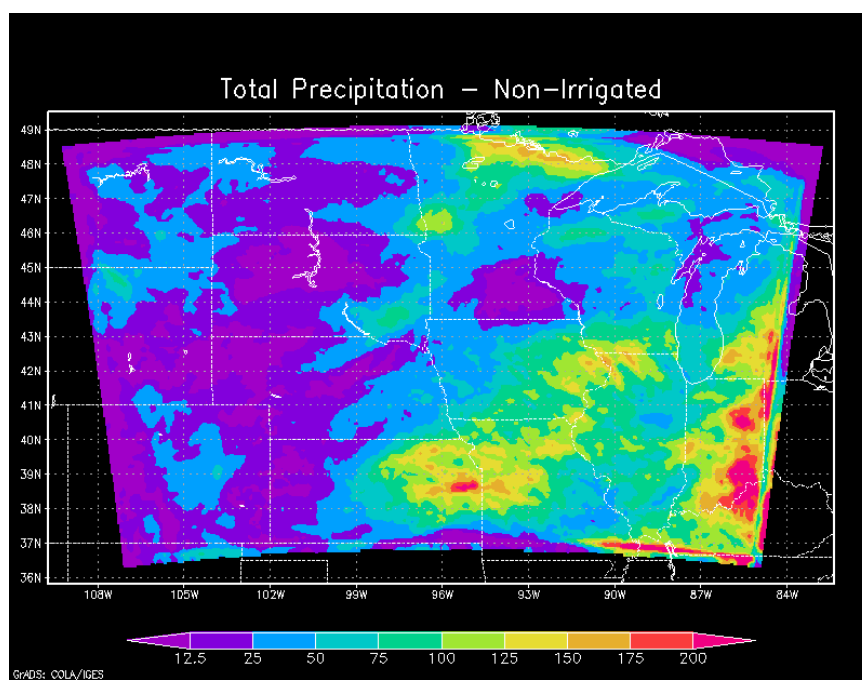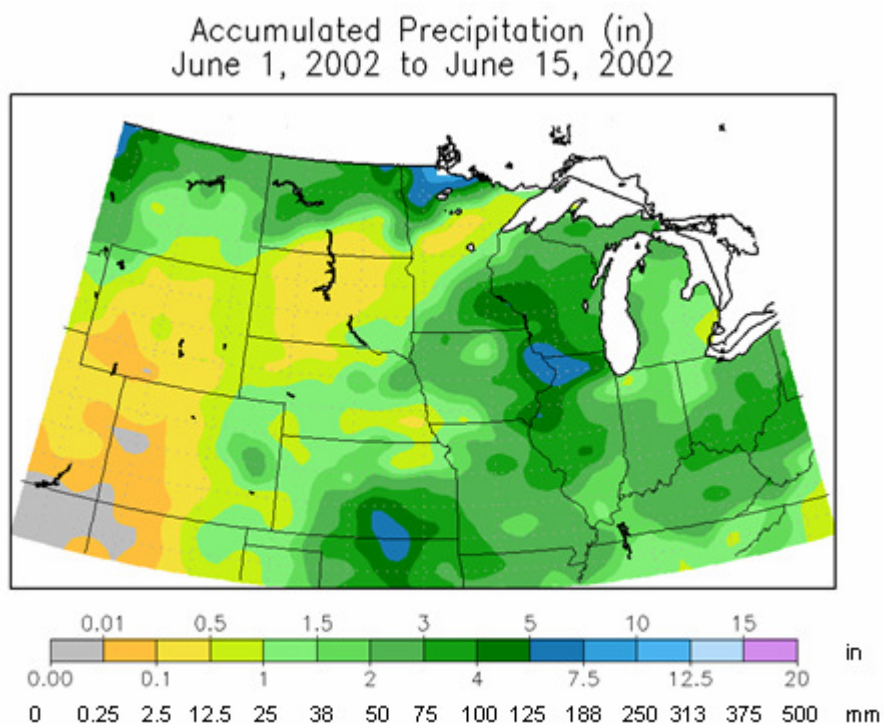
Figure 12 – [top] June 1-15 precipitation from cli-MATE (inches), which is obtained from the Midwestern Regional Climate Center. [bottom] Total simulated precipitation (mm) from the non-irrigated WRF model run, spanning June 1 at 00Z to June 15 at 21Z.
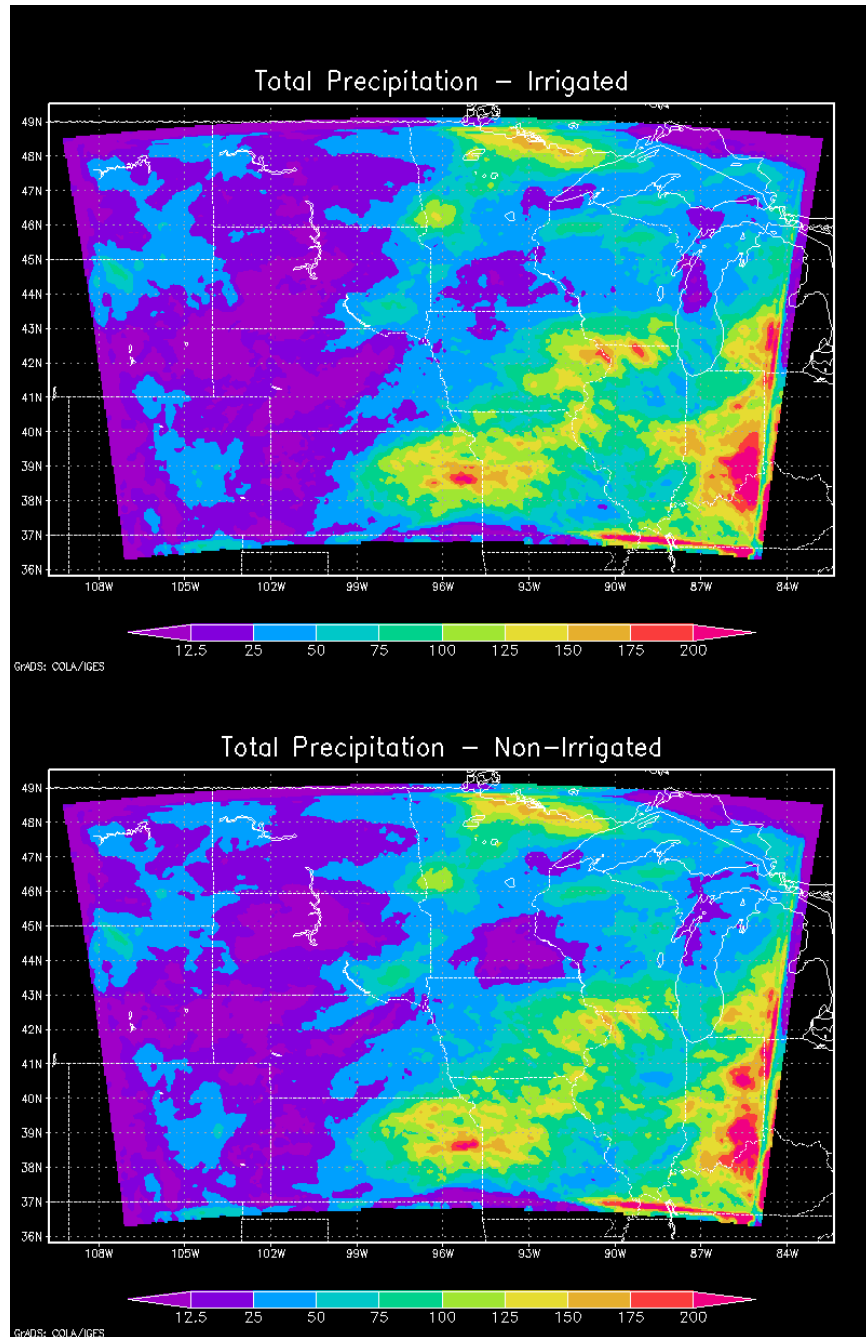
Figure 13 – [top] Total simulated precipitation (mm) from the irrigated WRF model run, spanning June 1 at 00Z to June 15 at 21Z. [bottom] Same as above, but for the non-irrigated WRF model run.
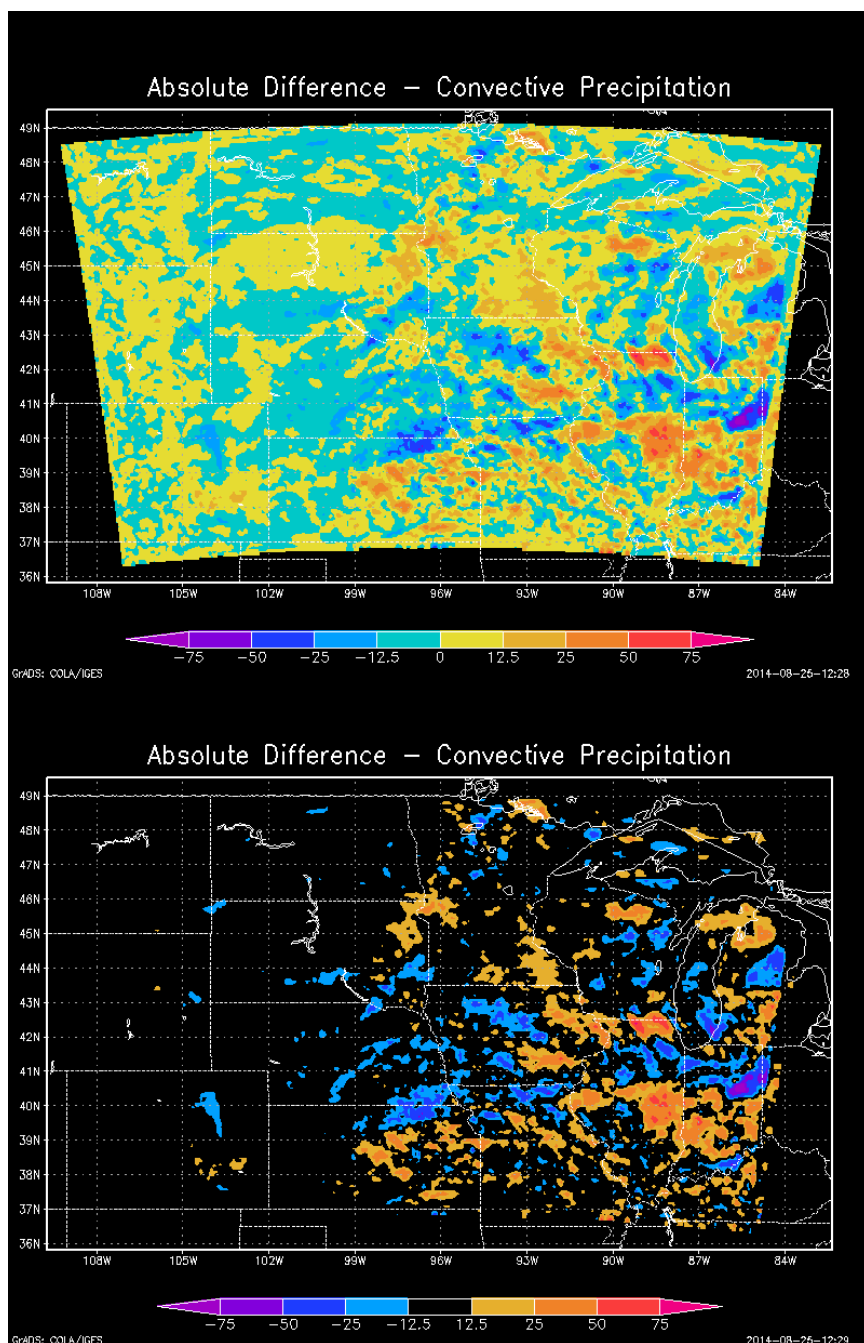
Figure 14 – [top] Absolute difference in total convective precipitation (mm) between the irrigated and non-irrigated WRF model runs for the whole 15-day period. [bottom] Same as top, but with all values less than 12.5 mm masked out.
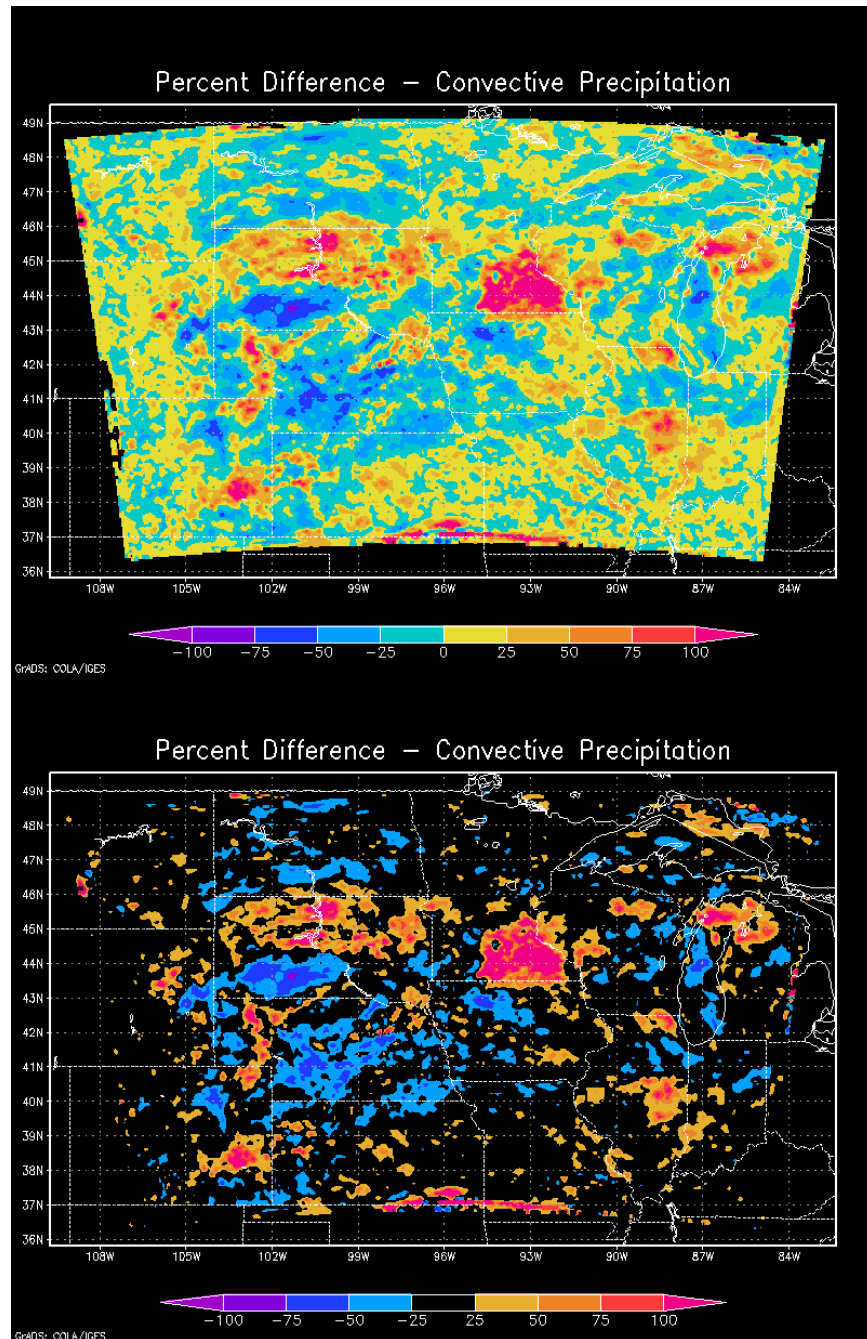
Figure 15 - [top] Percent difference in total convective precipitation (%) between the irrigated and non-irrigated WRF model runs for the whole 15-day period. [bottom] Same as top, but with all values less than 25% masked out.

Daily rain 37 43 −96 −90.5 — MWW

Daily rain 37 43 −90.5 −85 — MWE

Daily rain 43 48.5 −96 −90.5 — UMW

Daily rain 43 48.5 −90.5 −85 — UME

Daily rain 43 48.5 −107 −101.5 — NPW

Daily rain 43 48.5 −101.5 −96 — NPE

Daily rain 40 43 −104 −96 — NE

Daily rain 37 40 −104 −96 — KS
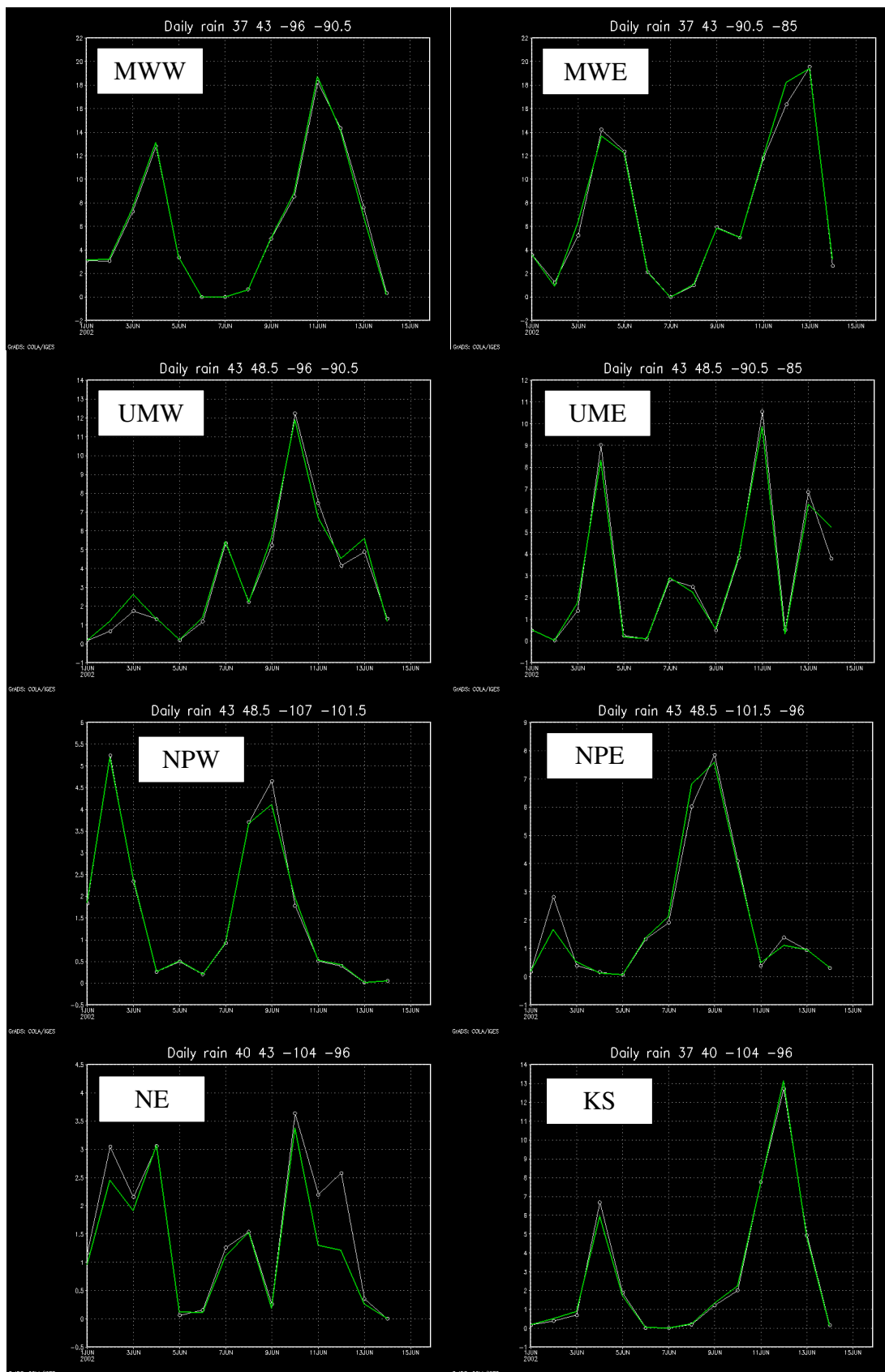
Figure 16 – Time series of daily precipitation intensities (mm) averaged over each given subregion for the irrigated (green) and non-irrigated (white) model runs. Note that the precipitation on a given date represents the precipitation that fell for the 24 hours *after* the initial time. For example, precipitation listed for June 12 would represent the precipitation that fell from 00Z on June 12 to 00Z on June 13. Subregion abbreviations are defined in Figure 1.
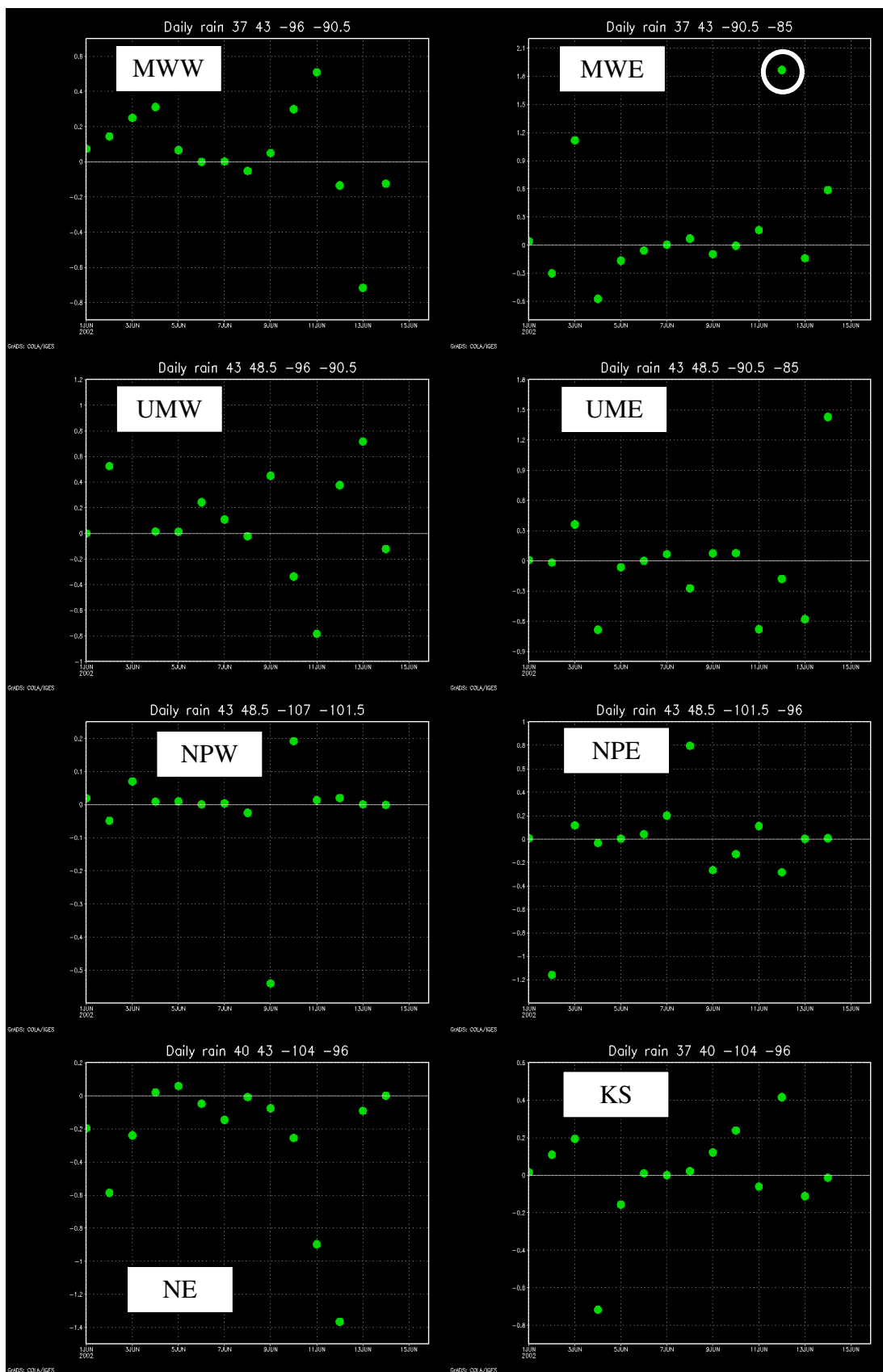
Figure 17 – Absolute changes in daily precipitation intensity (mm) averaged over each subregion. The white circle in the MWE subregion is the data point for the event that is examined in detail in the text. Subregion abbreviations are defined in Figure 1.

Daily rain 37 43 -96 -90.5

MWW

Daily rain 37 43 -90.5 -85

MWE

Daily rain 43 48.5 -96 -90.5

UMW

Daily rain 43 48.5 -90.5 -85

UME

Daily rain 43 48.5 -107 -101.5

NPW

Daily rain 43 48.5 -101.5 -96

NPE

Daily rain 40 43 -104 -96

NE

Daily rain 37 40 -104 -96

KS
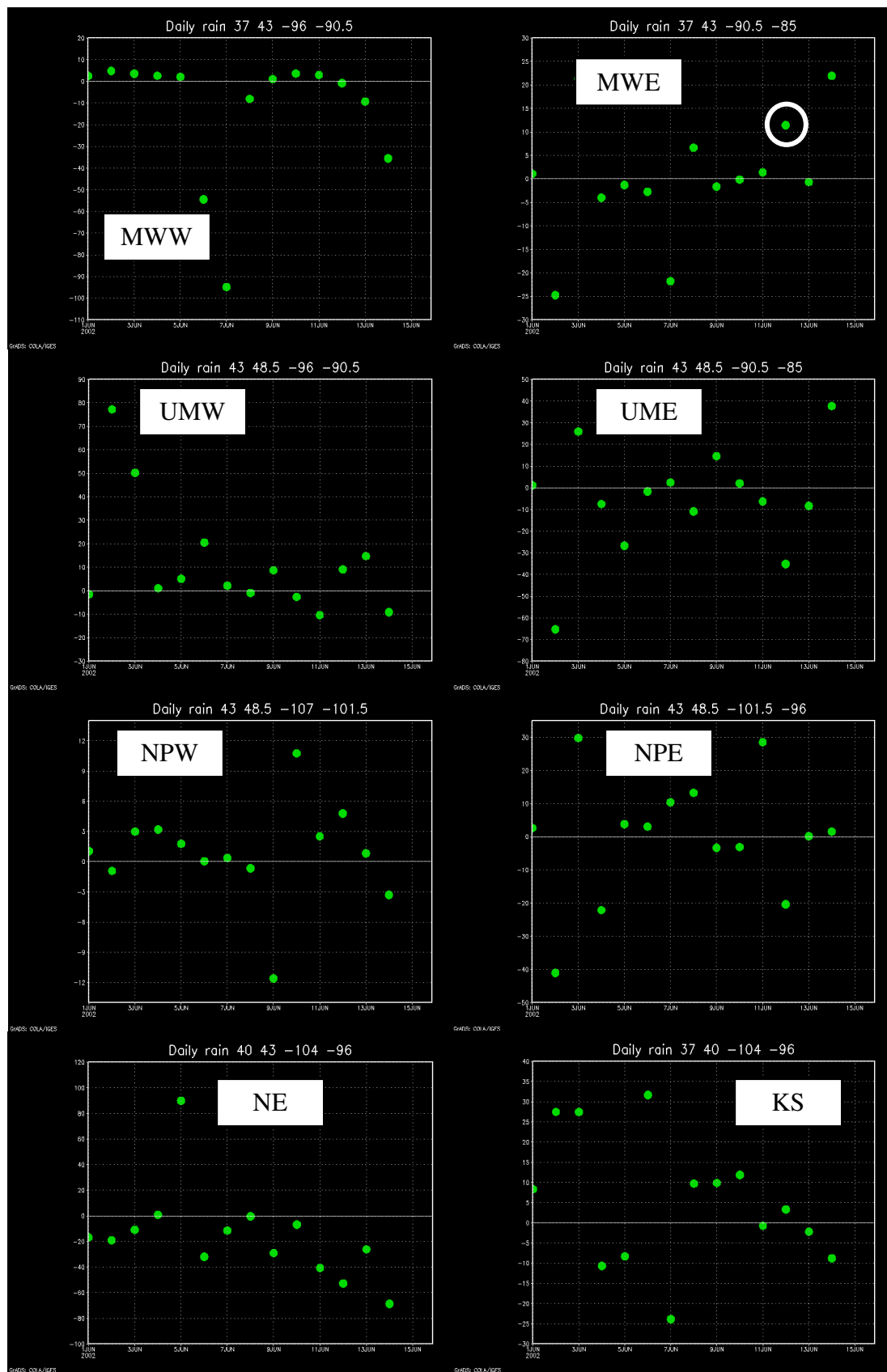
Figure 18 – Same as for Figure 7, but for percent changes in daily precipitation intensity (%) averaged over each subregion.
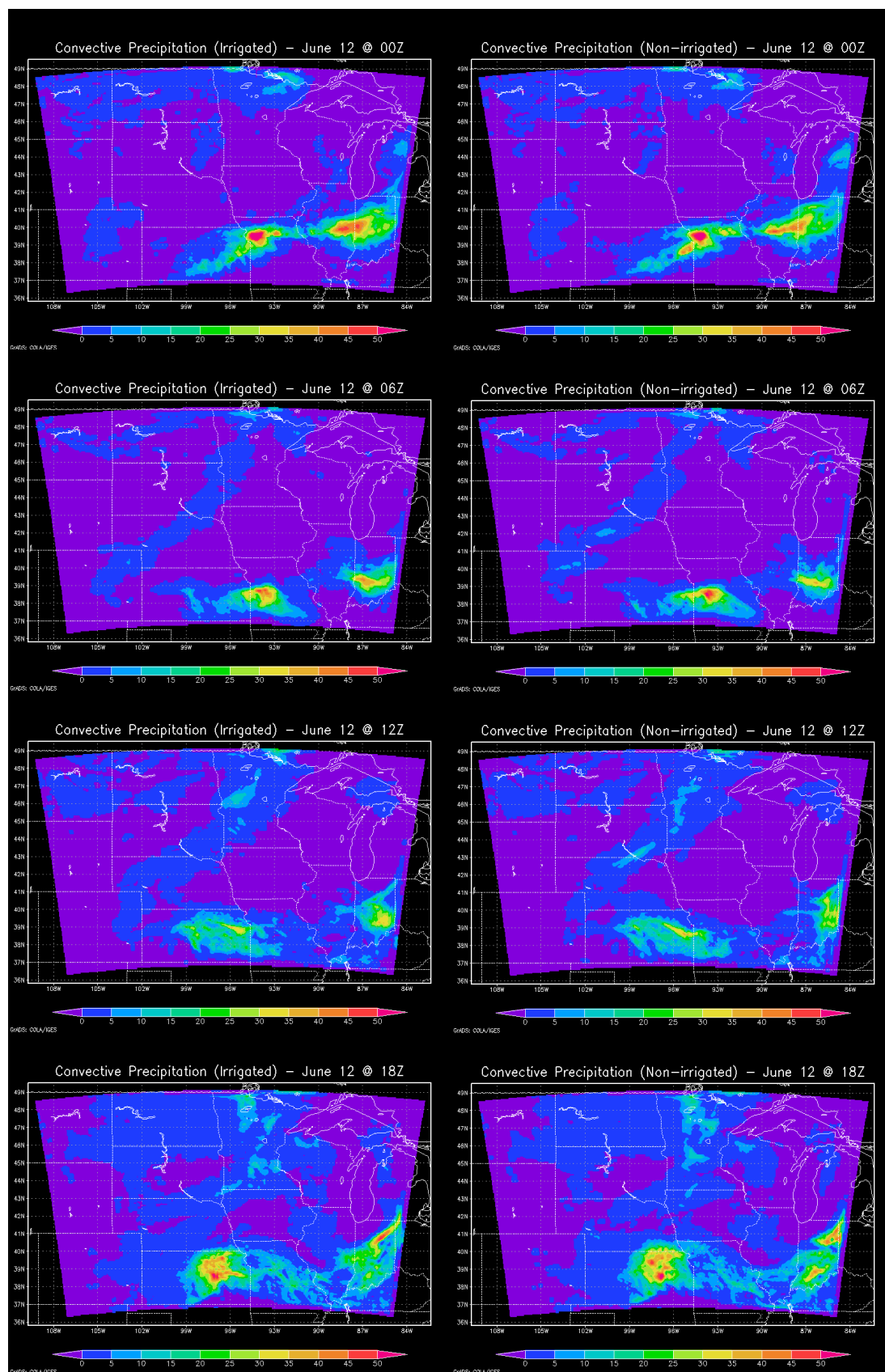
Figure 19 – [left] 6-hour convective precipitation (mm) for the irrigated model run beginning at the time specified in each panel. [right] 6-hour convective precipitation (mm) for the non-irrigated model run beginning at the time specified in each panel.

Diff in Convective Precip – June 12 @ 00Z

Percent Diff in Convective Precip – June 12 @ 00Z

Diff in Convective Precip – June 12 @ 06Z

Percent Diff in Convective Precip – June 12 @ 06Z

Diff in Convective Precip – June 12 @ 12Z

Percent Diff in Convective Precip – June 12 @ 12Z

Diff in Convective Precip – June 12 @ 18Z

Percent Diff in Convective Precip – June 12 @ 18Z
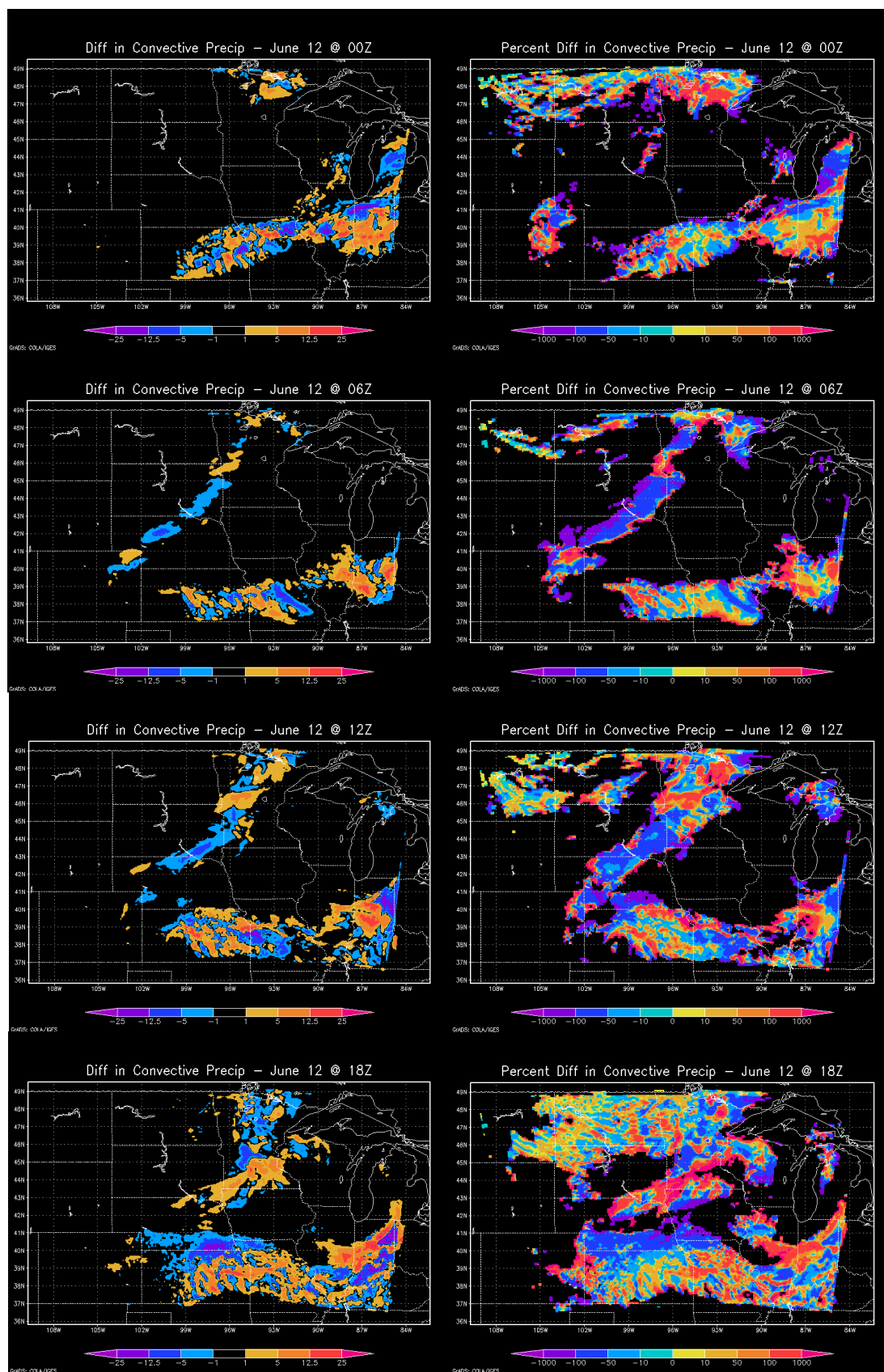
Figure 20 – [left] Absolute difference (mm) in 6-hour convective precipitation (mm) between the irrigated and non-irrigated model runs beginning at the time specified in each panel. [right] Percent difference (%) in 6-hour convective precipitation (mm) between the irrigated and non-irrigated model runs beginning at the time specified in each panel.
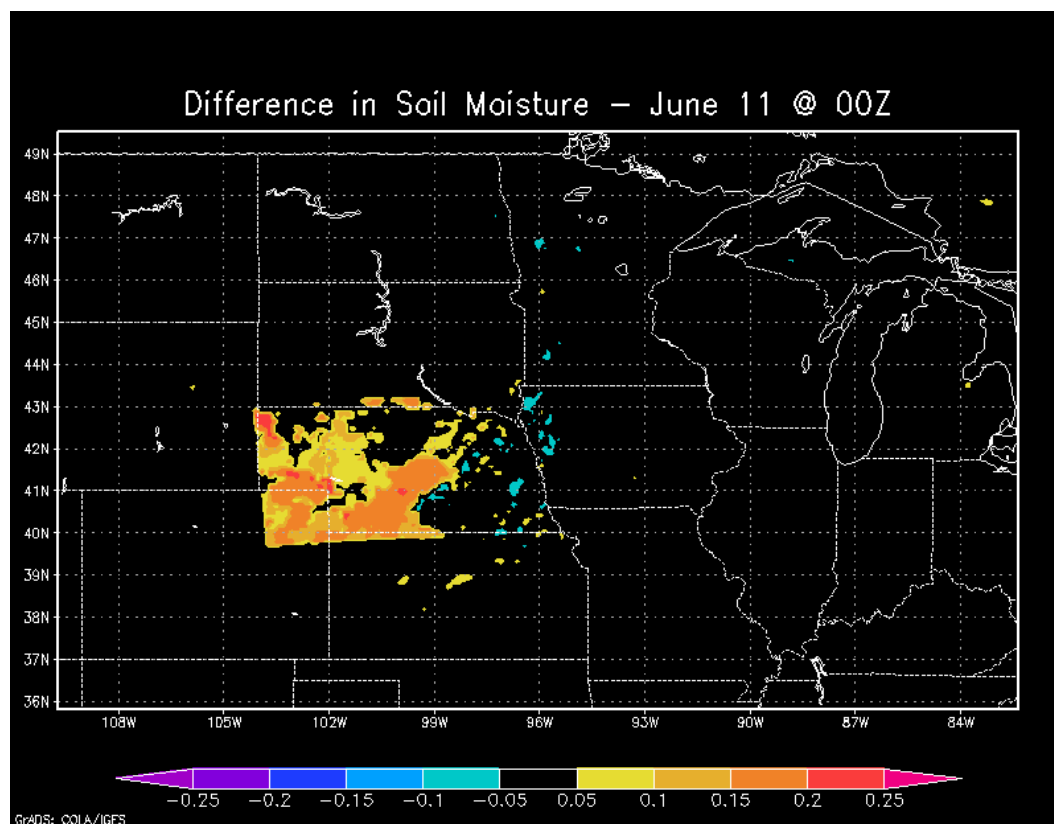
Figure 21 – Absolute difference (m^3 m^{-3}) in soil moisture between the irrigated and non-irrigated model runs on June 11 at 00Z. This plot is representative of the soil moisture anomaly for the entire 15-day simulation period.

Diff in Latent Heat Flux (sfc) — June 11 @ 18Z

Diff in Latent Heat Flux (sfc) — June 12 @ 18Z

Diff in Upward Moisture Flux (sfc) — June 11 @ 18Z

Diff in Upward Moisture Flux (sfc) — June 12 @ 18Z

Diff in Dewpoint Temperature — June 12 @ 18Z

Diff in Dewpoint Temperature — June 11 @ 18Z

Diff in Relative Humidity (sfc) — June 11 @ 18Z

Diff in Relative Humidity (sfc) — June 12 @ 18Z
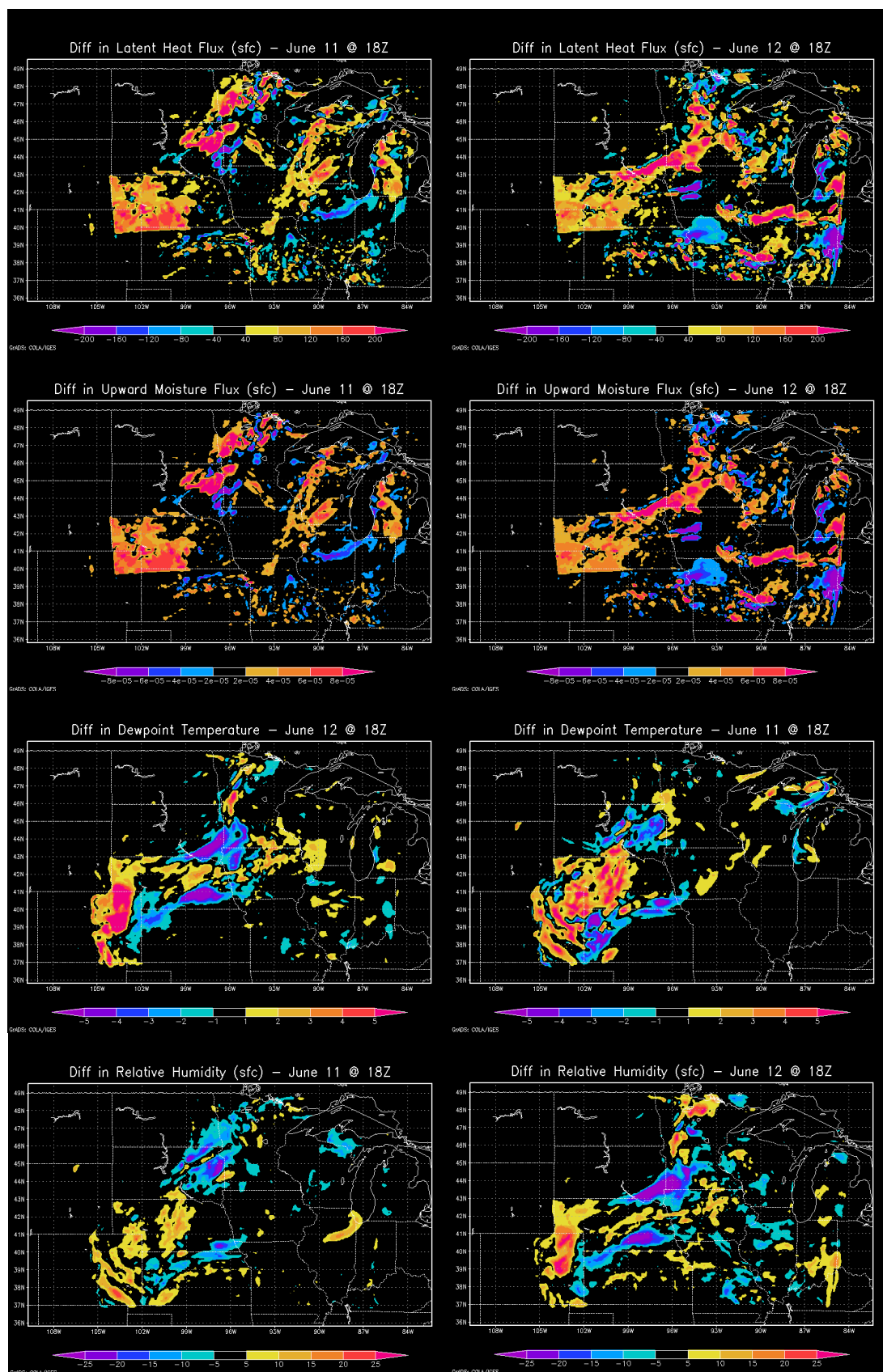
Figure 22 – [first row] Absolute difference in latent heat flux (W m^{-2}) between the
irrigated and non-irrigated model runs at 18Z on June 11 and 12. [second row] Same as
first row, but for upward moisture flux (W m^{-2}). [third row] Same as first row but for
dewpoint temperature (K). [fourth row] Same as first row, but for relative humidity
(percentage points).
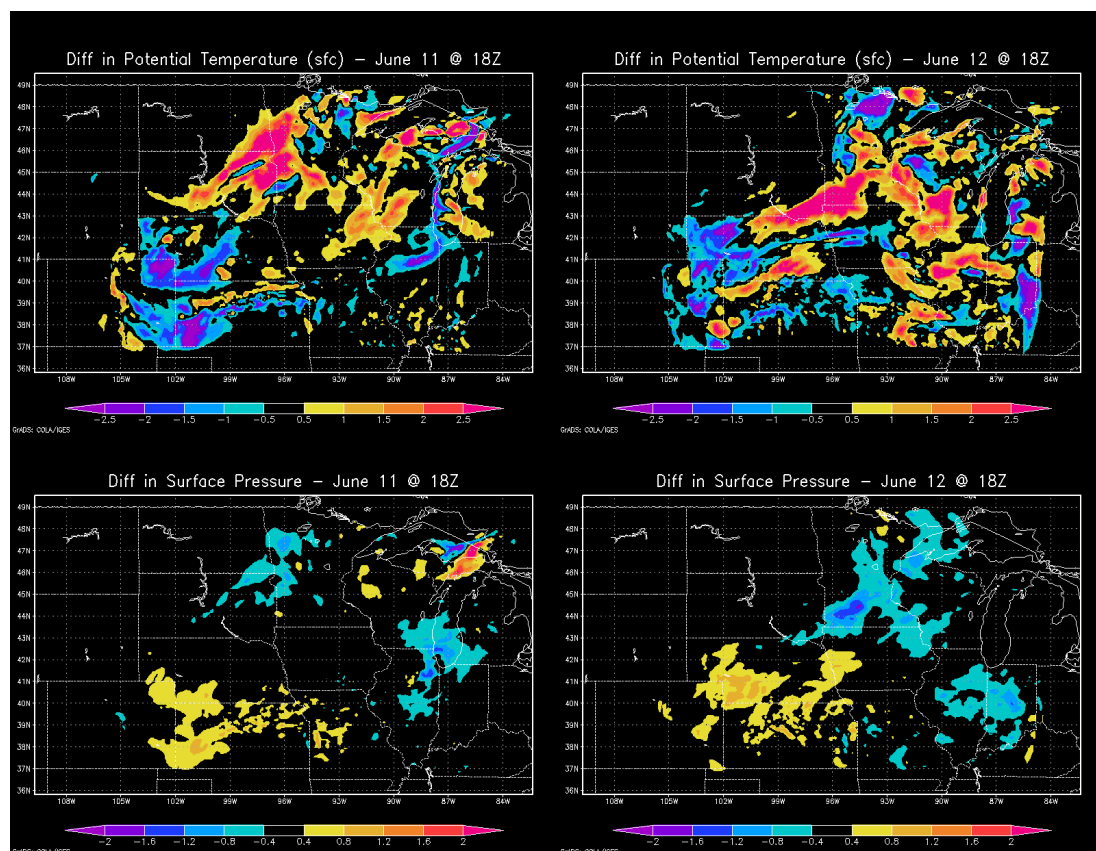
Figure 23 – Same as Figure 12, but for [top] potential temperature (K), and for [bottom] surface pressure (hPa).
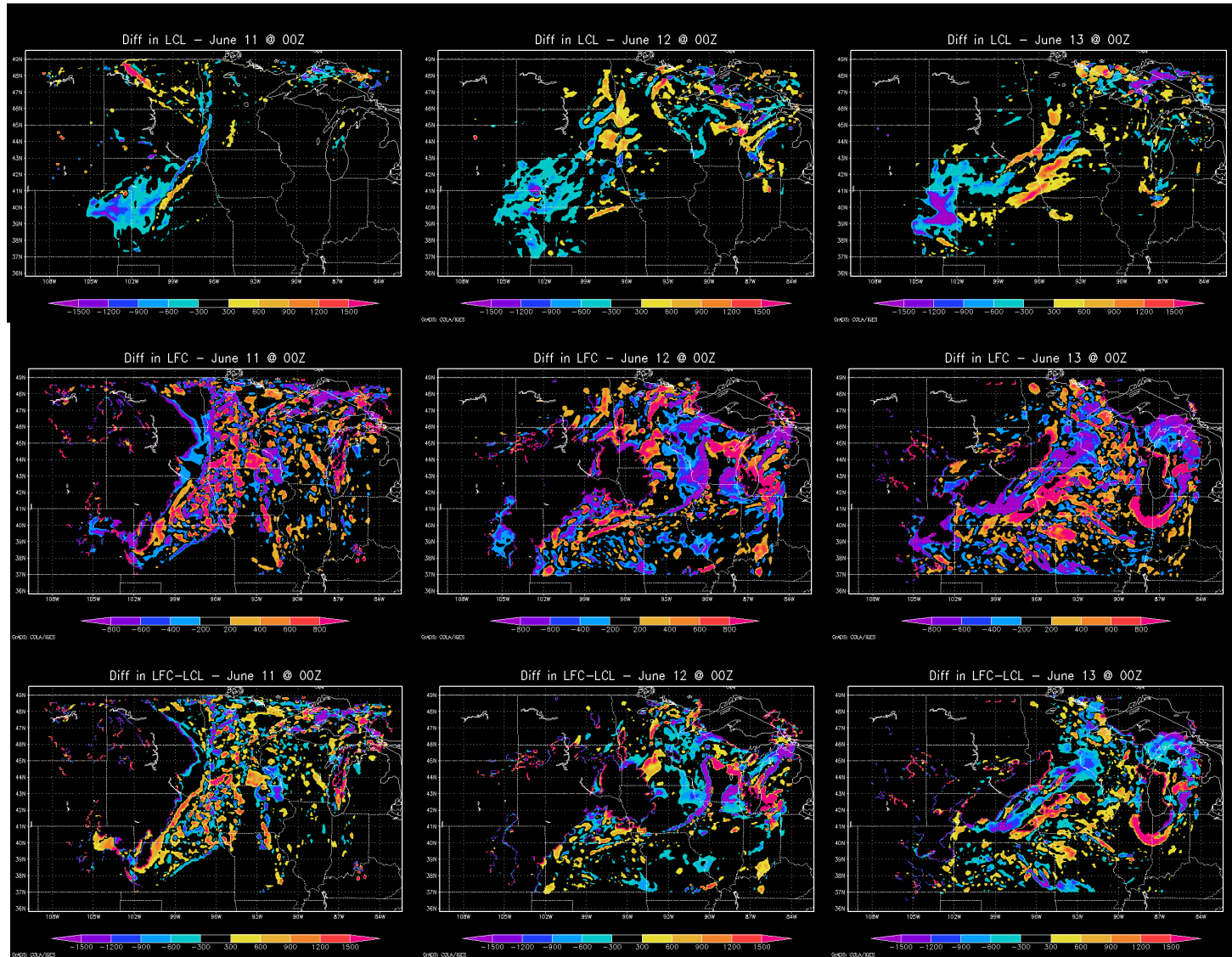
Figure 24 – [top row] Absolute difference in lifting condensation level (LCL) (m) between the irrigated and non-irrigated model runs at 00Z on June 11, 12, and 13. [middle row] Same as top row, but for level of free convection (LFC) (m). [bottom row] Same as top row, but for the difference between the LFC and LCL (m).
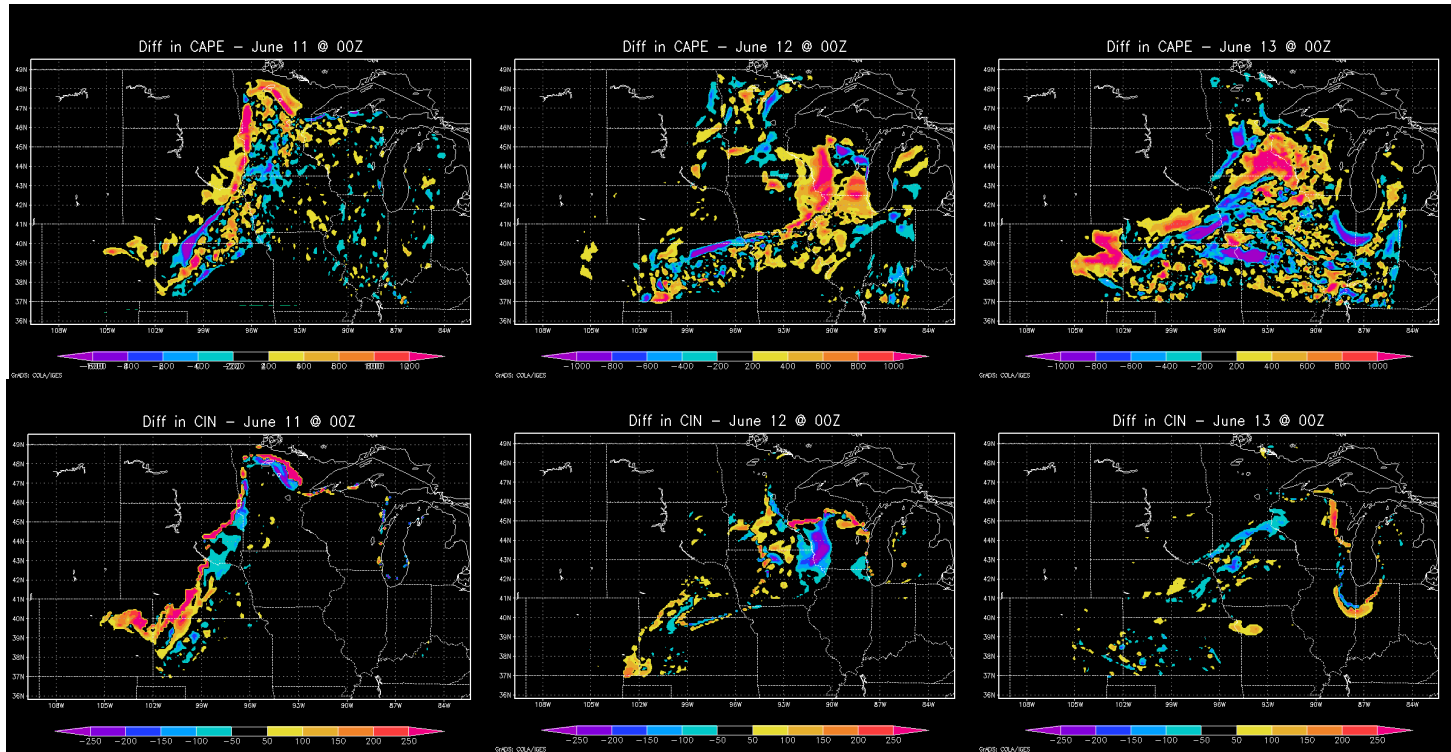
Figure 25 – [top] Same as in Figure 14, but for convective available potential energy (CAPE) (J kg^{-1}). [bottom] Same as in Figure 14, but for convective inhibition (CIN) (J kg^{-1}).
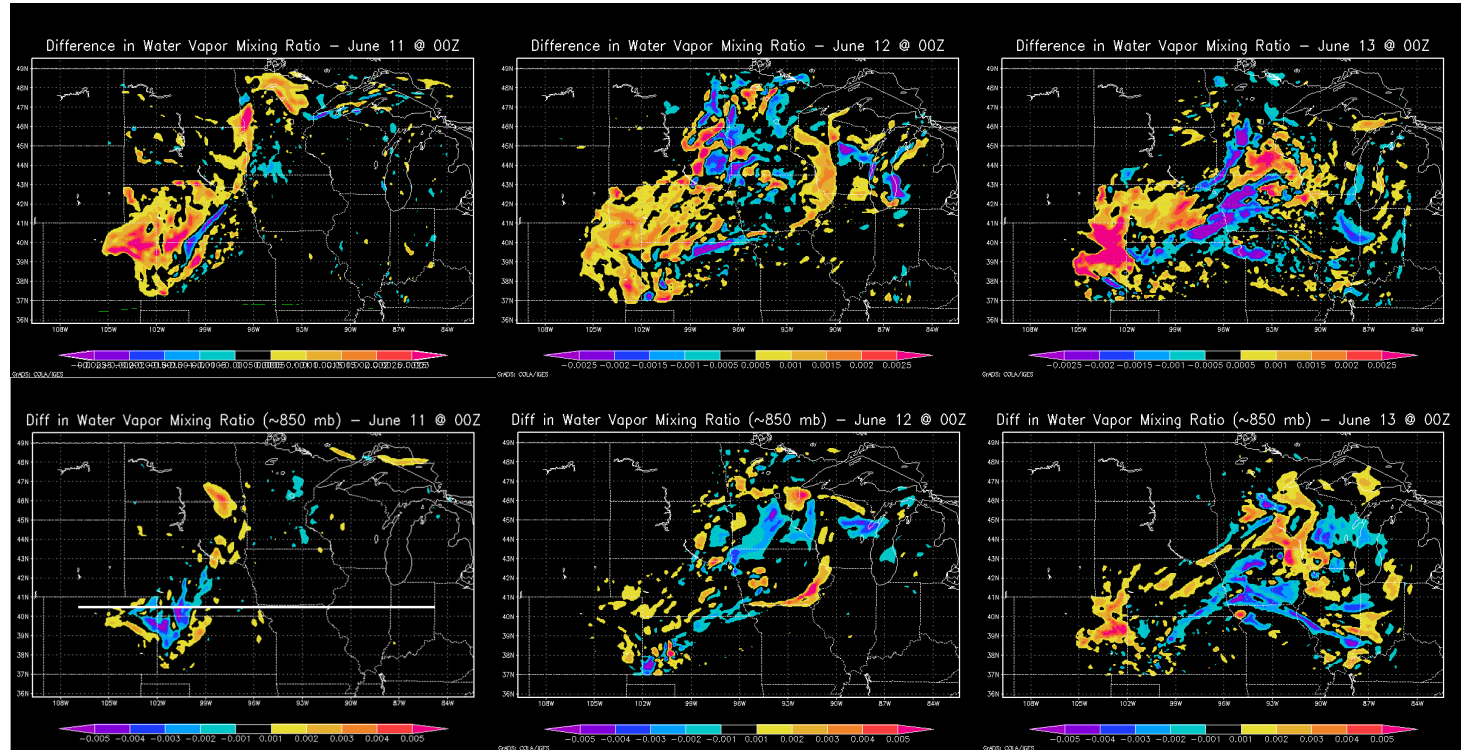
Figure 26 – Same as Figure 14, but for water vapor mixing ratio (kg kg^{-1}) [top] at the surface, and [bottom] at the 850 mb pressure level. Note that the white horizontal line drawn in the bottom left panel is the line through which the cross-section in the next figure (and for all other cross-sections) is derived.
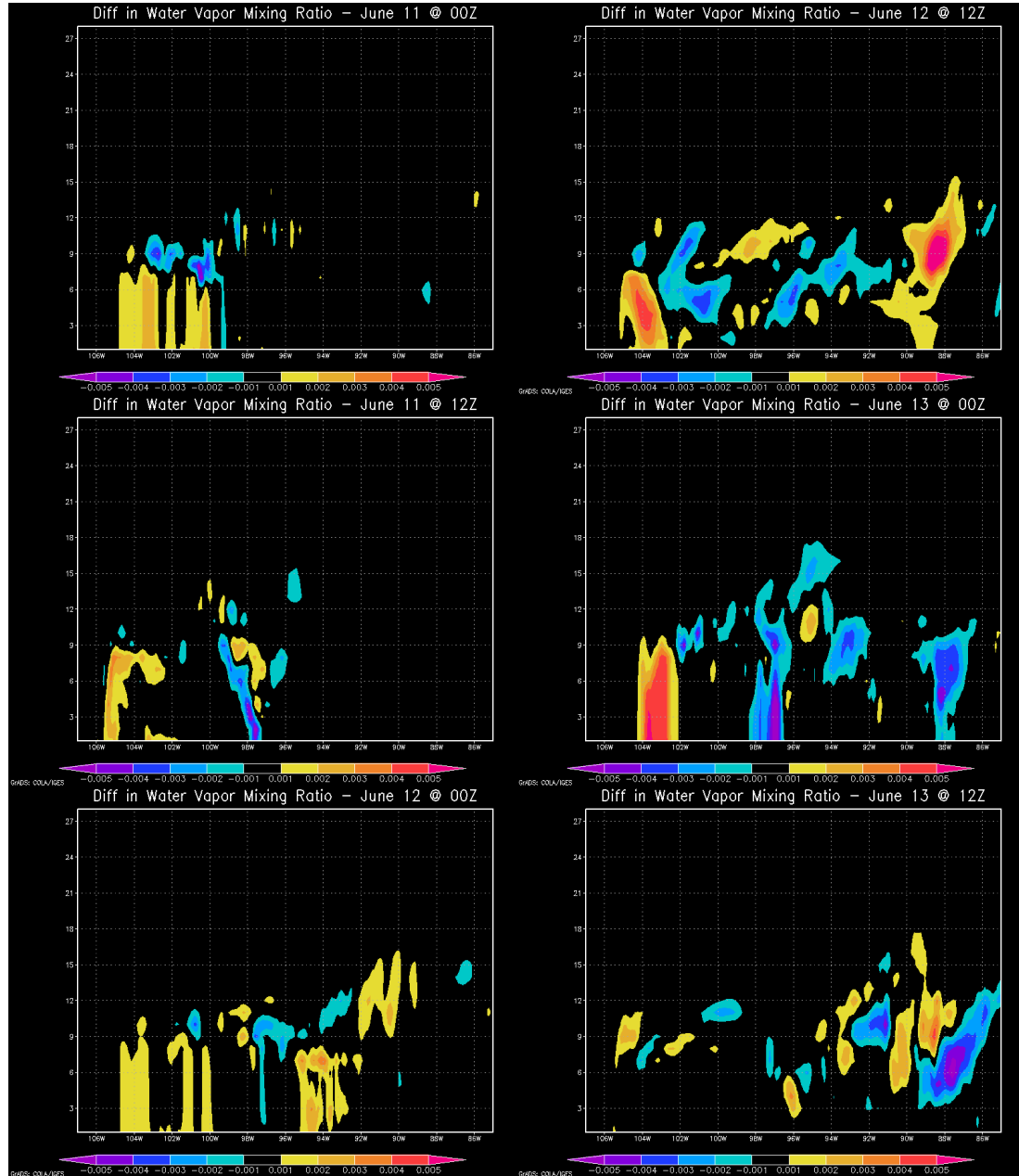
Figure 27 – Time series of cross-sections for the absolute difference of water vapor mixing ratio (kg kg^{-1}) between the irrigated and non-irrigated model runs in 12-hour increments between 00Z on June 11 and 12Z on June 13. Time increases going down the columns.
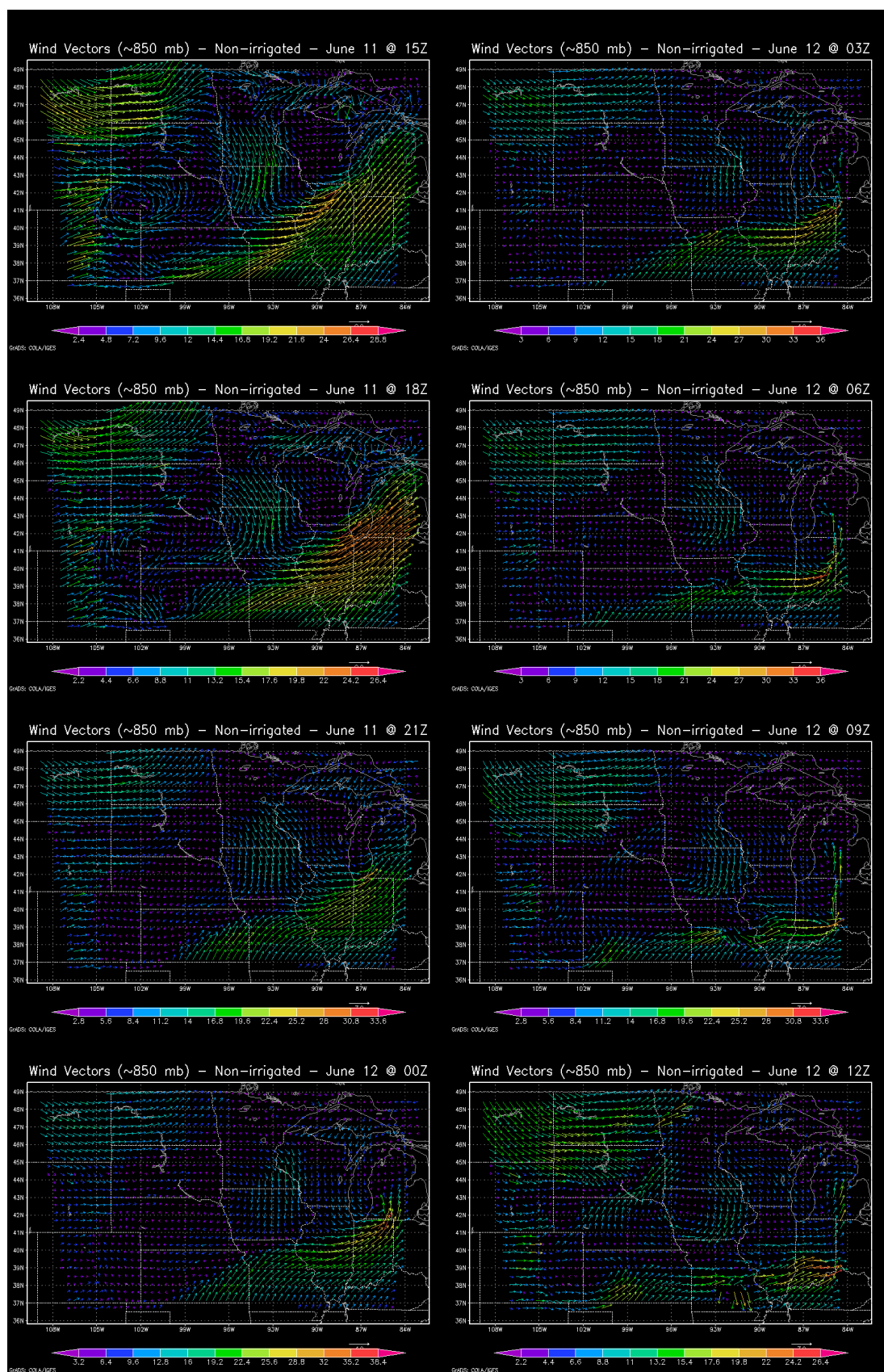
Figure 28 – A timeseries of wind vectors (m s^{-1}) for the non-irrigated model run at the 850 mb pressure level from 15Z on June 11 to 12Z on June 12 in 3-hour increments. Time increases going down the columns.
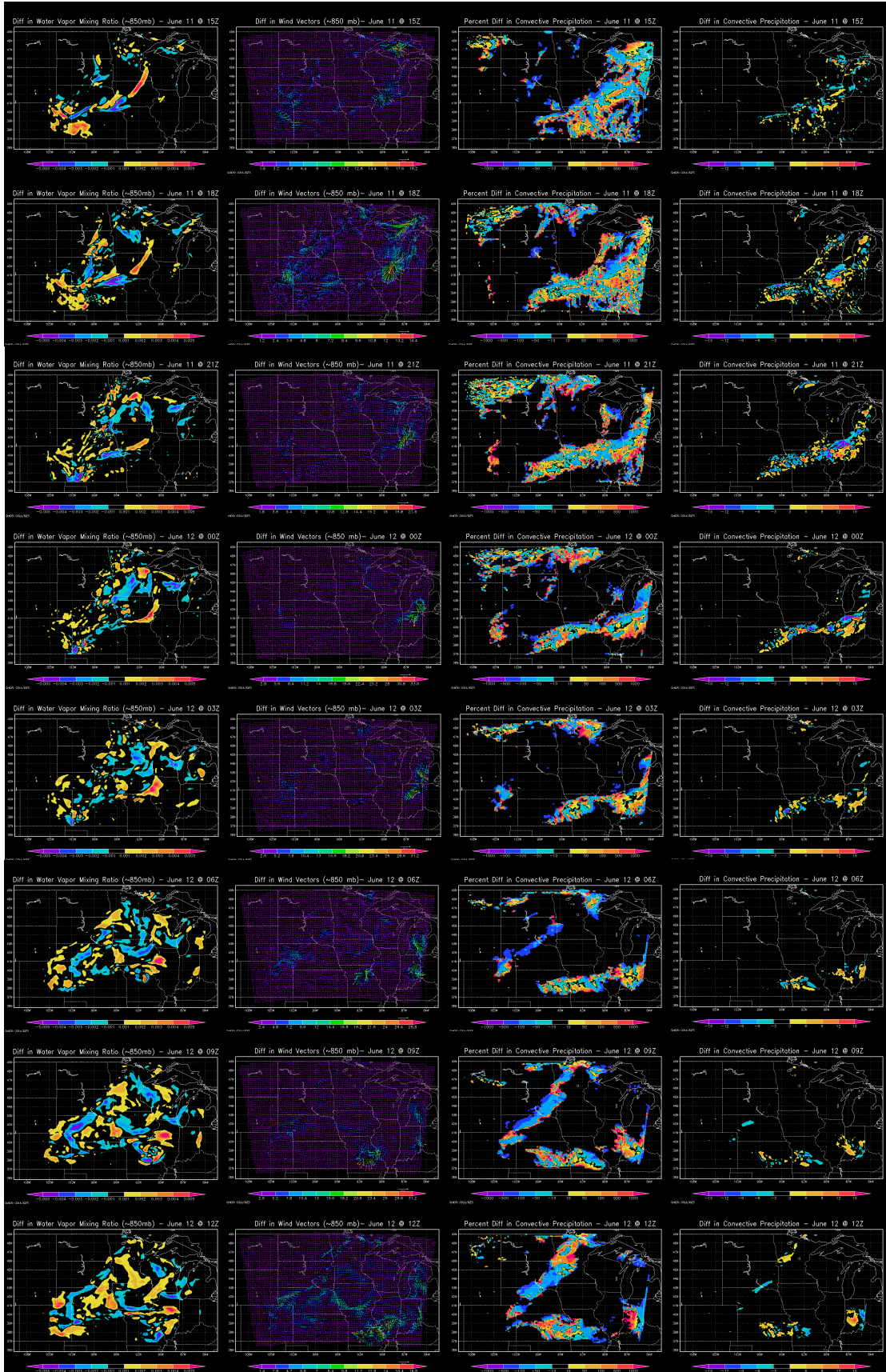
Figure 29 – Same as Figure 19, but for [left] absolute difference in water vapor mixing ratio at the 850 mb pressure level (kg kg^{-1}), [second from left] absolute difference in wind vectors at the 850 mb pressure level (m s^{-1}), [second from right] percent difference in 6-hour convective precipitation (%) beginning at the specified time, and [right] absolute difference in 6-hour convective precipitation (mm) beginning at the specified time.

Figure 30 – A time series of cross-sections for the absolute difference in wind vectors (m

s^{-1}) between the irrigated and non-irrigated model runs between 15Z on June 11 and 12Z

on June 12. Time increases going down the columns.

BIBLIOGRAPHY

Adegoke, J. O., R. A. Pielke, J. Eastman, R. Mahmood, and K. G. Hubbard, 2003: Impact of Irrigation on Midsummer Surface Fluxes and Temperature under Dry Synoptic Conditions: A Regional Atmospheric Model Study of the U.S. High Plains. *Mon. Weather Rev.*, **131**, 556–564.
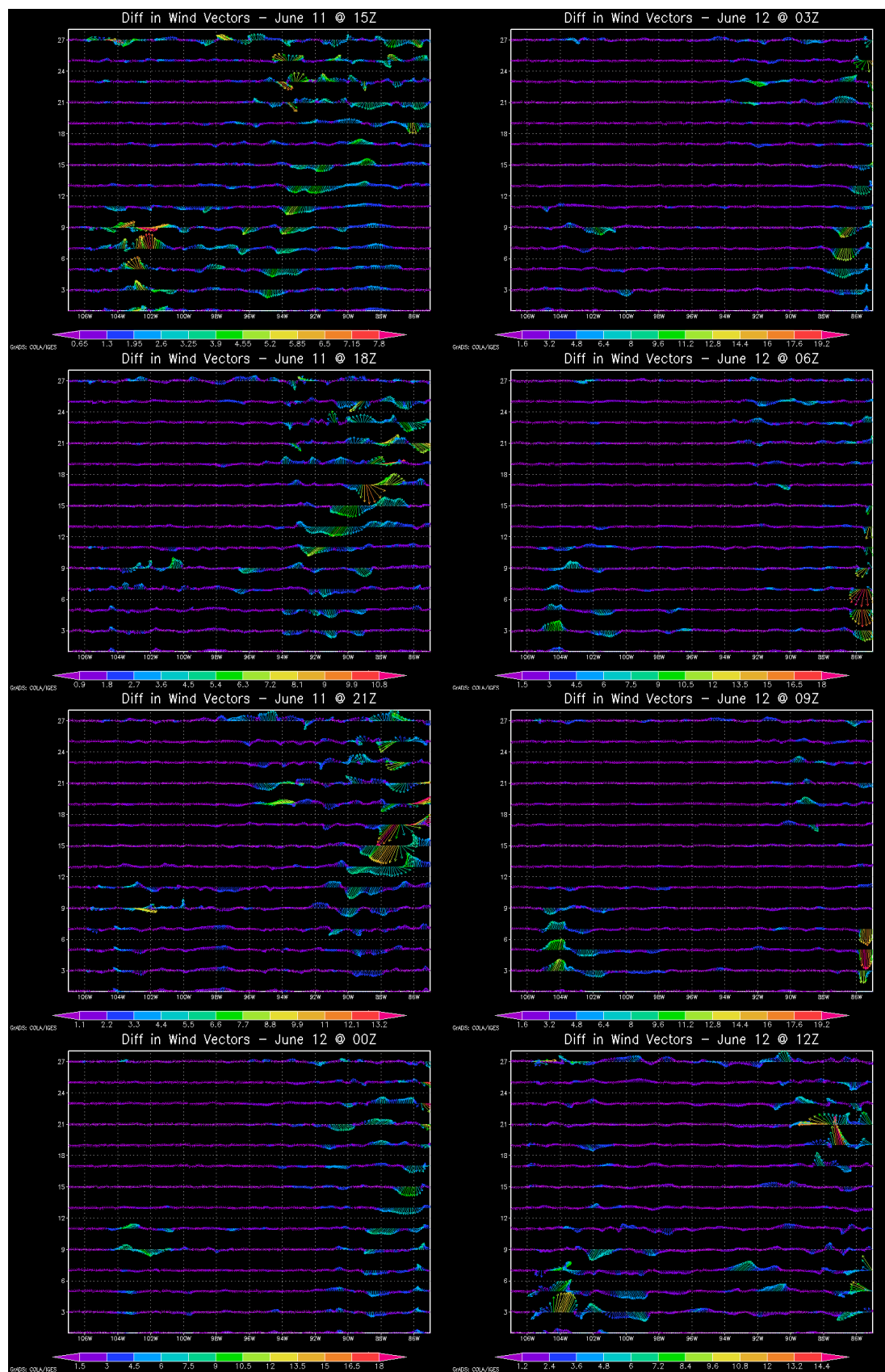
Adegoke, J. O., R. Pielke, and A. M. Carleton, 2007: Observational and modeling studies of the impacts of agriculture-related land use change on planetary boundary layer processes in the central U.S. *Agric. For. Meteorol.*, **142**, 203–215.

Alexander, L. V., et al., 2006: Global observed changes in daily climate extremes of temperature and precipitation. *J. Geophys. Res.*, **111**, D05109, doi:10.1029/2005JD006290.

Allard, J., and A. M. Carleton, 2010: Mesoscale Associations Between Midwest Land Surface Properties and Convective Cloud Development in the Warm Season. *Phys. Geogr.*, **31**, 107–136.

Angel, J. R., and F. A. Huff, 1997: Changes in Heavy Rainfall in Midwestern United States. *J. Water Resour. Plan. Manag.*, **123**, 246–249.

Baidya Roy, S., G. C. Hurtt, C. P. Weaver, and S. W. Pacala, 2003: Impact of historical land cover change on the July climate of the United States. *J. Geophys. Res. Atmos.*, **108**, 4793, doi:10.1029/ 2003JD003565.

Barnston, A. G., and P. T. Schickedanz, 1984: The Effect of Irrigation on Warm Season Precipitation in the Southern Great Plains. *J. Clim. Appl. Meteorol.*, **23**, 865–888.

Betts, A. K., 2004: Understanding Hydrometeorology Using Global Models. *Bull. Am. Meteorol. Soc.*, **85**, 1673–1688.

Betts, A. K., J. H. Ball, A. C. M. Beljaars, M. J. Miller, and P. A. Viterbo, 1996: The land surface-atmosphere interaction: A review based on observational and global modeling perspectives. *J. Geophys. Res.*, **101**, 7209, doi:10.1029/95JD02135.

Bonan, G. B., 1997: Effects of land use on the climate of the United States. *Clim. Change,* **37**, 449–486.

Bonan, G. B., 2001: Observational Evidence for Reduction of Daily Maximum Temperature by Croplands in the Midwest United States. *J. Clim.*, **14**, 2430–2442.

Boucher, O., Myhre, G. and Myhre, A., 2004: Direct human influence of irrigation on atmospheric water vapour and climate. *Clim. Dyn.*, **22**(6-7), 597-603.

Brown, P. J., and A. T. DeGaetano, 2013: Trends in U.S. Surface Humidity, 1930–2010. *J. Appl. Meteorol. Climatol.*, **52**, 147–163.

Carleton, A. M., J. Adegoke, J. Allard, D. L. Arnold, and D. J. Travis, 2001: Summer season land cover-convective cloud associations for the midwest U.S. "Corn Belt." *Geophys. Res. Lett.*, **28**, 1679–1682.

Carleton, A. M., D. L. Arnold, D. J. Travis, S. Curran, and J. O. Adegoke, 2008: Synoptic Circulation and Land Surface Influences on Convection in the Midwest U.S. "Corn Belt" during the Summers of 1999 and 2000. Part I: Composite Synoptic Environments. *J. Clim.*, **21**, 3389–3415.

Changnon, S., and K. Kunkel, 1995: Climate-related fluctuations in midwestern floods during 1921-1985. *J. Water Resour. Plan. Manag.*, **121**, 326-334.

DeAngelis, A., F. Dominguez, Y. Fan, A. Robock, M. D. Kustu, and D. Robinson, 2010: Evidence of enhanced precipitation due to irrigation over the Great Plains of the United States. *J. Geophys. Res.*, **115**, D15115, doi:10.1029/2010JD013892.

Degu, A. M., F. Hossain, D. Niyogi, R. Pielke Sr., J. M. Shepherd, N. Voisin, and T. Chronis, 2011: The influence of large dams on surrounding climate and precipitation patterns, *Geophys. Res. Lett.*, **38**, L04405, doi:10.1029/2010GL046482.

De Ridder, K., and H. Gallée, 1998: Land Surface–Induced Regional Climate Change in Southern Israel. *J. Appl. Meteorol.*, **37**, 1470–1485.

Diffenbaugh, N. S., 2009: Influence of modern land cover on the climate of the United States, *Clim. Dyn.*, **33**, 945-958.

Dominguez, F., P. Kumar, X.-Z. Liang, and M. Ting, 2006: Impact of Atmospheric Moisture Storage on Precipitation Recycling. *J. Clim.*, **19**, 1513–1530.

Douglas, E. M., A. Beltrán-Przekurat, D. Niyogi, R. A. Pielke, and C. J. Vörösmarty, 2009: The impact of agricultural intensification and irrigation on land–atmosphere interactions and Indian monsoon precipitation — A mesoscale modeling perspective. *Glob. Planet. Change*, **67**, 117–128.

Eltahir, E. A. B., 1998: A Soil Moisture-Rainfall Feedback Mechanism: 1. Theory and observations. *Water Resour. Res.*, **34**, 765–776.

Eltahir, E. A. B., and R. L. Bras, 1996: Precipitation recycling. *Rev. Geophys.*, **34**, 367, doi:10.1029/96RG01927.

Findell, K. L., and E. A. B. Eltahir, 2003a: Atmospheric Controls on Soil Moisture–Boundary Layer Interactions. Part I: Framework Development. *J. Hydrometeorol.*, **4**, 552–569.

Findell, K. L., and E. A. B. Eltahir, 2003b: Atmospheric Controls on Soil Moisture–Boundary Layer Interactions. Part II: Feedbacks within the Continental United States. *J. Hydrometeorol.*, **4**, 570–583.

Freydank, K. and S. Siebert, 2008: Towards mapping the extent of irrigation in the last century: time series of irrigated area per country. *Frankfurt Hydrology Paper* 08, Institute of Physical Geography, University of Frankfurt, Frankfurt am Main, Germany, 46 pp, DOI:10.13140/2.1.1743.1687.

Groisman, P. Y., R. W. Knight, T. R. Karl, D. R. Easterling, B. Sun, and J. H. Lawrimore, 2004: Contemporary Changes of the Hydrological Cycle over the Contiguous United States: Trends Derived from In Situ Observations. *J. Hydrometeorol.*, **5**, 64–85.

Groisman, P. Y., R. W. Knight, D. R. Easterling, T. R. Karl, G. C. Hegerl, and V. N. Razuvaev, 2005: Trends in intense precipitation in the climate record, *J. Clim.*, **18**, 1326–1350.

Groisman, P. Y., R. W. Knight, and T. R. Karl, 2012: Changes in Intense Precipitation over the Central United States. *J. Hydrometeorol.*, **13**, 47–66.

Guimberteau M., K. Laval, A. Perrier, and J. Polcher, 2011: Global effect of irrigation and its impact on the onset of the Indian summer monsoon. *Clim Dyn.*, **39,** 1329-1348, DOI:10.1007/s00382-011-1252-5.

Guru, M. V, and J. E. Horne, 2000: *The Ogallala Aquifer*. The Kerr Center for Sustainable Agriculture.

Harding, K. J., and P. K. Snyder, 2012a: Modeling the Atmospheric Response to Irrigation in the Great Plains. Part II: The Precipitation of Irrigated Water and Changes in Precipitation Recycling. *J. Hydrometeorol.*, **13**, 1687–1703.

Harding, K. J., and P. K. Snyder, 2012b: Modeling the Atmospheric Response to Irrigation in the Great Plains. Part I: General Impacts on Precipitation and the Energy Budget. *J. Hydrometeorol.*, **13**, 1667–1686.

Hennessy, K. J., J. M. Gregory, and J. F. B. Mitchell, 1997: Changes in daily precipitation under enhanced greenhouse conditions. *Clim. Dyn.*, **13**, 667–680.

Higgins, R. W., and V. E. Kousky, 2013: Changes in Observed Daily Precipitation over the United States between 1950–79 and 1980–2009. *J. Hydrometeorol.*, **14**, 105–121.

Hossain, F., I. Jeyachandran, and R. Pielke, 2009: Have Large Dams Altered Extreme Precipitation Patterns? *Eos, Trans. Am. Geophys. Union*, **90**, 453, doi:10.1029/2009EO480001.

Huber, D., D. Mechem, and N. Brunsell, 2014: The Effects of Great Plains Irrigation on the Surface Energy Balance, Regional Circulation, and Precipitation. *Climate*, **2**, 103–128.

Im, E.-S., M. P. Marcella, and E. A. B. Eltahir, 2014: Impact of Potential Large-Scale Irrigation on the West African Monsoon and Its Dependence on Location of Irrigated Area. *J. Clim.*, **27**, 994–1009.

IPCC, 2013. Collins, M., R. Knutti, J. Arblaster, J.-L. Dufresne, T. Fichefet, P. Friedlingstein, X. Gao, W.J. Gutowski, T. Johns, G. Krinner, M. Shongwe, C. Tebaldi, A.J. Weaver and M. Wehner, 2013: Long-term Climate Change: Projections, Commitments and Irreversibility. In: *Climate Change 2013: The Physical Science Basis. Contribution of Working Group I to the Fifth Assessment Report of the Intergovernmental Panel on Climate Change* [Stocker, T.F., D. Qin, G.-K. Plattner, M. Tignor, S.K. Allen, J. Boschung, A. Nauels, Y. Xia, V. Bex and P.M. Midgley (eds.)]. Cambridge University Press, Cambridge, United Kingdom and New York, NY, USA, pp. 1029–1136, doi:10.1017/CBO9781107415324.024.

Jódar, J., J. Carrera, and A. Cruz, 2010: Irrigation enhances precipitation at the mountains downwind. *Hydrol. Earth Syst. Sci.*, **14**, 2003–2010.

Jones, A. R., and N. A. Brunsell, 2009: Energy Balance Partitioning and Net Radiation Controls on Soil Moisture–Precipitation Feedbacks. *Earth Interact.*, **13**, 1–25.

Karl, T. R., and R. W. Knight, 1998: Secular Trends of Precipitation Amount, Frequency, and Intensity in the United States. *Bull. Am. Meteorol. Soc.*, **79**, 231–241.

Karl, T. R., R. W. Knight, D. R. Easterling, and R. G. Quayle, 1996: Indices of Climate Change for the United States. *Bull. Am. Meteorol. Soc.*, **77**, 279–292.

Karl, T. R., and W. J. Koss, 1984: Regional and National Monthly, Seasonal, and Annual Temperature Weighted by Area, 1895-1983. Historical Climatology Series 4-3, National Climatic Data Center, Asheville, NC, 38 pp.

Kunkel, K. E., D. R. Easterling, K. Redmond, and K. Hubbard, 2003: Temporal variations of extreme precipitation events in the United States: 1895 – 2000, *Geophys. Res. Lett.*, **30** (17), 1900, doi:10.1029/2003GL018052.

Kustu, M. D., Y. Fan, and A. Robock, 2010: Large-scale water cycle perturbation due to irrigation pumping in the US High Plains: A synthesis of observed stream flow changes. *J. Hydrology*, **390**, 222-244, doi:10.1016/j.jhydrol.2010.06.045.

Kustu, M. D., Y. Fan, and M. Rodell, 2011: Possible link between irrigation in the U.S. High Plains and increased summer streamflow in the Midwest, *Water Resour. Res.*, **47**, W03522, doi:10.1029/2010WR010046.

Lee, E., W. J. Sacks, T. N. Chase, and J. A. Foley, 2011: Simulated impacts of irrigation on the atmospheric circulation over Asia. *J. Geophys. Res.*, **116**, D08114, doi:10.1029/2010JD014740.

Lo, M., and J. S. Famiglietti, 2013: Irrigation in California's Central Valley strengthens the southwestern U.S. water cycle. *Geophys. Res. Lett.*, **40**, 301–306.

Lobell, D. B., C. J. Bonfils, L. M. Kueppers, and M. A. Snyder, 2008: Irrigation cooling effect on temperature and heat index extremes. *Geophys. Res. Lett.*, **35**, L09705, doi:10.1029/2008GL034145.

Mahmood, R., and K. Hubbard, 2002: Anthropogenic land-use change in the North American tall grass-short grass transition and modification of near-surface hydrologic cycle. *Clim. Res.*, **21**, 83–90.

Mahmood, R., K. G. Hubbard, and C. Carlson, 2004: Modification of growing-season surface temperature records in the northern great plains due to land-use transformation: verification of modelling results and implication for global climate change. *Int. J. Climatol.*, **24**, 311–327.

Mahmood, R., S. Foster, T. Keeling, K. Hubbard, C. Carlson, and R. Leeper, 2006: Impacts of irrigation on 20th century temperature in the northern Great Plains. *Glob. Planet. Change*, **54**, 1–18.

Mahmood, R., K. G. Hubbard, R. D. Leeper, and S. A. Foster, 2008: Increase in Near-Surface Atmospheric Moisture Content due to Land Use Changes: Evidence from the Observed Dewpoint Temperature Data. *Mon. Weather Rev.*, **136**, 1554–1561.

Melillo, J. M., T. C. Richmond, and G. W. Yohe, Eds., 2014: *Climate Change Impacts in the United States: The Third National Climate Assessment*. U.S. Global Change Research Program, 841 pp. doi:10.7930/J0Z31WJ2.

Menne M. J., I. Durre, R. S. Vose, B. E. Gleason, and T. G. Houston, 2012: An Overview of the Global Historical Climatology Network-Daily Database. *J. Atmos. Oceanic Technol.*, **29**, 897–910, doi: http://dx.doi.org/10.1175/JTECH-D-11-00103.1

Moore, N., and S. Rojstaczer, 2002: Irrigation's influence on precipitation: Texas High Plains, U.S.A. *Geophys. Res. Lett.*, **29**, 1755, doi:10.1029/2002GL014940.

MRCC, 2014. Cli-MATE Database. Midwestern Regional Climate Center. Accessed June 15, 2014 <http://mrcc.isws.illinois.edu/CLIMATE/#>.

NASS, cited 2013: The United States Department of Agriculture National Agricultural Statistics Service. [Available online at http://www.nass.usda.gov/.]

NCAR, 2011. WRF User's Guide for the Advanced Research WRF (ARW) Modeling System Version 3.3. WRF Users Page. University Corporation for Atmospheric Research <http://www2.mmm.ucar.edu/wrf/users/docs/user_guide_V3.3/contents.html>.

NCDC, 2013. Climate at a Glance. National Climatic Data Center. Accessed May 1, 2013 <www.ncdc.noaa.gov/cag>.

NRCS, 2013: Groundwater Irrigation and Water Withdrawals: The Ogallala Aquifer Initiative. The United States Department of Agriculture National Resources Conservation Service. Economic Series Number 1.

Ozdogan, M., M. Rodell, H. K. Beaudoing, and D. L. Toll, 2010: Simulating the Effects of Irrigation over the United States in a Land Surface Model Based on Satellite-Derived Agricultural Data. *J. Hydrometeorol.*, **11**, 171–184.

Pal, J. S., and E. A. B. Eltahir, 2001: Pathways Relating Soil Moisture Conditions to Future Summer Rainfall within a Model of the Land–Atmosphere System. *J. Clim.*, **14**, 1227–1242.

Peterson, T. C., et al., 2013: Monitoring and Understanding Changes in Heat Waves, Cold Waves, Floods, and Droughts in the United States: State of Knowledge. *Bull. Amer. Meteor. Soc.*, **94**, 821–834. doi: http://dx.doi.org/10.1175/BAMS-D-12-00066.1

Pielke, R. A., 2001: Influence of the spatial distribution of vegetation and soils on the prediction of cumulus convective rainfall. *Rev. Geophys.*, **39**, 151–177.

Pielke, R. A., and X. Zeng, 1989: Influence on Severe Storm Development of Irrigated Land. *Natl. Weather Dig.*, **14**, 16–17.

Pryor, S. C., J. A. Howe, and K. E. Kunkel, 2009: How spatially coherent and statistically robust are temporal changes in extreme precipitation in the contiguous USA? *Int. J. Climatol.*, **29**, 31–45.

Puma, M. J., and B. I. Cook, 2010: Effects of irrigation on global climate during the 20th century. *J. Geophys. Res.*, **115**, D16120, doi:10.1029/2010JD014122.

Qian, Y., M. Huang, B. Yang, and L. K. Berg, 2013: A Modeling Study of Irrigation Effects on Surface Fluxes and Land–Air–Cloud Interactions in the Southern Great Plains. *J. Hydrometeorol.*, **14**, 700–721.

Raddatz, R. L., 2007: Evidence for the influence of agriculture on weather and climate through the transformation and management of vegetation: Illustrated by examples from the Canadian Prairies. *Agric. For. Meteorol.*, **142**, 186–202.

Ramankutty, N., and J.A. Foley (1999). Estimating historical changes in global land cover: croplands from 1700 to 1992. *Global Biogeochemical Cycles*, **13**(4), 997-1027.

Sacks, W. J., B. I. Cook, N. Buenning, S. Levis, and J. H. Helkowski, 2009: Effects of global irrigation on the near-surface climate. *Clim. Dyn.*, **33**, 159–175.

Segal, M., R. Avissar, M. C. McCumber, and R. A. Pielke, 1988: Evaluation of Vegetation Effects on the Generation and Modification of Mesoscale Circulations. *J. Atmos. Sci.*, **45**, 2268–2293.

Segal, M., Z. Pan, R. W. Turner, and E. S. Takle, 1998: On the Potential Impact of Irrigated Areas in North America on Summer Rainfall Caused by Large-Scale Systems. *J. Appl. Meteorol.*, **37**, 325–331.

Stidd, C. K., W. B. Fowler, and J. D. Helvey, 1975: Irrigation increases rainfall? *Science*, **188**, 279–281.

Sun, Y., S. Solomon, A. Dai, and R. W. Portmann, 2006: How often does it rain? *J. Clim.*, **19**, 916–934.

Sun, B., T. R. Karl, and D. J. Seidel, 2007: Changes in Cloud-Ceiling Heights and Frequencies over the United States since the Early 1950s. *J. Clim.*, **20**, 3956–3970.

Sun Y., S. Solomon, A. Dai, and R. W. Portmann, 2007: How often will it rain? *J. Clim.*, **20,** 4801–4818.

Suyker, A. E., and S. B. Verma, 2008: Interannual water vapor and energy exchange in an irrigated maize-based agroecosystem. *Agric. For. Meteorol.*, **148**, 417–427.

Tao, W.-K., J.-P. Chen, Z. Li, C. Wang, and C. Zhang, 2012: Impact of aerosols on convective clouds and precipitation, *Rev. Geophys.*, **50**, RG2001, doi:10.1029/2011RG000369.

Trenberth, K. E., A. Dai, R. M. Rasmussen, and D. B. Parsons, 2003: The Changing Character of Precipitation. *Bull. Am. Meteorol. Soc.*, **84**, 1205–1217.

USGS, 2013: High Plains Water-Level Monitoring Study (Groundwater Resource Program): Physical/Cultural Setting. United States Geological Survey. Accessed at http://ne.water.usgs.gov/ogw/hpwlms/physsett.html.

Utsumi, N., S. Seto, S. Kanae, E. E. Maeda, and T. Oki, 2011: Does higher surface temperature intensify extreme precipitation? *Geophys. Res. Lett.*, **38**, L16708, doi:10.1029/2011GL048426.

Villarini, G., J. A. Smith, and G. A. Vecchi, 2013: Changing Frequency of Heavy Rainfall over the Central United States. *J. Clim.*, **26**, 351–357.

Wang, H., A. J. Pitman, M. Zhao, and R. Leemans, 2003: The impact of land-cover modification on the June meteorology of China since 1700, simulated using a regional climate model. *Int. J. Climatol.*, **23**, 511–527.

Weaver, C. P., 2004: Coupling between Large-Scale Atmospheric Processes and Mesoscale Land–Atmosphere Interactions in the U.S. Southern Great Plains during Summer. Part II: Mean Impacts of the Mesoscale. *J. Hydrometeorol.*, **5**, 1247–1258.

Weaver, S. J., and S. Nigam, 2008: Variability of the Great Plains Low-Level Jet: Large-Scale Circulation Context and Hydroclimate Impacts. *J. Clim.*, **21**, 1532–1551.

Wei, J., P. A. Dirmeyer, D. Wisser, M. G. Bosilovich, and D. M. Mocko, 2013: Where Does the Irrigation Water Go? An Estimate of the Contribution of Irrigation to Precipitation Using MERRA. *J. Hydrometeorol.*, **14**, 275–289.

Zangvil, A., D. H. Portis, and P. J. Lamb, 2004: Investigation of the Large-Scale Atmospheric Moisture Field over the Midwestern United States in Relation to Summer Precipitation. Part II: Recycling of Local Evapotranspiration and Association with Soil Moisture and Crop Yields. *J. Clim.*, **17**, 3283–3301.